

**International
Progress Report**

IPR-07-07

Äspö Hard Rock Laboratory

Temperature Buffer Test

**Sensors data report
(Period 030326-070101)
Report No:9**

Reza Goudarzi

Mattias Åkesson

Harald Hökmark

Clay Technology AB

January 2007

Svensk Kärnbränslehantering AB

Swedish Nuclear Fuel
and Waste Management Co
Box 5864
SE-102 40 Stockholm Sweden
Tel 08-459 84 00
+46 8 459 84 00
Fax 08-661 57 19
+46 8 661 57 19



| | |
|------------------------|---------------------|
| Report no. | No. |
| IPR-07-07 | F12K |
| Author | Date |
| Reza Goudarzi | January 2007 |
| Mattias Åkesson | |
| Harald Hökmark | |
| Checked by | Date |
| Bertrand Vignal | 2007-05-11 |
| Approved | Date |
| Anders Sjöland | 2007-06-21 |

Äspö Hard Rock Laboratory

Temperature Buffer Test

**Sensors data report
(Period 030326-070101)
Report No:9**

Reza Goudarzi
Mattias Åkesson
Harald Hökmark

Clay Technology AB

January 2007

Keywords: Field test, Data, Repository, Bentonite, Rock, Canister, Measurements, Water pressure, Total pressure, Relative humidity, Temperature, Displacements

This report concerns a study which was conducted for SKB. The conclusions and viewpoints presented in the report are those of the author(s) and do not necessarily coincide with those of the client.

Résumé

TBT (Test de Barrière ouvragée en Température) est un projet mené par SKB et l'ANDRA, soutenu par ENRESA (en modélisation) et DBE (en instrumentation) qui vise à comprendre et modéliser le comportement thermo-hydro-mécanique de barrières ouvragées à base d'argile gonflante soumises à des températures élevées ($> 100^{\circ}\text{C}$) pendant leur hydratation.

L'essai est conduit dans le HRL d'Äspö dans une alvéole verticale de 8 m de profondeur et 1,75 m de diamètre. Deux sondes chauffantes (chacune de 3 m de long et 0,6 m de diamètre) sont entourées d'argile gonflante, une bentonite MX 80 qui est confinée par un bouchon ancré dans la roche par 9 câbles. L'essai fonctionne depuis le printemps 2003. Les sondes ont été chauffées chacune à la puissance nominale de 1500 W du 15^{ème} au 1171^{ème} jour et à 1600 W depuis.

Ce rapport présente les données de TBT enregistrées depuis son début le 26 mars 2003 jusqu'au premier janvier 2007.

Dans la bentonite la pression totale est mesurée en 29 points, la pression de pore en 8 points et l'humidité relative en 35 points. La température est mesurée en 92 points et aussi à l'emplacement de chaque capteur dont la mesure nécessite d'être compensée en température.

Des mesures additionnelles sont faites : température en 40 points dans la roche alentour, en 11 points à la surface et 6 à l'intérieur des sondes. La force de confinement est mesurée sur trois des neuf câbles. Le déplacement vertical du bouchon est mesuré en trois points. Le débit et la pression d'eau fournie au système sont également mesurés.

Des mesures de température et de pression dans les zones chaudes du test obtenues par des capteurs à fibres optiques installés par DBE sont rapportées dans l'Appendix B.

Globalement, le système de mesure et de transmission des données fonctionne bien et les capteurs fournissent des valeurs fiables. Une exception concerne la mesure d'humidité relative au droit de la sonde inférieure où plusieurs capteurs ne fonctionnent plus.

La densité des dispositifs de mesure de température par thermocouples à mi-hauteur de chaque sonde chauffante s'est révélée utile pour observer de façon qualitative les cycles saturation - désaturation. Dans la section du bas des indications claires de désaturation sont apparues très tôt dans l'expérience sur une zone annulaire de 0.15 m autour de la sonde chauffante. Cette partie se resature très lentement à l'heure actuelle.

Dans la bentonite, la plupart des mesures d'humidité ne sont plus significatives, car le matériau est désormais trop proche de la saturation. Cependant dans la section supérieure (au Ring 9), le fait que les pressions de pore tendent à s'équilibrer avec la pression d'eau du filtre de sable indique une quasi saturation de l'argile.

Ce filtre de sable disposé entre la roche et la colonne de bentonite permet une alimentation artificielle du système en eau. Plus de la totalité de l'eau théoriquement nécessaire au remplissage du filtre et à la saturation de la bentonite a été injectée, ce qui montre que le système n'est pas hydrauliquement clos mais fuit dans l'environnement rocheux (EDZ). La pression croissante nécessaire pour maintenir le débit d'injection prouve la fragilité du système d'injection (colmatage des embouts des injecteurs).

La baisse de pression totale et la hausse de la succion observées entre le 225^{ème} et le 370^{ème} jour autour de la sonde supérieure ont été provoquées par un déficit en eau inattendu du haut du filtre de sable. Lorsque ce filtre a été de nouveau rempli, la pression totale dans la bentonite s'est rétablie et la succion s'est remise à décroître.

Abstract

TBT (Temperature Buffer Test) is a joint project between SKB/ANDRA and supported by ENRESA (modeling) and DBE (instrumentation), which aims at understanding and modeling the thermo-hydro-mechanical behavior of buffers made of swelling clay submitted to high temperatures (over 100°C) during the water saturation process.

The test is carried out in Åspö HRL in a 8 meters deep and 1.75 m diameter deposition hole, with two canisters (3 m long, 0.6 m diameter), surrounded by a MX 80 bentonite buffer and a confining plug on top anchored with 9 rods. It was installed during spring 2003. The canisters were heated with 1500 W power from day 15 to day 1171. The power was raised to 1600 W since day 1171.

This report presents data from the measurements in the Temperature Buffer Test from 030326 to 070101 (26 March 2003 to 01 January 2007).

The following measurements are made in the bentonite: Temperature is measured in 92 points, total pressure in 29 points, pore water pressure in 8 points and relative humidity in 35 points. Temperature is also measured by all gauges as an auxiliary measurement used for compensation.

The following additional measurements are done: Temperature is measured in 40 points in the rock, in 11 points on the surface of each canister and in 6 points inside each canister. The force on the confining plug is measured in 3 of the 9 rods and its vertical displacement is measured in three points. The water inflow and water pressure in the outer sand filter is also measured.

Temperature and total pressure measurements obtained in the hot parts of the system with fiber optic sensors installed by DBE are reported in Appendix B.

A general conclusion is that the measuring systems and transducers work well and almost all sensors deliver reliable values. An exception is the Relative Humidity sensors in the high temperature area around the lower canister, where sensors have failed.

The dense arrays of thermocouples at the mid-height of the two heaters appear to be useful for examining the dehydration/hydration process qualitatively. In the lower section there are clear signs of early dehydration in a 0.15 m annular zone around the heater. Resaturation of this part is now slowly in progress.

In the bentonite buffer, most humidity sensors measurements are now insignificant, the material being too close to saturation. However in the upper section (Ring 9), the fact that pore pressure start equilibrating with the water pressure in the sand slot indicates a quasi saturation of the clay material.

This sand slot set between the bentonite column and the surrounding rock is used for artificial wetting. More than the water theoretically needed to fill up the sand slot and to saturate the bentonite has already been injected, which proves that the system is not hydraulically closed but leaks towards the rock (EDZ). The high sand slot injection pressure required to maintain the inflow shows the weakness of the injection system (clogging of the filter tips).

The decrease in total pressure and increase in suction that was recorded around the upper canister from day 225 to day 370 has been caused by an unexpected lack of water supply in the upper part of the sand slot. When this slot got filled again with water, the total pressure resumed and increased and the suction decreased again.

Sammanfattning

TBT (Temperature Buffer Test) är ett gemensamt SKB/ANDRA projekt med deltagande av ENRESA (modellering) och DBE (instrumentering). Syftet är att öka förståelsen för de termiska, hydrauliska och mekaniska processerna i en buffert gjord av svällande lera som utsätts för höga temperaturer (över 100 °C) under vattenmätnadsfasen och att kunna modellera dessa processer.

Försöket görs på 420-metersnivån i Äspö HRL i ett 8 m djupt deponeringshål med diametern 1,75 m, där två kapslar, omgivande bentonitbuffert och en ovanliggande plugg, som förankrats med 9 stag, installerades våren 2003. Kapslarna värmdes med en effekt på 1500 W från dag 15 till dag 1171. Effekten på kapslarna ökades till 1600 W dag 1171.

I denna rapport presenteras data från mätningar i TBT under perioden 030326-070101.

Följande mätningar görs i bentoniten: Temperaturen mäts i 92 punkter, totaltryck i 29 punkter, porvattentryck i 8 punkter och relativa fuktigheten i 35 punkter. Temperaturen mäts även i alla relativa fuktighetsmätare, för att kompensera för temperaturens inverkan på mätresultaten.

Följande övriga mätningar görs: Temperaturen mäts i 40 punkter i berget, i 11 punkter på ytan av varje kapsel och i 6 punkter inne varje kapsel. Kraften på den ovanliggande pluggen mäts i 3 av de 9 stagen och vertikala förskjutningen av pluggen mäts i tre punkter. Vatteninflödet och vattentrycket i den yttre sandfyllda spalten mäts också.

Temperaturer och totaltryck registrerade med fiberoptiska sensorer, installerade av DBE, rapporteras i Appendix B.

En generell slutsats är att mätsystemen och givarna fungera bra och i stort sett alla givare leverar pålitliga mätvärden. Ett undantag är mätningarna av relativa fuktigheten i högtemperaturområdet runt den nedre kapseln, där ett flertal givare inte fungerar.

De tätta linjerna av termoelement vid de två värmarnas höjdcentrum visar sig vara användbara för att undersöka torkning/mätnadsprocessen kvalitativt. I den undre sektionen finns det tydliga tecken på uttorkning inom ett avstånd av 0,15 m från värmarytan. En långsam återmättnad av denna zon pågår

Resultaten från de flesta relativ fuktighetsmätarna är nu mindre signifikanta, eftersom bentonitbufferten är för nära mättnad. Portrycksgivarna i Ring 9 börjar emellertid komma i jämvikt med vattentrycket i sandfiltret, vilket indikerar att full mättnad har uppnåtts i denna del.

Sandfiltret mellan bentonitblocken och omgivande berg används för artificiell bevätning. Mer vatten än den teoretiska mängden som behövs för att mätta hela systemet har nu tillförts. Detta visar att systemet inte är hydrauliskt stängt, utan att det finns ett läckage (sannolikt ut i berget). Det injekteringstryck i sandspalten som fordras för att upprätthålla inflödet visar på en svaghet hos injekteringssystemet. Detta beror sannolikt på en igensättning av filterspetsarna.

Den sänkning av totaltrycket och höjning av buffertens *suction* som noterats runt den översta kapseln mellan dag 225 och dag 370 orsakades av en brist på vattentillgång i övre delen av sandfiltret. När sandfiltret vattenfylldes och trycksattes höjdes totaltrycket åter medan buffertens *suction* minskade.

Contents

| | | |
|-------------------|---|-----------|
| 1 | Introduction | 11 |
| 2 | Comments | 13 |
| 2.1 | General | 13 |
| 2.2 | Total pressure, Geokon (App. A, pages 49-57) | 15 |
| 2.3 | Suction, Wescore Psychrometers (App. A, pages 58-62) | 15 |
| 2.4 | Relative humidity, Vaisala and Rotronic (App. A, pages 63-68) | 15 |
| 2.5 | Pore water pressure, Geokon (App. A, pages 69-70) | 16 |
| 2.6 | Water flow and water pressure in the sand (App. A, pages 71-72) | 16 |
| 2.7 | Forces on the plug (App. A, page 73) | 16 |
| 2.8 | Displacement of the plug (App. A, page 74) | 17 |
| 2.9 | Canister power (App A, page 75-76) | 17 |
| 2.10 | Temperature in the buffer (App. A, pages 77-82) | 17 |
| 2.11 | Temperature in the rock (App. A, pages 83-86) | 18 |
| 2.12 | Temperature on the canister surface (App. A, pages 87-88) | 18 |
| 2.13 | Temperature inside the canister (App. A, pages 89-90) | 18 |
| 3 | Coordinate system | 19 |
| 4 | Location of instruments | 21 |
| 4.1 | Brief description of the instruments | 21 |
| | Measurements of temperature | 21 |
| | Measurement of total pressure in the buffer | 21 |
| | Measurement of pore water pressure in the buffer | 21 |
| | Measurement of the water saturation process | 21 |
| | Measurements of forces on the plug | 22 |
| | Measurements of plug displacement | 22 |
| | Measurement of water flow into the sand | 22 |
| 4.2 | Strategy for describing the position of each device | 22 |
| 4.3 | Position of each instrument in the bentonite | 23 |
| 4.4 | Instruments in the rock | 28 |
| | Temperature measurements | 28 |
| 4.5 | Instruments in the canister | 29 |
| 4.6 | Instruments on the plug | 31 |
| 5 | Discussion of results | 33 |
| 5.1 | General | 33 |
| 5.2 | Total inflow of water | 33 |
| 5.3 | Temperatures | 35 |
| | Thermal gradients and conductivities | 36 |
| 5.4 | Relative humidity/suction | 38 |
| 5.5 | Pore pressure | 39 |
| 5.6 | Total pressure | 40 |
| References | | 45 |
| Appendix A | | 47 |
| Appendix B | | 91 |

1 Introduction

The installation of the Temperature Buffer Test was made during spring 2003 in Äspö Hard Rock Laboratory, Sweden.

The Temperature Buffer Test, TBT, is a full-scale experiment that ANDRA and SKB carry out at the SKB Äspö Hard Rock Laboratory. In addition ENRESA supports TBT with THM modelling and DBE has installed a number of optic pressure sensors.

The test aims at understanding and modelling the thermo-hydro-mechanical behaviour of buffers made of swelling clay submitted to high temperatures (over 100°C) during the water saturation process. No other full scales tests have been carried out with buffer temperatures exceeding 100°C so far.

The test consists of a full-scale KBS3 deposition hole, 2 steel canisters equipped with electrical heaters simulating the power of radioactive decay and a mechanical plug at the top. Figure 1-1 shows the layout and denomination of blocks and canisters. The canisters are embedded in dense clay buffer consisting of blocks (cylindrical and ring shaped) of compacted bentonite powder.

An artificial water pressure is applied in the outer slot between the buffer and the rock, which is filled with compacted sand and functions as a filter.

The upper canister is surrounded by sand in order to reduce the temperature in the bentonite.

The buffer material is instrumented with pressure cells (total and water pressure), thermocouples and moisture gauges. Thermocouples are also installed in the rock.

A retaining plug is built in order to confine the buffer swelling.

Measured results and general comments concerning the collected data are given in chapter 2. A test overview with the positions of the measuring points and a brief description of the instruments are presented in chapters 3 and 4. Finally analyses and discussions of the results are given in chapter 5.

In general the data in this report are presented in diagrams covering the time period 030326 to 070101¹. The time axis in the diagrams represents days from 030326. The diagrams are attached in Appendix A.

Results regarding the fibre optic sensing system are attached in Appendix B.

¹ YYMMDD (Swedish way of expressing dates implying that the first two numbers are the year, the next two numbers are the month and the final two numbers are the date)

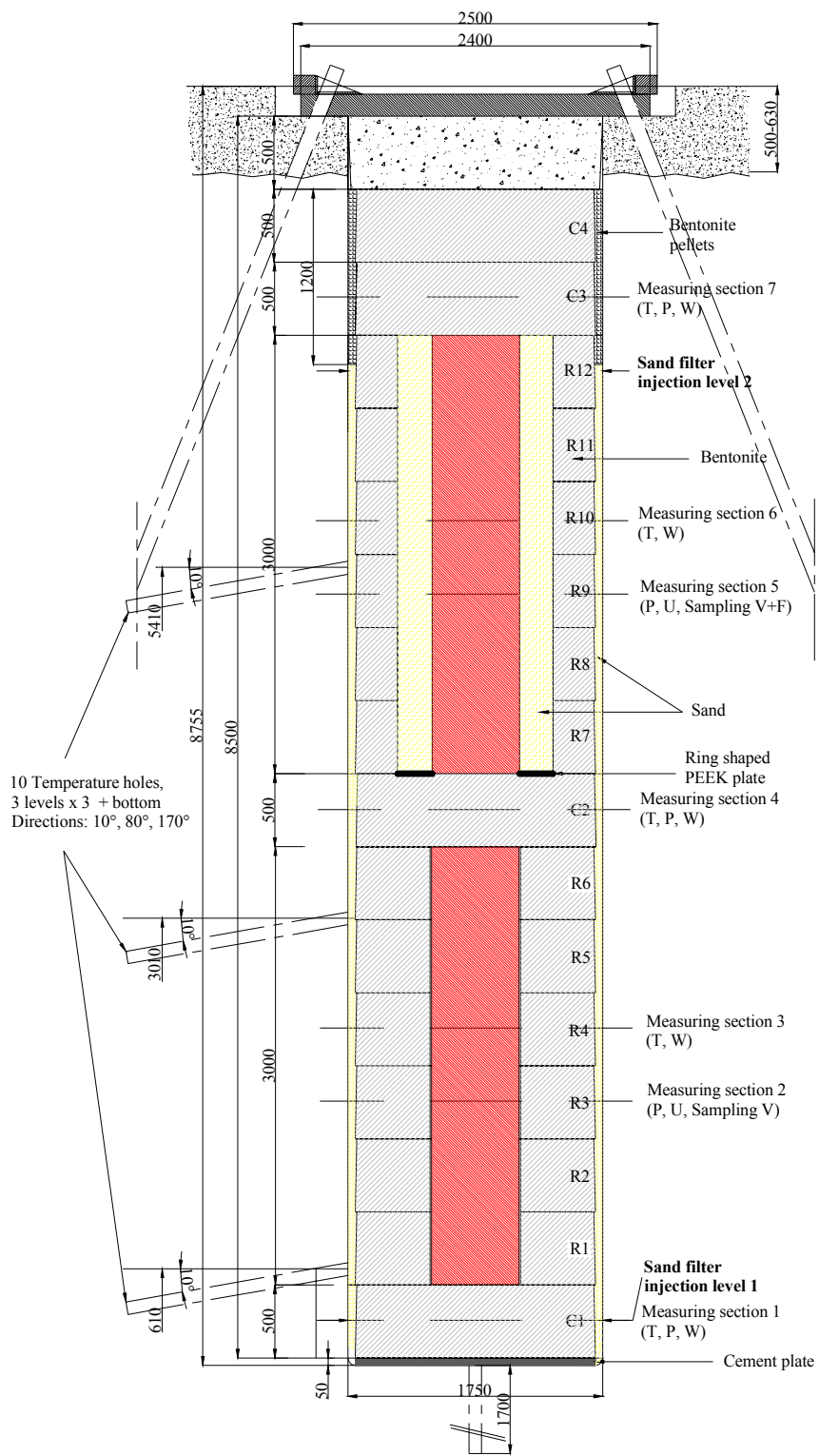


Figure 1-1. Schematic view showing the layout of the experiment and the numbering of bentonite blocks. The lower heater is denominated No. 1 and the upper heater is No. 2.

2 Comments

2.1 General

In this chapter short comments on general trends in the measurements are given. Sensors that are not delivering reliable data or no data at all are noted and comments on the data in general are given but no evaluation or comparison with predictions will be given here.

The heating of both canisters started with an initially applied constant power of 900 W on 030326. This date is also marked as start date. The power was raised to 1200 W on 030403. The power was further raised to 1500 W on 030410. Several power failures have occurred. The power was raised to 1600 W at 20060609 (day 1171).

Important events and dates are shown in Table 2-1.

Table 2-1. Key dates for TBT

| Activity | Date (time) | Day No. |
|--|---|---------|
| 900 W power applied | 030326 | 0 |
| Start water filling of filter | 030327 | 1 |
| 1200 W power applied | 030403 | 8 |
| 1500 W power applied | 030410 | 15 |
| Finished water filling | ~030604 | ~70 |
| Power failure heater 1 | 030423 (~20.00)-030424 (~10.00) | 27-28 |
| Power failure heater 1 | 030527 (~01.00)-030527 (~12.00) | 62 |
| Power failure heater 1 | 030603 (~12.00)-030603 (~14.00) | 69 |
| Power failure heater 1 | 030606 (~19.00)-030609 (~10.00) | 72-75 |
| Power failure heater 1 | 030612 (~12.00)-030612 (~14.00) | 78 |
| Power failure heaters 1 and 2 | 030923 (~12.00 ¹⁾)-030923 (~18.00 ¹⁾) | 181 |
| Power failure heaters 1 and 2 | 031028 (~18.00 ¹⁾)-031029 (~11.00 ¹⁾) | 216 |
| Injection pump replaced by gas tube | 031104 | 223 |
| Power failure heater 1 | 040120 (~16.00)-040120 (~19.00) | 300 |
| Power failure heater 2 | 040120 (~18.00)-040120 (~20.00) | 300 |
| Filling and pressurisation of the sand filter also through the upper tubes | 040406 | 377 |

| | | |
|---|---------------|---------------|
| Flushing and pressurisation of filters through both upper and lower tubes (160 kPa) | 040615-040616 | 448-449 |
| Pressurisation of filters through both upper and lower tubes | 041011-041014 | 565-568 |
| Filling and pressurisation of the sand filter through AS205 and AS207 | 041014 | 568 |
| Filling and pressurisation of the sand filter through AS201, AS202, AS204, AS205, AS206 and AS208 | 041110 | 595 |
| Power failure heater 2 50 w more power | 050629-050706 | 826- 833 |
| Filling and pressurisation of the sand filter through AS201, AS203, AS204, AS205, AS207 and AS208 | 050728 | 856 |
| Water filling of filter mats. | 051209 | 989 |
| Airvents AS212-AS215 closed. | | |
| AS209 connected to artificial saturation. | | |
| AS210 connected to artificial saturation. | 051212 | 992 |
| Back flushing of filters through both upper and lower tubes. Only AS203 is still closed. | 060517-060614 | 1148- 1176 |
| 1600 W power applied | 060609- | 1171- |
| Power failure heater 1 | 060903-060904 | 1257-1258 |

1) The duration of the power loss is not known since no data was recorded between the times noted.

The water filling was done through four tubes leading to the bottom of the sand filter. The filling was slow due to flow resistance in the sand and the rate was increased by pressurizing the water (see chapter 2.6). The filling was completed after 60-80 days. The water pressure in the bottom of the sand filter has been kept with periodical interruptions (see chapter 2.6) but the valves to the 4 upper tubes leading out water from the top of the sand filter have been open at all times until 040615.

On day 377 (040406) water was supplied to the sand filter also through the tubes leading to the top of the sand filter and a small pressure applied. On days 448-449 the filters were flushed and a water pressure of 160 kPa was applied on the sand filter through both the top tubes and the bottom tubes.

This report is the ninth one and covers the results up to 070101.

2.2 Total pressure, Geokon (App. A, pages 49-57)

The measured pressure ranges from 5.7 to 9.0 MPa. The start of the pressure increase takes place shortly after the water filling has reached the level of the different transducer.

Notable is that all transducers in ring 9 around heater 2 except the one at the rock are recording decreasing total pressure in a period between day ~230 and day ~370. The reason for this and other observations are discussed in chapter 5.

The pressure increase by sensor placed in Cyl.3 at 20051209 (day 989) due to water filling of the filter mats between Cyl.3 and Cyl.4.

Seven transducers are out of order.

2.3 Suction, Wescore Psychrometers (App. A, pages 58-62)

Wescor psychrometers are only working at suction below ~7000 kPa, which correspond to high relative humidity (higher than 95%).

Eleven transducers have started yielding interpretable values, which means that they are close to water saturation. Two of them have ceased functioning. Notable is that two transducers around heater 2 are yielding increasing suction (drying) during a period of about 80 days, which is consistent with the measured decrease in total pressure. On the other hand the suction of those transducers is again dropping in suction during the last 2 months, which is also in consistence with the total pressure observations.

WB233 placed in Cyl.3 has begun to react during this measuring period due to water injection to the mat between Cyl.3 and Cyl.4.

Two transducers (WB213 and WB220) are out of order.

2.4 Relative humidity, Vaisala and Rotronic (App. A, pages 63-68)

Relative humidity and temperature measured with Vaisala and Rotronic transducers are shown on pages 67-72. For most transducers RH starts to increase just after the filling of water has reached the sensor level. Only one sensor in the buffer shows an obvious reduction in RH, namely WB206, which is located in the high temperature zone close to the lower heater. Sensors WB221 and WB222 are located in the sand in contact with the bentonite rings 9 and 10. The high initial RH measured by WB221 may be caused by the free water in the sand that had the water content of about 1% from start.

WB206 indicate an increasing from 62% to 78% during this measuring period (from day 860).

8 of 23 sensors are presently out of order for other reasons than high degree of saturation. Four of them are placed in ring 4.

2.5 Pore water pressure, Geokon (App. A, pages 69-70)

Transducers UB208 and UB204 show pore water pressure about 0.35 MPa and 0.15 MPa at the end of this measuring period.

Transducers UB206 and UB207 have begun to increased with about 0.1 MPa in the last month.

The other water pressure sensors yield pressure close to zero.

2.6 Water flow and water pressure in the sand (App. A, pages 71-72)

Water filling and measurement of water inflow into the sand started on 030327. The total inflow to the sand has since that date been 3480 litre. The total volume of voids in the sand filter was initially about 790 litres. The inflow rate has been in average about 1.74 l/day since day 110. The inflow rate has been in average about 0.64 l/day in the last sex month.

There was also an outflow that started after completed filling since the valves from the top of the sand filter was kept open. The outflow stopped rather early and the total outflow of water has been 44 litres.

The water injection pressure upstream the filter tips is shown on page 76. The water pressure was increased to 800 – 900 kPa during the first 50 days and then kept “constant” until day ~370. However, problems with the water pump have lead to many interruptions in the applied pressure. At day 377 the water pressure was reduced in connection with the start of water supply also from the tubes leading to the top of the filter.

It should be noted that the actual water pressure in the sand filter is only measured at those injection points that are closed to the atmosphere and not pressurized, at present (2007-01-01) only point AS203.

2.7 Forces on the plug (App. A, page 73)

The forces on the plug have been measured since 030404. The total force is about 13380 kN at 070101. The influence of the additional water supply from the upper tubes after ~370 days is clearly seen.

During the first about 15 days the plug was only fixed with 3 rods. When the total force exceeded 1100 kN the rest of the 9 rods were fixed in a prescribed manner. This procedure took place 10-11 April 2003 that is 15-16 days after test start. From that time only every third anchor is measured and the results should thus be multiplied with 3. The diagram shows both the actual measurements and after multiplication with 3.

2.8 Displacement of the plug (App. A, page 74)

The three displacement gauges were placed and started to measure displacements from 030409 (day 14) (except for zero reading that was done day 0). One of them (DP201) did not work well and was replaced on 030923 with a new transducer.

Transducer DP203 did not work well during this measuring period.

The measured displacements are in good agreement with the measured forces.

2.9 Canister power (App A, page 75-76)

The heating of both canisters started with an initially applied constant power of 900 W on 030326 and was raised to 1500 W according to Table 2-1. Only one out of three heaters in each canister is presently used (RAH1 and RAH2).

The failure in one of heater (RCH2) in canister 2 caused increasing of power with 50 W on 2005-06-29 to 2005-07-05.

The power has increased to 1600 W in both canisters on 2006-06-09 (day1171).

2.10 Temperature in the buffer (App. A, pages 77-82)

Temperature is measured in a large number of points. The plotting of results is done so that the effect of wetting and cracking can be traced, since sensors placed close to each other are collected in the same diagrams.

The highest measured temperature in the bentonite is 138 °C by sensor TB215 located in the midplane of canister 1 at the distance 15 mm from the canister surface. The corresponding temperature on the canister surface is 140 °C, which shows that the temperature drop at the slot between the canister and the bentonite ring is very small.

Temperature is also measured (TB254, TB255 and TB256) in the sand around canister 2 (page 82), where the temperature drop is rather large (~2.5 °C/cm).

The increase in temperature with about one degree °C seen in the upper part of the buffer in the beginning of June (day ~435) is judged to be caused by the increase in tunnel air temperature that takes place in the summer (page 84).

On day ~335 three additional transducers (TB290, TB291 and TB292) placed in Ring 12 were connected to the data scanner and are reported on page 83. One of them was out of order from start.

The increase in temperature in the beginning of June 2006 (day ~1171) depends to increasing of power with 100 W.

9 of 92 transducers are out of order.

2.11 Temperature in the rock (App. A, pages 83-86)

The maximum temperature measured in the rock (72 degrees) is measured in the central section on the surface of the deposition hole. The deviation from axial symmetry of the temperature measured in the rock is caused by the influence from the heating of the neighbouring Canister Retrieval Test.

On October 11 (day 930) the power in Canister Retrieval Test was switched off.

2.12 Temperature on the canister surface (App. A, pages 87-88)

The maximum temperature measured on the surface of canister 1 is about 140 °C and on the surface of canister 2 about 146 °C on 070101. There are strong temperature differences in the canisters, both radial and axial. The highest measured difference on the surface is 22 °C on canister 1 and 38 °C on canister 2.

The steady increase in temperature of heater 1 has turned into a slow decrease. The temperature of heater 2 has decreased since day 50.

One sensor (TH1 SE0) has stopped to work since day 1234.

2.13 Temperature inside the canister (App. A, pages 89-90)

The maximum temperature measured inside canister 1 is about 165 °C and about 171 °C in canister 2 on 070101.

The very high value from sensor TH2 SI3 0° is not reliable before day 1080.

3 Coordinate system

Measurements are done in 7 measuring sections placed on different levels (see Figure 1-1). On each level, sensors are placed in eight main directions A, AB, B, BC, C, CD, D and DA according to Figure 3-1. Direction A and C are placed in the tunnels axial direction with A headed against the end of the tunnel i.e. almost to the South (see Figure 1-1, 3-1 and 4-1). The angle α is counted anti-clockwise from direction A. The z-coordinate is counted from the bottom of the deposition hole (the cement base).

The bentonite blocks are called cylinders and rings. The cylinders are numbered C1-C4 and the rings R1-R12 respectively (see Figure 1-1).

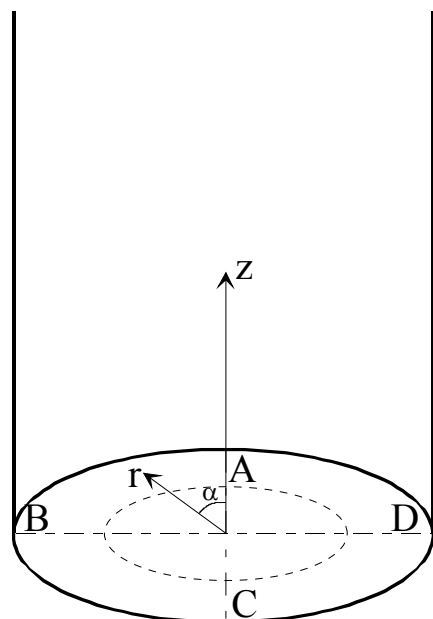


Figure 3-1. Figure describing the coordinate system used when determining the instrument positions.

4 Location of instruments

4.1 Brief description of the instruments

The different instruments that are used in the experiment are briefly described in this chapter. For additional information, see /4-1/.

Measurements of temperature

Buffer

Thermocouples from Pentronic have been installed for measuring temperature in the buffer. Measurements are done in 92 points in the test hole. In addition, temperature gauges are built in into the capacitive relative humidity sensors (23 sensors) as well as in the pressure gauges of vibrating wire type (37 gauges). Temperature is also measured in the psychrometers.

Canister

Temperature is measured in 11 points on the surface of each canister. Temperature is also measured in each canister insert in 6 points.

Rock

Temperature in the rock and on the rock surface of the hole is measured in 40 points with thermocouples from Pentronic.

Measurement of total pressure in the buffer

Total pressure is the sum of the swelling pressure and the pore water pressure. It is measured with Geokon total pressure cells with vibrating wire transducers. 29 cells of this type have been installed.

Measurement of pore water pressure in the buffer

Pore water pressure is measured with Geokon pore pressure cells with vibrating wire transducer. 8 cells of this type have been installed.

Measurement of the water saturation process

The water saturation process is recorded by measuring the relative humidity in the pore system, which can be converted into water ratio or total suction (negative water pressure). The following techniques and devices are used:

- Vaisala relative humidity sensor of capacitive type. 29 cells of this type have been installed. The measuring range is 0-100 % RH.
- Wescor psychrometers measure the dry and the wet temperature in the pore system. The measuring range is 95.5-99.6 % RH corresponding to the pore water pressure -0.5 to -6MPa. 12 cells of this type have been installed.

Measurements of forces on the plug

The force on the plug caused by the swelling pressure of the bentonite is measured in 3 of the 9 anchors. The force transducers are of the type GLÖTZL.

Measurements of plug displacement

Due to straining of the anchors the swelling pressure of the bentonite will cause not only a force on the plug but also displacement of the plug. The displacement is measured in three points with transducers of the type LVDT with the range 0 – 50 mm.

Measurement of water flow into the sand

An artificial water pressure is applied in the outer slot, which is filled with sand. Titanium tubes equipped with filter tips are placed in the sand on two levels, 250 mm and 6750 mm from bottom (four at each level).

4.2 Strategy for describing the position of each device

Every instrument is named with a unique name consisting of 1 letter describing the type of measurement, (T-Temperature, P-Total Pressure, U-Pore Pressure, W-Relative Humidity, C-Chemical sampling, D-Displacement and A-Artificial water), 1 letter describing where the measurement takes place (B-Buffer, H-Heater, S-Sand, R-Rock and P-plug), 1 figure denoting the deposition hole (1 is used for the CRT test and 2 is used for this experiment), and 2 figures specifying the position in the buffer according to a separate list (see Table 4-1 to 4-7). Every instrument position is described with three coordinates according to Figure 3-1. The r-coordinate is the horizontal distance from the centre of the hole and the z-coordinate is the height from the bottom of the hole (the block height is set to 500mm). The coordinate is the angle from the vertical direction A (almost South).

The position of each instrument is described in the legend in the diagrams according to the following strategy:

Buffer: Three positions according to Figure 3-1: ($z \setminus \alpha \setminus r$) meaning (z-coordinate in m. from the bottom \ the angle α \ the radius in m.)

The cells measuring total pressure have been installed in three different directions in order to measure the radial stress (R), the axial stress (A) and the tangential stress (T). The direction of the pressure measurement is added in Table 4-2 and in the legend for each cell.

Rock: Three positions with the following meaning: (distance in meters from the bottom \ α according to Fig 3-1 \ distance in meters from the rock surface)

The bentonite blocks are called cylinders and rings. The cylinders are numbered C1-C4 and the rings R1-R12 respectively (Figure 1-1).

Canister: The denomination of the instruments in the canister differs a little from the other instruments. At first there are two letters and one figure describing the type of measurement and the place (TH for temperature and heater) and which heater (1 for lower heater and 2 for upper). Then there are again two letters describing if it is an external or internal sensor (SE or SI) and one figure describing the position on the canister (0-4 according to Figure 4-2). Finally the angle clockwise from direction A is written.

4.3 Position of each instrument in the bentonite

Measurements are done in 7 measuring sections placed on different levels (see Figure 1-1). On each level, sensors are placed in eight main directions A, AB, B, BC, C, CD, D and DA according to Figure 4-1. The bentonite blocks are called cylinders and rings. The cylinders are numbered C1-C4 and the rings R1-R12 respectively (see Figure 1-1).

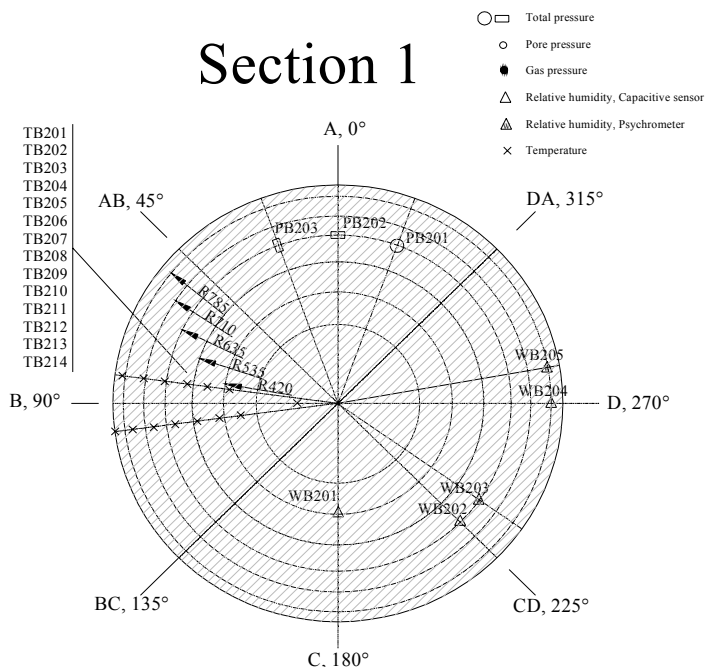


Figure 4-1. Schematic view, showing the main directions of the instrument positioning. The drawing shows the instrumentation in measuring section 1.

An overview of the positions of the instruments is shown in Fig 1-1 and 4-1. Exact positions are described in Tables 4-1 to 4-6. These tables have been updated since the last report and the measured exact position of the transducers have been inserted.

The instruments are located in three main levels in each instrumented block, the surface of the block (only total pressure cells measuring the horizontal pressure) and 50 mm and 250 mm from the upper block surface. The thermocouples and the total pressure cells are placed in the 50 mm level by practical reasons and the other sensors in the 250 mm level.

Table 4-1. Numbering and position of instruments for measuring temperature (T)

| Type and number | Measuring section | Block | Instrument position in block | | | | Instrument Fabricate |
|-----------------|-------------------|--------|------------------------------|--------------------|--------|--------|----------------------|
| | | | Direction | α degree | r m | Z m | |
| TB201 | 1 | Cyl. 1 | B | 90 | 0,150 | 0,452 | Pentronic |
| TB202 | 1 | Cyl. 1 | B | 95 | 0,360 | 0,452 | Pentronic |
| TB203 | 1 | Cyl. 1 | B | 85 | 0,400 | 0,452 | Pentronic |
| TB204 | 1 | Cyl. 1 | B | 95 | 0,440 | 0,452 | Pentronic |
| TB205 | 1 | Cyl. 1 | B | 85 | 0,480 | 0,452 | Pentronic |
| TB206 | 1 | Cyl. 1 | B | 95 | 0,520 | 0,452 | Pentronic |
| TB207 | 1 | Cyl. 1 | B | 85 | 0,560 | 0,452 | Pentronic |
| TB208 | 1 | Cyl. 1 | B | 95 | 0,600 | 0,452 | Pentronic |
| TB209 | 1 | Cyl. 1 | B | 85 | 0,640 | 0,452 | Pentronic |
| TB210 | 1 | Cyl. 1 | B | 95 | 0,680 | 0,452 | Pentronic |
| TB211 | 1 | Cyl. 1 | B | 85 | 0,720 | 0,452 | Pentronic |
| TB212 | 1 | Cyl. 1 | B | 95 | 0,760 | 0,452 | Pentronic |
| TB213 | 1 | Cyl. 1 | B | 85 | 0,800 | 0,452 | Pentronic |
| TB214 | 1 | Cyl. 1 | B | 95 | 0,840 | 0,452 | Pentronic |
| TB215 | 3 | Ring 4 | B | 97,5 | 0,320 | 2,469 | Pentronic |
| TB216 | 3 | Ring 4 | B | 82,5 | 0,360 | 2,469 | Pentronic |
| TB217 | 3 | Ring 4 | B | 97,5 | 0,390 | 2,469 | Pentronic |
| TB218 | 3 | Ring 4 | B | 92,5 | 0,420 | 2,469 | Pentronic |
| TB219 | 3 | Ring 4 | B | 87,5 | 0,435 | 2,469 | Pentronic |
| TB220 | 3 | Ring 4 | B | 82,5 | 0,450 | 2,469 | Pentronic |
| TB221 | 3 | Ring 4 | B | 97,5 | 0,465 | 2,469 | Pentronic |
| TB222 | 3 | Ring 4 | B | 92,5 | 0,480 | 2,469 | Pentronic |
| TB223 | 3 | Ring 4 | B | 87,5 | 0,495 | 2,469 | Pentronic |
| TB224 | 3 | Ring 4 | B | 82,5 | 0,510 | 2,469 | Pentronic |
| TB225 | 3 | Ring 4 | B | 97,5 | 0,525 | 2,469 | Pentronic |
| TB226 | 3 | Ring 4 | B | 92,5 | 0,540 | 2,469 | Pentronic |
| TB227 | 3 | Ring 4 | B | 87,5 | 0,555 | 2,469 | Pentronic |
| TB228 | 3 | Ring 4 | B | 82,5 | 0,570 | 2,469 | Pentronic |
| TB229 | 3 | Ring 4 | B | 97,5 | 0,585 | 2,469 | Pentronic |
| TB230 | 3 | Ring 4 | B | 92,5 | 0,600 | 2,469 | Pentronic |
| TB231 | 3 | Ring 4 | B | 87,5 | 0,615 | 2,469 | Pentronic |
| TB232 | 3 | Ring 4 | B | 82,5 | 0,630 | 2,469 | Pentronic |
| TB233 | 3 | Ring 4 | B | 97,5 | 0,645 | 2,469 | Pentronic |
| TB234 | 3 | Ring 4 | B | 92,5 | 0,660 | 2,469 | Pentronic |
| TB235 | 3 | Ring 4 | B | 87,5 | 0,690 | 2,469 | Pentronic |
| TB236 | 3 | Ring 4 | B | 92,5 | 0,720 | 2,469 | Pentronic |
| TB237 | 3 | Ring 4 | B | 87,5 | 0,750 | 2,469 | Pentronic |
| TB238 | 3 | Ring 4 | B | 92,5 | 0,780 | 2,469 | Pentronic |
| TB239 | 3 | Ring 4 | B | 87,5 | 0,810 | 2,469 | Pentronic |
| TB240 | 4 | Cyl. 2 | B | 90 | 0,150 | 3,983 | Pentronic |
| TB241 | 4 | Cyl. 2 | B | 95 | 0,360 | 3,983 | Pentronic |
| TB242 | 4 | Cyl. 2 | B | 85 | 0,400 | 3,983 | Pentronic |
| TB243 | 4 | Cyl. 2 | B | 95 | 0,440 | 3,983 | Pentronic |
| TB244 | 4 | Cyl. 2 | B | 85 | 0,480 | 3,983 | Pentronic |
| TB245 | 4 | Cyl. 2 | B | 95 | 0,520 | 3,983 | Pentronic |

| Type and number | Measuring section | Block | Instrument position in block | | | Instrument Fabricate | |
|-----------------|-------------------|---------|------------------------------|----------|-------|----------------------|-----------|
| | | | Direction | α | r | | |
| | | | degree | m | m | | |
| TB246 | 4 | Cyl. 2 | B | 85 | 0,560 | 3,983 | Pentronic |
| TB247 | 4 | Cyl. 2 | B | 95 | 0,600 | 3,983 | Pentronic |
| TB248 | 4 | Cyl. 2 | B | 85 | 0,640 | 3,983 | Pentronic |
| TB249 | 4 | Cyl. 2 | B | 95 | 0,680 | 3,983 | Pentronic |
| TB250 | 4 | Cyl. 2 | B | 85 | 0,720 | 3,983 | Pentronic |
| TB251 | 4 | Cyl. 2 | B | 95 | 0,760 | 3,983 | Pentronic |
| TB252 | 4 | Cyl. 2 | B | 85 | 0,800 | 3,983 | Pentronic |
| TB253 | 4 | Cyl. 2 | B | 95 | 0,825 | 3,983 | Pentronic |
| TB254 | 6 | Ring 10 | B | 90 | 0,343 | 6,056 | Pentronic |
| TB255 | 6 | Ring 10 | B | 90 | 0,400 | 6,056 | Pentronic |
| TB256 | 6 | Ring 10 | B | 90 | 0,463 | 6,056 | Pentronic |
| TB257 | 6 | Ring 10 | B | 97,5 | 0,540 | 6,006 | Pentronic |
| TB258 | 6 | Ring 10 | B | 92,5 | 0,555 | 6,006 | Pentronic |
| TB259 | 6 | Ring 10 | B | 87,5 | 0,570 | 6,006 | Pentronic |
| TB260 | 6 | Ring 10 | B | 82,5 | 0,585 | 6,006 | Pentronic |
| TB261 | 6 | Ring 10 | B | 97,5 | 0,600 | 6,006 | Pentronic |
| TB262 | 6 | Ring 10 | B | 92,5 | 0,615 | 6,006 | Pentronic |
| TB263 | 6 | Ring 10 | B | 87,5 | 0,630 | 6,006 | Pentronic |
| TB264 | 6 | Ring 10 | B | 82,5 | 0,645 | 6,006 | Pentronic |
| TB265 | 6 | Ring 10 | B | 97,5 | 0,660 | 6,006 | Pentronic |
| TB266 | 6 | Ring 10 | B | 92,5 | 0,675 | 6,006 | Pentronic |
| TB267 | 6 | Ring 10 | B | 87,5 | 0,690 | 6,006 | Pentronic |
| TB268 | 6 | Ring 10 | B | 82,5 | 0,705 | 6,006 | Pentronic |
| TB269 | 6 | Ring 10 | B | 97,5 | 0,720 | 6,006 | Pentronic |
| TB270 | 6 | Ring 10 | B | 92,5 | 0,735 | 6,006 | Pentronic |
| TB271 | 6 | Ring 10 | B | 87,5 | 0,750 | 6,006 | Pentronic |
| TB272 | 6 | Ring 10 | B | 82,5 | 0,765 | 6,006 | Pentronic |
| TB273 | 6 | Ring 10 | B | 97,5 | 0,780 | 6,006 | Pentronic |
| TB274 | 6 | Ring 10 | B | 92,5 | 0,795 | 6,006 | Pentronic |
| TB275 | 6 | Ring 10 | B | 87,5 | 0,810 | 6,006 | Pentronic |
| TB276 | 7 | Cyl. 3 | B | 90 | 0,150 | 7,524 | Pentronic |
| TB277 | 7 | Cyl. 3 | B | 95 | 0,360 | 7,524 | Pentronic |
| TB278 | 7 | Cyl. 3 | B | 85 | 0,400 | 7,524 | Pentronic |
| TB279 | 7 | Cyl. 3 | B | 95 | 0,440 | 7,524 | Pentronic |
| TB280 | 7 | Cyl. 3 | B | 85 | 0,480 | 7,524 | Pentronic |
| TB281 | 7 | Cyl. 3 | B | 95 | 0,520 | 7,524 | Pentronic |
| TB282 | 7 | Cyl. 3 | B | 85 | 0,560 | 7,524 | Pentronic |
| TB283 | 7 | Cyl. 3 | B | 95 | 0,600 | 7,524 | Pentronic |
| TB284 | 7 | Cyl. 3 | B | 85 | 0,640 | 7,524 | Pentronic |
| TB285 | 7 | Cyl. 3 | B | 95 | 0,680 | 7,524 | Pentronic |
| TB286 | 7 | Cyl. 3 | B | 85 | 0,720 | 7,524 | Pentronic |
| TB287 | 7 | Cyl. 3 | B | 95 | 0,760 | 7,524 | Pentronic |
| TB288 | 7 | Cyl. 3 | B | 85 | 0,800 | 7,524 | Pentronic |
| TB289 | 7 | Cyl. 3 | B | 95 | 0,825 | 7,524 | Pentronic |
| TB290 | | Ring 12 | B | 90 | 0,360 | 6,881 | Pentronic |
| TB291 | | Ring 12 | B | 90 | 0,420 | 6,881 | Pentronic |
| TB292 | | Ring 12 | B | 90 | 0,480 | 6,881 | Pentronic |

Table 4-2. Numbering and position of instruments measuring total pressure (P)

| Type and number | Measuring section | Block | Instrument position in block | | | | Instrument Fabricate | Direction of pressure measurement |
|-----------------|-------------------|--------|------------------------------|----------|-------|-------|----------------------|-----------------------------------|
| | | | Direction | α | r | z | | |
| | | | | degree | m | m | | |
| PB201 | 1 | Cyl. 1 | A | 340 | 0,635 | 0,502 | Geokon | Axial |
| PB202 | 1 | Cyl. 1 | A | 0 | 0,635 | 0,452 | Geokon | Radial |
| PB203 | 1 | Cyl. 1 | A | 20 | 0,635 | 0,452 | Geokon | Tangential |
| PB204 | 2 | R3 | D | 250 | 0,420 | 1,968 | Geokon | Radial |
| PB205 | 2 | R3 | D | 290 | 0,420 | 2,018 | Geokon | Axial |
| PB206 | 2 | R3 | A | 8 | 0,535 | 1,968 | Geokon | Radial |
| PB207 | 2 | R3 | A | 20 | 0,535 | 1,968 | Geokon | Tangential |
| PB208 | 2 | R3 | AB | 45 | 0,585 | 2,018 | Geokon | Axial |
| PB209 | 2 | R3 | B | 100 | 0,635 | 1,968 | Geokon | Tangential |
| PB210 | 2 | R3 | C | 170 | 0,710 | 1,968 | Geokon | Tangential |
| PB211 | 2 | R3 | C | 180 | 0,710 | 1,968 | Geokon | Radial |
| PB212 | 2 | R3 | D | 260 | 0,748 | 2,018 | Geokon | Axial |
| PB213 | 2 | R3 | D | 270 | 0,875 | 1,950 | Geokon | Radial on rock |
| PB214 | 4 | Cyl. 2 | A | 340 | 0,635 | 4,033 | Geokon | Axial |
| PB215 | 4 | Cyl. 2 | A | 0 | 0,635 | 3,983 | Geokon | Radial |
| PB216 | 4 | Cyl. 2 | A | 20 | 0,635 | 3,983 | Geokon | Tangential |
| PB217 | 5 | Ring 9 | D | 270 | 0,535 | 5,319 | Geokon | Radial,against sand |
| PB218 | 5 | Ring 9 | A | 340 | 0,635 | 5,554 | Geokon | Axial |
| PB219 | 5 | Ring 9 | A | 0 | 0,635 | 5,504 | Geokon | Radial |
| PB220 | 5 | Ring 9 | A | 20 | 0,635 | 5,504 | Geokon | Tangential |
| PB221 | 5 | Ring 9 | B | 70 | 0,710 | 5,554 | Geokon | Axial |
| PB222 | 5 | Ring 9 | B | 110 | 0,710 | 5,504 | Geokon | Radial |
| PB223 | 5 | Ring 9 | C | 160 | 0,745 | 5,554 | Geokon | Axial |
| PB224 | 5 | Ring 9 | C | 180 | 0,770 | 5,504 | Geokon | Radial |
| PB225 | 5 | Ring 9 | C | 200 | 0,740 | 5,504 | Geokon | Tangential |
| PB226 | 5 | Ring 9 | D | 270 | 0,875 | 5,450 | Geokon | Radial on rock |
| PB227 | 7 | Cyl. 3 | A | 340 | 0,635 | 7,574 | Geokon | Axial |
| PB228 | 7 | Cyl. 3 | A | 0 | 0,635 | 7,524 | Geokon | Radial |
| PB229 | 7 | Cyl. 3 | A | 20 | 0,635 | 7,524 | Geokon | Tangential |
| PB230 | 2 | R3 | C | 180 | 0,315 | 1,968 | DBE | Radial |
| PB231 | 5 | R9 | C | 180 | 0,535 | 5,504 | DBE | Radial |

Table 4-3. Numbering and position of instruments measuring pore pressure (U)

| Type and number | Measuring section | Block | Instrument position in block | | | | Instrument Fabricate | Remark |
|-----------------|-------------------|--------|------------------------------|----------|-------|-------|----------------------|---------|
| | | | Direction | α | r | z | | |
| | | | | degree | m | m | | |
| UB201 | 2 | Ring 3 | D | 270 | 0,420 | 1,768 | Geokon | |
| UB202 | 2 | Ring 3 | A | 350 | 0,535 | 1,768 | Geokon | |
| UB203 | 2 | Ring 3 | B | 90 | 0,635 | 1,768 | Geokon | |
| UB204 | 2 | Ring 3 | D | 280 | 0,785 | 1,768 | Geokon | |
| US205 | 5 | Ring 9 | D | 270 | 0,510 | 5,304 | Geokon | In sand |
| UB206 | 5 | Ring 9 | DA | 315 | 0,635 | 5,304 | Geokon | |
| UB207 | 5 | Ring 9 | B | 90 | 0,710 | 5,304 | Geokon | |
| UB208 | 5 | Ring 9 | CD | 225 | 0,785 | 5,304 | Geokon | |
| UB209 | 2 | Ring 3 | C | 200 | 0,315 | 1,968 | DBE | |
| UB210 | 5 | Ring 9 | C | 150 | 0,510 | 5,304 | DBE | |

Table 4-4. Numbering and position of instruments measuring water content (W)

| Type and number | Measuring section | Block | Instrument position in block | | | | Instrument Fabricate | Remark |
|-----------------|-------------------|---------|------------------------------|--------------------|--------|--------|----------------------|---------|
| | | | Direction | α degree | r m | Z m | | |
| WB201 | 1 | Cyl.1 | C | 180 | 0,420 | 0,252 | Rotronic | |
| WB202 | 1 | Cyl.1 | CD | 225 | 0,635 | 0,252 | Vaisala | |
| WB203 | 1 | Cyl.1 | CD | 235 | 0,635 | 0,252 | Wescor | |
| WB204 | 1 | Cyl.1 | D | 270 | 0,785 | 0,252 | Rotronic | |
| WB205 | 1 | Cyl.1 | D | 280 | 0,785 | 0,252 | Wescor | |
| WB206 | 3 | Ring 4 | BC | 135 | 0,360 | 2,269 | Vaisala | |
| WB207 | 3 | Ring 4 | C | 180 | 0,420 | 2,269 | Rotronic | |
| WB208 | 3 | Ring 4 | CD | 225 | 0,485 | 2,269 | Vaisala | |
| WB209 | 3 | Ring 4 | D | 270 | 0,560 | 2,269 | Rotronic | |
| WB210 | 3 | Ring 4 | DA | 315 | 0,635 | 2,269 | Vaisala | |
| WB211 | 3 | Ring 4 | DA | 325 | 0,635 | 2,269 | Wescor | |
| WB212 | 3 | Ring 4 | A | 0 | 0,710 | 2,269 | Rotronic | |
| WB213 | 3 | Ring 4 | A | 10 | 0,710 | 2,269 | Wescor | |
| WB214 | 3 | Ring 4 | AB | 45 | 0,785 | 2,269 | Vaisala | |
| WB215 | 3 | Ring 4 | AB | 55 | 0,785 | 2,269 | Wescor | |
| WB216 | 4 | Cyl.2 | C | 180 | 0,420 | 3,783 | Rotronic | |
| WB217 | 4 | Cyl.2 | CD | 225 | 0,635 | 3,783 | Vaisala | |
| WB218 | 4 | Cyl.2 | CD | 235 | 0,635 | 3,783 | Wescor | |
| WB219 | 4 | Cyl.2 | D | 270 | 0,785 | 3,783 | Rotronic | |
| WB220 | 4 | Cyl.2 | D | 280 | 0,785 | 3,783 | Wescor | |
| WS221 | 5 | Ring 9 | BC | 135 | 0,525 | 5,304 | Vaisala | In sand |
| WS222 | 6 | Ring 10 | BC | 135 | 0,525 | 5,806 | Vaisala | In sand |
| WB223 | 6 | Ring 10 | C | 180 | 0,585 | 5,806 | Rotronic | |
| WB224 | 6 | Ring 10 | CD | 225 | 0,635 | 5,806 | Vaisala | |
| WB225 | 6 | Ring 10 | D | 270 | 0,685 | 5,806 | Rotronic | |
| WB226 | 6 | Ring 10 | D | 280 | 0,685 | 5,806 | Wescor | |
| WB227 | 6 | Ring 10 | DA | 315 | 0,735 | 5,806 | Vaisala | |
| WB228 | 6 | Ring 10 | DA | 325 | 0,735 | 5,806 | Wescor | |
| WB229 | 6 | Ring 10 | A | 0 | 0,785 | 5,806 | Rotronic | |
| WB230 | 6 | Ring 10 | A | 10 | 0,785 | 5,806 | Wescor | |
| WB231 | 7 | Cyl.3 | C | 180 | 0,420 | 7,374 | Rotronic | |
| WB232 | 7 | Cyl.3 | CD | 225 | 0,635 | 7,374 | Vaisala | |
| WB233 | 7 | Cyl.3 | CD | 235 | 0,635 | 7,374 | Wescor | |
| WB234 | 7 | Cyl.3 | D | 270 | 0,785 | 7,374 | Rotronic | |
| WB235 | 7 | Cyl.3 | D | 280 | 0,785 | 7,374 | Wescor | |

4.4 Instruments in the rock

Temperature measurements

40 thermocouples are located in ten boreholes in the rock (see Figure 1-1). The depth of each borehole is 1.5 m. In each borehole 4 thermocouples are placed at different distances from the rock surface. Observe that the coordinate system does not count the radius but the radial distance from the rock surface of the deposition hole. The position of each instrument is described in Table 4-5.

Table 4-5. Numbering and positions of thermocouples in the rock

| Mark | Level | Direction | Distance from rock surface | Instrument Fabricate |
|-------|-------|-----------|----------------------------|-------------------------|
| | m | degree | m | |
| TR201 | 0 | Center | 0,000 | Pentronic |
| TR202 | 0 | Center | 0,375 | Pentronic |
| TR203 | 0 | Center | 0,750 | Pentronic |
| TR204 | 0 | Center | 1,500 | Pentronic |
| TR205 | 0,61 | 10° | 0,000 | Pentronic |
| TR206 | 0,61 | 10° | 0,375 | Pentronic |
| TR207 | 0,61 | 10° | 0,750 | Pentronic |
| TR208 | 0,61 | 10° | 1,500 | Pentronic |
| TR209 | 0,61 | 80° | 0,000 | Pentronic |
| TR210 | 0,61 | 80° | 0,375 | Pentronic |
| TR211 | 0,61 | 80° | 0,750 | Pentronic |
| TR212 | 0,61 | 80° | 1,500 | Pentronic |
| TR213 | 0,61 | 170° | 0,000 | Pentronic |
| TR214 | 0,61 | 170° | 0,375 | Pentronic |
| TR215 | 0,61 | 170° | 0,750 | Pentronic |
| TR216 | 0,61 | 170° | 1,500 | Pentronic |
| TR217 | 3,01 | 10° | 0,000 | Pentronic |
| TR218 | 3,01 | 10° | 0,375 | Pentronic |
| TR219 | 3,01 | 10° | 0,750 | Pentronic |
| TR220 | 3,01 | 10° | 1,500 | Pentronic |
| TR221 | 3,01 | 80° | 0,000 | Pentronic |
| TR222 | 3,01 | 80° | 0,375 | Pentronic |
| TR223 | 3,01 | 80° | 0,750 | Pentronic |
| TR224 | 3,01 | 80° | 1,500 | Pentronic |
| TR225 | 3,01 | 170° | 0,000 | Pentronic |
| TR226 | 3,01 | 170° | 0,375 | Pentronic |
| TR227 | 3,01 | 170° | 0,750 | Pentronic |
| TR228 | 3,01 | 170° | 1,500 | Pentronic |
| TR229 | 5,41 | 10° | 0,000 | Pentronic |
| TR230 | 5,41 | 10° | 0,375 | Pentronic |
| TR231 | 5,41 | 10° | 0,750 | Pentronic |
| TR232 | 5,41 | 10° | 1,500 | Pentronic |
| TR233 | 5,41 | 80° | 0,000 | Pentronic |
| TR234 | 5,41 | 80° | 0,375 | Pentronic |
| TR235 | 5,41 | 80° | 0,750 | Pentronic |
| TR236 | 5,41 | 80° | 1,500 | Pentronic |
| TR237 | 5,41 | 170° | 0,000 | Pentronic |
| TR238 | 5,41 | 170° | 0,375 | Pentronic |
| TR239 | 5,41 | 170° | 0,750 | Pentronic |
| TR240 | 5,41 | 170° | 1,500 | Pentronic |

4.5 Instruments in the canister

Temperature is measured both on the canister surface and inside the canister /4-2/. Eleven thermocouples are installed on each canisters surface. Three groups of three thermocouples are installed 100 mm from each heater end, and in the middle of the heater, with a distribution of 120°. Two additional thermocouples are installed in the centre of the bottom lid and the top cover. Temperature inside the canister insert is measured at 6 points with thermocouples.

Figure 4-2 shows how these thermocouples are placed (see also chapter 4.2). Table 4-6 and 4-7 show the positions.

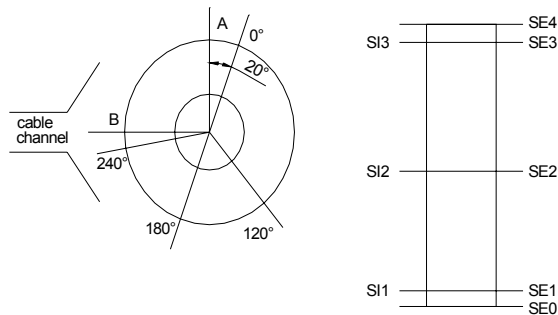
Table 4-6. Numbering and position of instruments for measuring the temperature on the heaters surface (T)

| Type and number | Heater | Instruments coordinates | | | | Instrument Fabricate | Remark |
|-----------------|--------|-------------------------|-------------|--------|--------|-------------------------|--------|
| | | Position | α degree | r m | z m | | |
| TH1 SE0 | 1 | Bottom | 0 | 0,000 | 0,500 | | |
| TH1 SE1 0° | 1 | Lower sec. | 0 | 0,305 | 0,600 | | |
| TH1 SE1 240° | 1 | Lower sec. | 240 | 0,305 | 0,600 | | |
| TH1 SE1 120° | 1 | Lower sec. | 120 | 0,305 | 0,600 | | |
| TH1 SE2 0° | 1 | Middle sec. | 0 | 0,305 | 2,000 | | |
| TH1 SE2 240° | 1 | Middle sec. | 240 | 0,305 | 2,000 | | |
| TH1 SE2 120° | 1 | Middle sec. | 120 | 0,305 | 2,000 | | |
| TH1 SE3 0° | 1 | Upper sec. | 0 | 0,305 | 3,400 | | |
| TH1 SE3 240° | 1 | Upper sec. | 240 | 0,305 | 3,400 | | |
| TH1 SE3 120° | 1 | Upper sec. | 120 | 0,305 | 3,400 | | |
| TH1 SE4 | 1 | Top | 0 | 0,000 | 3,500 | | |
| TH2 SE0 | 2 | Bottom | 0 | 0,000 | 4,000 | | |
| TH2 SE1 0° | 2 | Lower sec. | 0 | 0,305 | 4,100 | | |
| TH2 SE1 240° | 2 | Lower sec. | 240 | 0,305 | 4,100 | | |
| TH2 SE1 120° | 2 | Lower sec. | 120 | 0,305 | 4,100 | | |
| TH2 SE2 0° | 2 | Middle sec. | 0 | 0,305 | 5,500 | | |
| TH2 SE2 240° | 2 | Middle sec. | 240 | 0,305 | 5,500 | | |
| TH2 SE2 120° | 2 | Middle sec. | 120 | 0,305 | 5,500 | | |
| TH2 SE3 0° | 2 | Upper sec. | 0 | 0,305 | 6,900 | | |
| TH2 SE3 240° | 2 | Upper sec. | 240 | 0,305 | 6,900 | | |
| TH2 SE3 120° | 2 | Upper sec. | 120 | 0,305 | 6,900 | | |
| TH2 SE4 | 2 | Top | 0 | 0,000 | 7,000 | | |

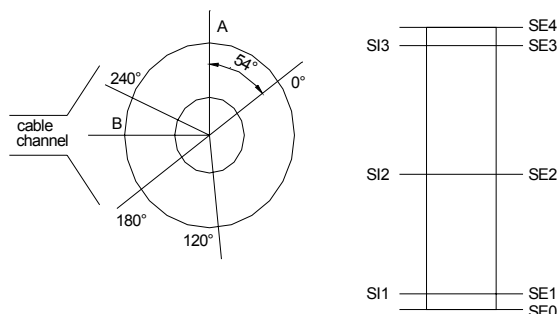
Table 4-7. Numbering and position of instruments for measuring the temperature inside the heaters (T)

| Type and number | Heater | Instruments coordinates | | | Instrument Fabricate | Remark |
|-----------------|--------|-------------------------|--------------------|--------|-------------------------|--------|
| | | Position | α degree | Z m | | |
| TH1 SI1 0° | 1 | Lower sec. | 0 | 0,60 | | |
| TH1 SI1 180° | 1 | Lower sec. | 180 | 0,60 | | |
| TH1 SI2 0° | 1 | Middle sec. | 0 | 2,00 | | |
| TH1 SI2 180° | 1 | Middle sec. | 180 | 2,00 | | |
| TH1 SI3 0° | 1 | Upper sec. | 0 | 3,40 | | |
| TH1 SI3 180° | 1 | Upper sec. | 180 | 3,40 | | |
| TH2 SI1 0° | 2 | Lower sec. | 0 | 0,60 | | |
| TH2 SI1 180° | 2 | Lower sec. | 180 | 0,60 | | |
| TH2 SI2 0° | 2 | Middle sec. | 0 | 2,00 | | |
| TH2 SI2 180° | 2 | Middle sec. | 180 | 2,00 | | |
| TH2 SI3 0° | 2 | Upper sec. | 0 | 3,40 | | |
| TH2 SI3 180° | 2 | Upper sec. | 180 | 3,40 | | |

Heater 2



Heater 1



Figur 4-2. Location of thermocouples inside (SI) and on (SE) the canisters.

4.6 Instruments on the plug

Three force transducers and three displacement transducers have been placed on the plug to measure the force of the anchors and the displacement of the plug. The location of these transducers can be described in relation to Fig 4-3, which shows a schematic view of the plug with the slots, rods and cables.

The rods are numbered 1-9 anti-clockwise and number 1 is the northern rod 18 degrees from direction A. The force transducers are placed on rods 3, 6, and 9. The displacement transducers are placed between the rods on the steel ring in the periphery of the plug. They are fixed on the rock surface and measure thus the displacement relative to the rock.

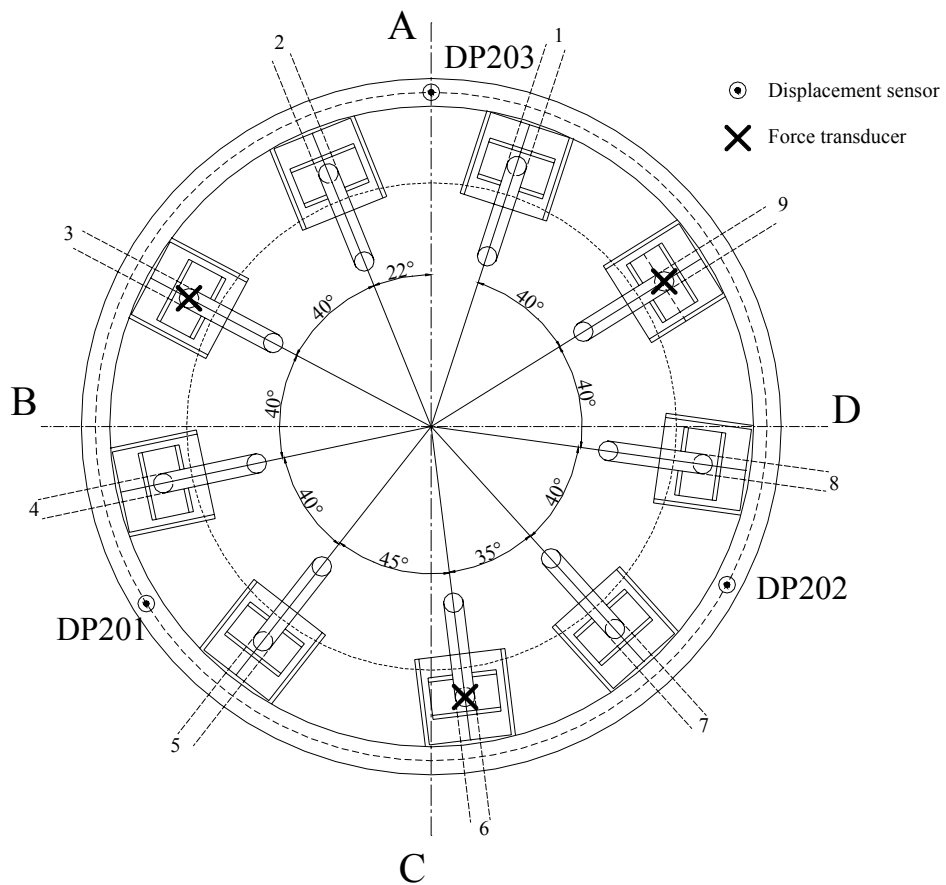


Figure 4-3. Schematic view showing the positions of the rods and the displacement and force transducers on the retaining plug.

5 Discussion of results

5.1 General

The aim of this chapter is two-parted: (i) to give an updated interpretation of the project as a whole; and (ii) to highlight the latest developments. More detailed discussions of earlier results can be found in previous data reports.

5.2 Total inflow of water

The total injected water volume is shown in (App.A\page 71) and was 3.5 m^3 at January 1, 2007. Table 5-1 shows the pore space available at the beginning of the test. The calculated available pore volume has thereby been exceeded with 0.8 m^3 . This discrepancy appears to be caused by a water leakage, possibly into the rock. This is elaborated below.

The inflow has varied significantly during the test period. During the first 75 days the inflow was about 15 l/d , while it dropped to about 1.3 l/d during the subsequent 250 days. On average during the test period, the flow rate was slightly below 2.5 l/d .

Two major events can be noticed in the applied scheme for pressurization (Table 5-2):

- During the first 377 days, the sand filter was only pressurized through the lower injection points, while the upper were open to the atmosphere. After this day, upper injection points have also been pressurized while none of the injection points has been open to the atmosphere.
- The second event was the installation of equipment for measuring pressure at each injection point at October 8, 2004 (day 562) (see Figure 5-1.). Since then, at least one out of eight injection points have been closed and used for monitoring of the actual pressure in the sand filter.

Table 5-1. TBT Pore space

| | Available at test start [m^3] | |
|----------------------------|--|------|
| Sand filter | 0.77 | |
| Pellets filling | 0.24 | 1.38 |
| Bentonite | 1.08 | |
| Heater/bentonite clearance | 0.06 | |
| Sand shield | 0.55 | |
| Total | 2.70 | |

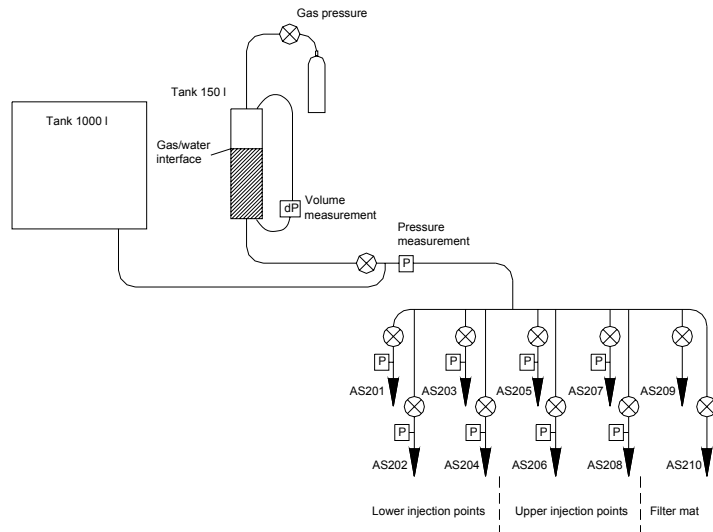


Figure 5-1. Schematic view of injection system.

Table 5-2. Injection point pressurization scheme (values are relative pressures). The actual water pressure in the sand filter is only measured at those points that are closed

| Intervals | Lower injection points | | | | Upper injection points | | | | Filter mat | | P (bar) | |
|------------------------------------|-----------------------------------|-----|-----|-----|------------------------|-----|-----|-----|------------|-----|------------|--|
| | 201 | 202 | 203 | 204 | 205 | 206 | 207 | 208 | 209 | 210 | | |
| 030326 – 040406 Day 0 - 377 | O | O | O | O | ⊕ | ⊕ | ⊕ | ⊕ | ⊗ | ⊗ | 7 | |
| 040406 – 040615 Day 377 - 447 | O | O | O | O | O | O | O | O | ⊗ | ⊗ | 0 | |
| 040615 – 040616 Day 447 - 448 | Hydraulic test I | | | | | | | | | | | |
| 040616 – 041008 Day 448 – 562 | O | O | O | O | O | O | O | O | ⊗ | ⊗ | 1.5 | |
| 041008 – 041014 Day 562 - 568 | Hydraulic test II | | | | | | | | | | | |
| 041014 – 041110 Day 568 - 595 | ⊗ | ⊗ | ⊗ | ⊗ | O | ⊗ | O | ⊗ | ⊗ | ⊗ | 5 | |
| 041110 – 050728 Day 595 - 856 | O | O | ⊗ | O | O | O | ⊗ | O | ⊗ | ⊗ | 5 | |
| 050728 – 051209 Day 856 - 989 | O | ⊗ | O | O | O | ⊗ | O | O | ⊗ | ⊗ | 5 | |
| 051209 – 051212 Day 989 - 992 | O | ⊗ | O | O | O | ⊗ | O | O | O | ⊗ | 5 | |
| 051212 – 060517 Day 992 – 1148 | O | ⊗ | O | O | O | ⊗ | O | O | O | O | 5 | |
| 060517 – 060614 Day 1148 - 1176 | Back flushing of injection points | | | | | | | | | | | |
| 060614 – 060807 Day 1176 – 1230 | O | O | ⊗ | O | O | O | O | O | O | O | 5 | |
| 060807 – 060811 Day 1230 – 1234 | Increase of injection pressure | | | | | | | | | | | |
| 060811 – 070101 Day 1234 - 1377 | O | O | ⊗ | O | O | O | O | O | O | O | 9 | |

O = Open and pressurized

⊕ = Open to atmosphere

⊗ = Closed

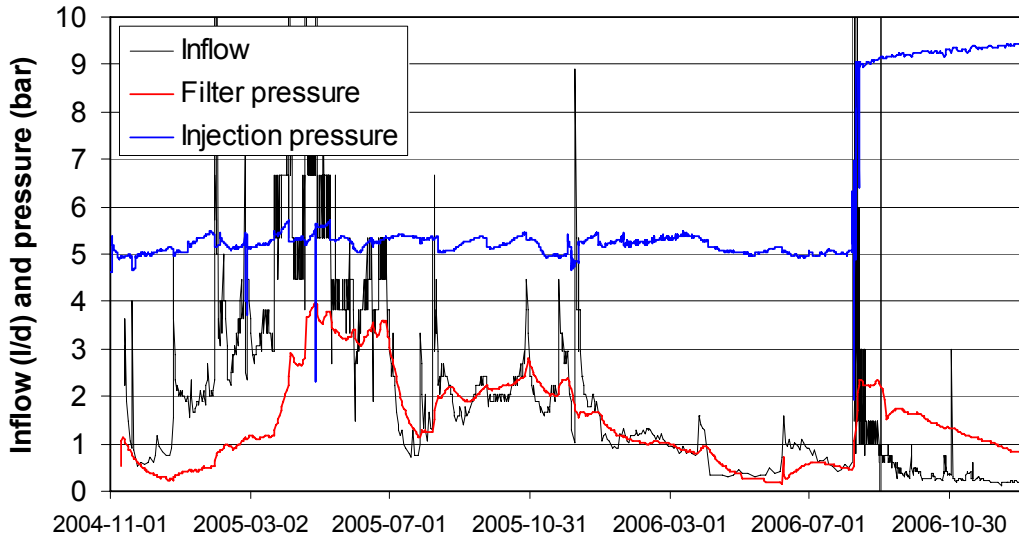


Figure 5-2. Development of relative pressures (injection and in sand filter) and inflow since the second hydraulic test.

Due to low pressure levels recorded in the sand filter, the injection pressure was increased from 5 to 9 bar during the period August 7 to August 11. The increase was followed by an increasing inflow and filter pressure. The inflow dropped however quite soon afterward this event. The filter pressure, on the other hand, has remained on a higher level than previously.

In the previous Sensor data report (/5-1/), a model for the relation between filter pressure, the inflow and an outflow was suggested. Since the inflow and the filter pressure was highly correlated from July 2005 to July 2006 (see Figure 5-2), it was suggested that the actual water uptake during this period was very limited and nearly all injected water was lost though leakage. From this followed that the conductivity of the leakage was approx. 1 l/d,bar.

With the new data, after the increase of the injection pressure, the relation between the filter pressure and the inflow has changed. With the proposed model and the specified conductivity, this would imply that there would be a net loss of water from the buffer. Since this does not appear to be realistic, an alternative interpretation should be sought after. One explanation could perhaps be that the conductivity of the leakage has reduced to approx. 0.2 l/d,bar after the event, but more data is needed before this can be elaborated. The cumulative water uptake therefore appears to be approximately the same as before, i.e. approx. 2.3 m³, which can be compared with the initial available pore volume of 2.7 m³.

5.3 Temperatures

Temperatures are monitored by use of thermocouples in three cylinders (C1, C2 and C3) and two rings (R4 and R10), cf. Figure 1-1. In addition, temperature readings are provided by the capacitance-type relative humidity (RH) sensors. In general, the temperature results exhibit consistent trends up to maximum values after about 200 days (App. A\ pages 77-82). A few exceptions have occurred for inner parts in Cyl 2 and the inner sand shield at Ring 10, where the maximum temperatures were reached after only about 40 and 60 days, respectively (App.A\pages79-80).

The temperature readings from January 1 2007 are compiled in Figure 5-3. It can be noted that the highest temperatures in the bentonite blocks are found in Ring 4, whereas the lowest can be found in cylinder C3. It can also be noted that the temperatures in Cylinder 2 at radius 350 – 450 mm is significant lower than in Ring 4 and Ring 10 at corresponding radii.

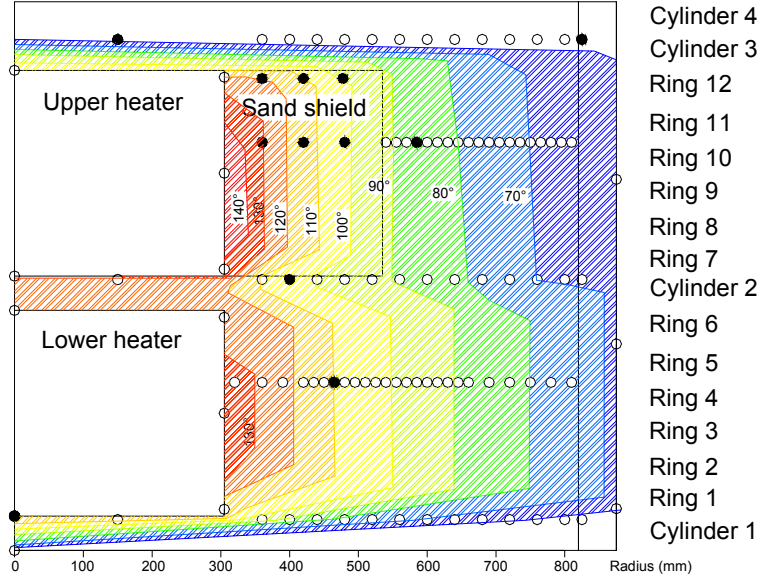


Figure 5-3. Temperature distribution at January 1, 2007. Rings indicate sensor positions. Filled rings indicate sensors out of order.

The TBT experiment is located 6 m from the CRT experiment. The latter was initiated approximately 880 days before the start of the TBT experiment and has therefore contributed with a certain heat flux. The CRT was terminated in October 2005. In order to compensate for this loss, the power output from the TBT heaters was increased from 1500 to 1600 W on June 9, 2006.

Thermal gradients and conductivities

Figure 5-4 shows Azimuth 90° temperatures measured in Ring 4 and 10. The effect of the wetting of the sand filter outside Ring 10 is obvious: Within the first 60 days of heating, the temperature drop across the filter had discernibly decreased, as would be expected in a system that had become water saturated and had potentially undergone some swelling pressure – induced compression.

Whereas the distributions have been fairly stable since day 200 with slowly decreasing temperature levels, the two latest scan-lines show a small but significant increase due to the increased power output.

The temperature distributions enable evaluations of the apparent thermal conductivity of the buffer materials. Distributions of such conductivities were presented in the previous Sensor data report (/5-1/). The development of conductivities at different radii in Ring 4 is shown in Figure 5-5. It can be noted that the innermost point, at 35 mm from the heater surface, dropped immediately after test start, but has thereafter increased steadily. In contrast, a point at 155 mm from the heater appears to have undergone a rapid increase in the beginning and has thereafter remained fairly constant.

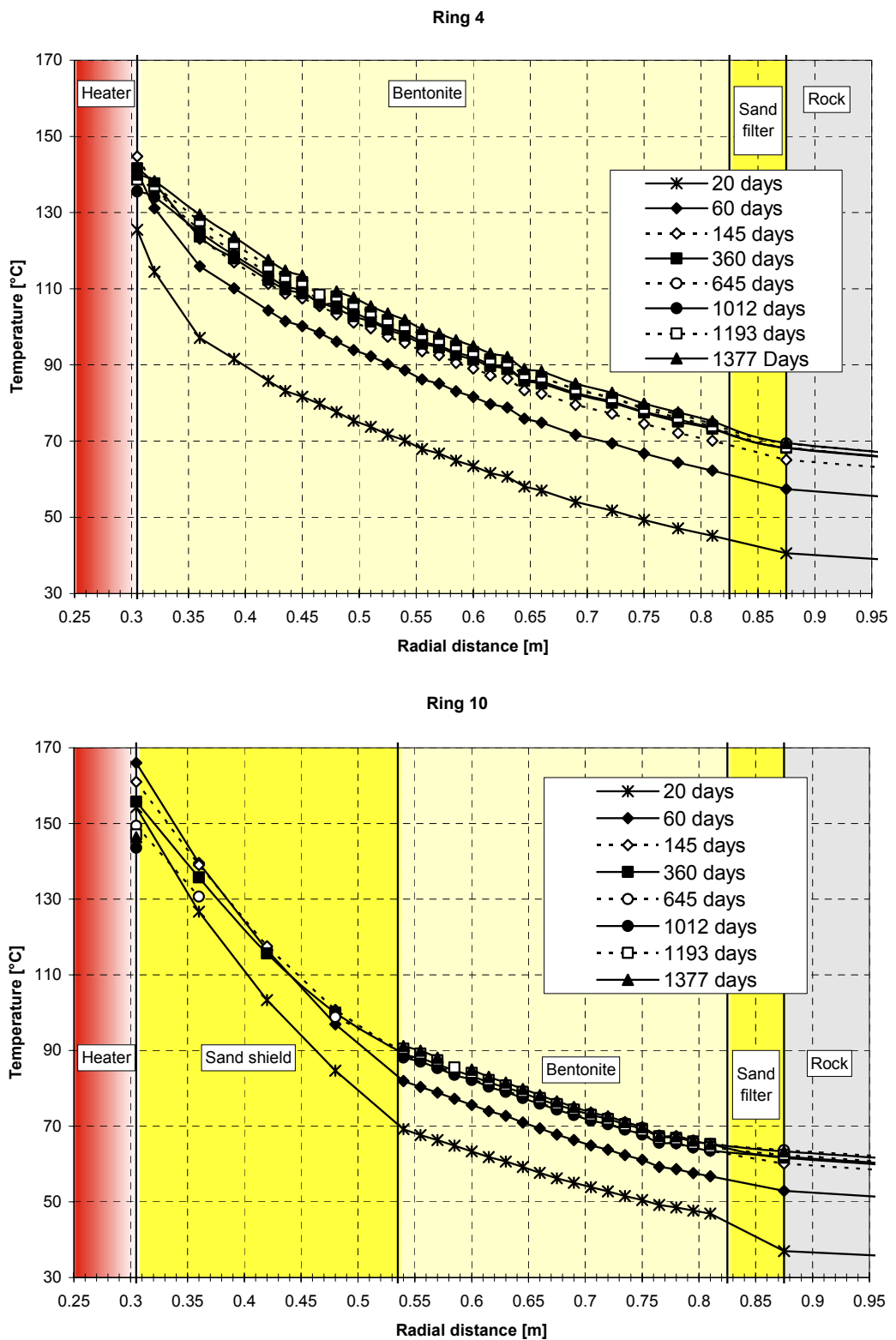


Figure 5-4. Temperatures measured at mid-height of heater 1 (Ring 4) and heater 2 (Ring 10).

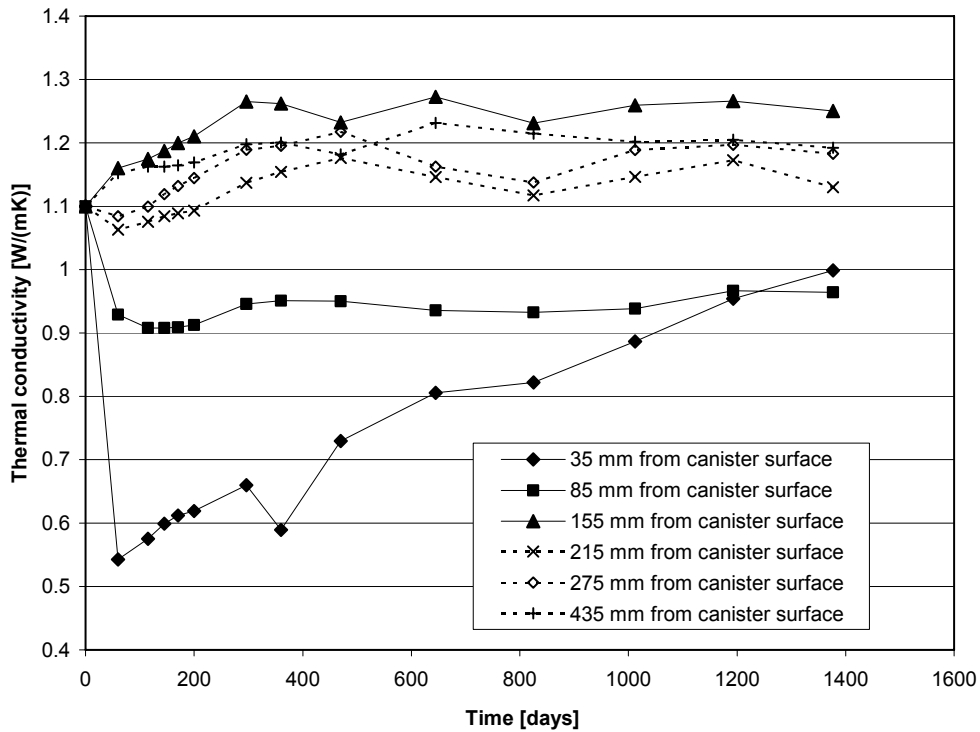


Figure 5-5. Thermal conductivity development in ring 4.

5.4 Relative humidity/suction

Recorded RH values and suctions indicate that moisture contents generally increase: RH from 72 to maximum 100 % (App.A\pages 63-68); suction between 6 and 1 MPa (App.A\pages 58-62).

A significant exception was the suction *increase* in Ring 10 at radius 785 and 735 mm after day 225 (App.A\page 61). Although this increase correlated with a general decrease in stresses in parts of Ring 9, it was most likely caused by a shortage in water supply, resulting in a localized desiccation cycle to occur. The trend was also reversed when water injection through the upper tubes was introduced (see Section 5.2), which supports the water supply explanation for these observations.

The hydration of the buffer, as recorded by the RH-sensors, is illustrated in Figure 5-6. Occasions when capacitive sensor signals showing $\text{RH} \approx 100\%$ (Vaisala and Rotronic), and all *active* signals from psychrometers, corresponding to $\text{RH} > 95\%$ (Wescor), are compiled. These occasions have earlier been taken as indication of *buffer* saturation. Recent results from the pore pressure sensors have however led to a reassessment of this interpretation. The occasions are instead taken as indications of *vapour* saturation. The current understanding is that the process of reaching full saturation is slow, and that only the bentonite at the mid-section around the upper heater has yet reached this condition.

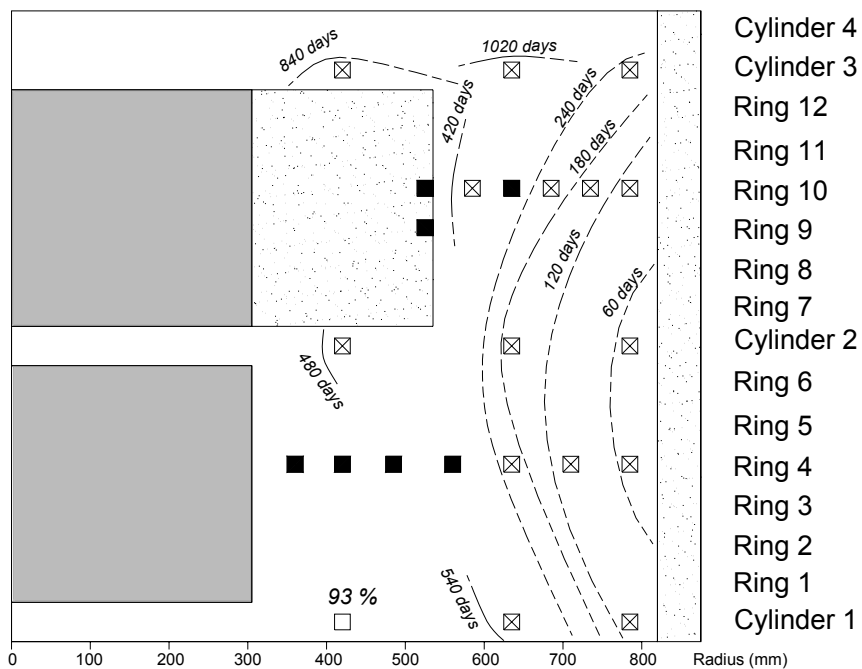


Figure 5-6. Occurrences of vapour saturation up till January 1, 2007. Boxes are sensor positions. Ticked boxes indicate saturation. Filled boxes indicate sensors out of order. Percentage is current RH values.

The activation of the filter mat between the upper cylinders is reflected by the most recent vapour saturation event in the upper part (see Figure 5-6).

The only capacitive sensor that still indicates unsaturated vapour, i.e. < 100 %RH, is the innermost sensor in Cylinder 1. The innermost sensor in Ring 4 failed in April 2006. At that time it showed 91 % RH.

5.5 Pore pressure

Ideally, pore pressure sensors should give a zero signal as long as the condition isn't totally saturated. At present, four sensors, the outermost in Ring 3 and all sensors in Ring 9 located in the bentonite, clearly show positive values (App.A\pages 69-70), which indicates that these parts are saturated. The build-up of the outermost sensor in Ring 9 coincided with the filter pressure increase in the beginning of 2005, whereas the other sensors responded within 200 days.

5.6 Total pressure

Results from pressure monitoring are shown in App.A\pages 51-59. A compilation of recent total pressures is shown in Figure 5-7. From this a number of observations can be made. Higher pressure levels occur in the outer parts throughout the experiment. An exception is the upper cylinders, which display the lowest pressure levels. The conditions in the lower and the mid-section cylinders are quite isostatic, while the sections around the heaters are characterized by deviatoric stresses, with relatively lower radial stresses. This appears to reflect that the largest displacements occur in radial direction around the heaters. In these sections, the sand filter and the sand shield, and perhaps also the dehydration of the inner parts around the lower heater, enable the radial swelling of the hydrating buffer.

The build-up of total pressures appears to have been interrupted during the period with lower filter pressures (July 2005 – June 2006). This trend is noticeable for all sections except Cylinder 3 and can be observed in Figure 5-8. In general, only the total pressures recorded in Cylinder 3 has increase significantly during the last 6 months.

Recent axial pressures, shown in Figure 5-7, appear to be quite similar in a band between radius 550 and 650 mm from Cylinder 1 to Ring 9. In contrast, the axial pressure in Cylinder 3 was significantly lower, although this can not be seen in Figure 5-7 due to the sensor failure in connection with the filter mat activation. The relation is further illustrated in Figure 5-8 in which results are shown from axial pressure sensors all located at radii 585 - 635 mm. Moreover, measured cable forces are here shown after conversion to pressures under the assumption that the forces are evenly distributed over the entire rock hole area (2.40 m^2).

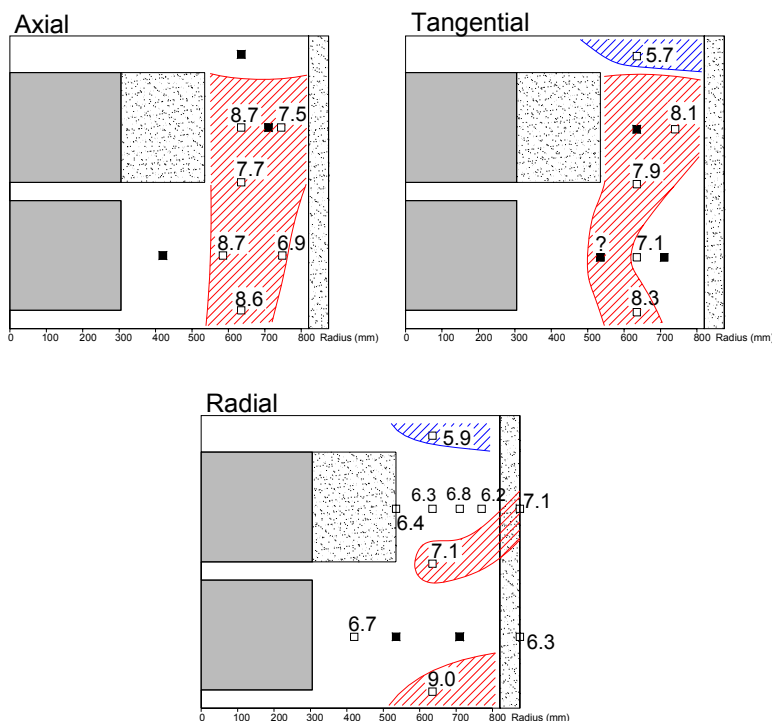


Figure 5-7. Total pressure distribution at January 2007. Values in MPa. Boxes are sensor positions. Filled boxes indicate sensors out of order. Levels above 7 MPa marked red; below 6 MPa marked blue.

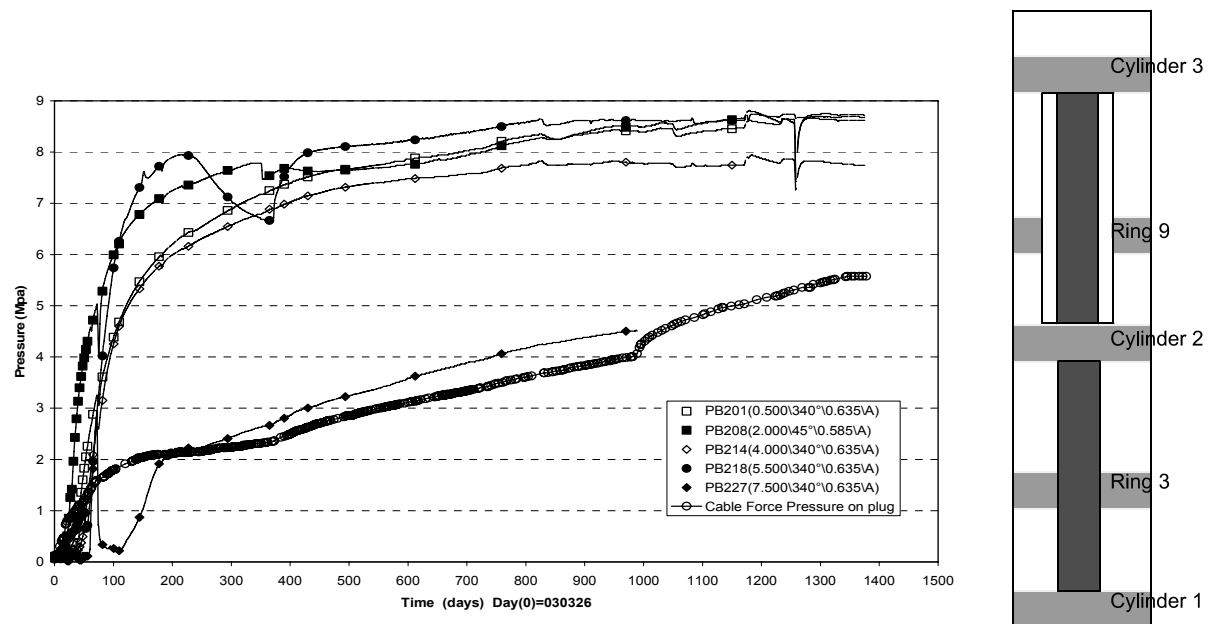


Figure 5-8. Axial pressure measured in different sections.

A fairly clear-cut grouping can be observed, which suggests that the vertical forces are predominantly transferred in a section corresponding to the buffer rings around the upper heater. The stress level around the heaters and in the lower cylinders has during the test period been significantly higher than the upper part of the experiment. This difference has however decreased during the test period. This has been further evaluated as a balance between the vertical forces acting on Ring 10 and the lid, respectively (/5-1/).

Hydro-mechanical evolution

Insight into the hydro-mechanical evolution can be gained through relating the stress condition with the prevailing suction level. Comparisons of different sensor results can be made for positions with approximately the same radii and the same heights. Figure 5-9 shows a schematic outline of all sensors for total pressure and relative humidity located in the bentonite buffer. Among the different sensors, eleven groups have been defined: one in each cylinder, five in Rings 3/4 and three in Rings 9/10. Each group has been defined for a certain radius. Additional RH-sensors with lower radii have been included in a few cases in order to cover the available data as much as possible.

Data are shown in Figures 5-10. For the results on total pressure, averages have been calculated from the available data and are denoted mean stresses. So as long as a sensor has been in operation, it has been included in the mean value. Relative humidity and temperature results have been transformed into suction values. Psychrometers (Wescor) and capacitive sensors (Vaisala) are presented separately.

The framework of presenting stress-paths like these is considered in the constitutive laws, e.g. Barcelona Basic Model (BBM), used for mechanical modeling. The experimental paths therefore correspond directly to those generated by the model. In general, a path is steep if the material expands (through swelling or unloading), whereas the path is flat if the material is compressed or shrinks. The behavior that some of the

paths intersect with the abscissa reflects the result that several RH-sensors show 100 %, i.e. that the vapor is saturated. In several cases, the total pressures have not reached their maximum values, which indicate that vapour saturation events did not coincide with the buffer saturation event. This is, however, only exhibited by the capacitive sensors.

Some sensors display signals that should be regarded as uncertain, e.g. the Vaisala signals for Ring 3:4 and the last values for Cylinder 2.

Finally it can be noted that the evolution displayed by the paths occurred quite fast after the launch of the test. In several cases, the main part of the paths had advanced already after 200 days.

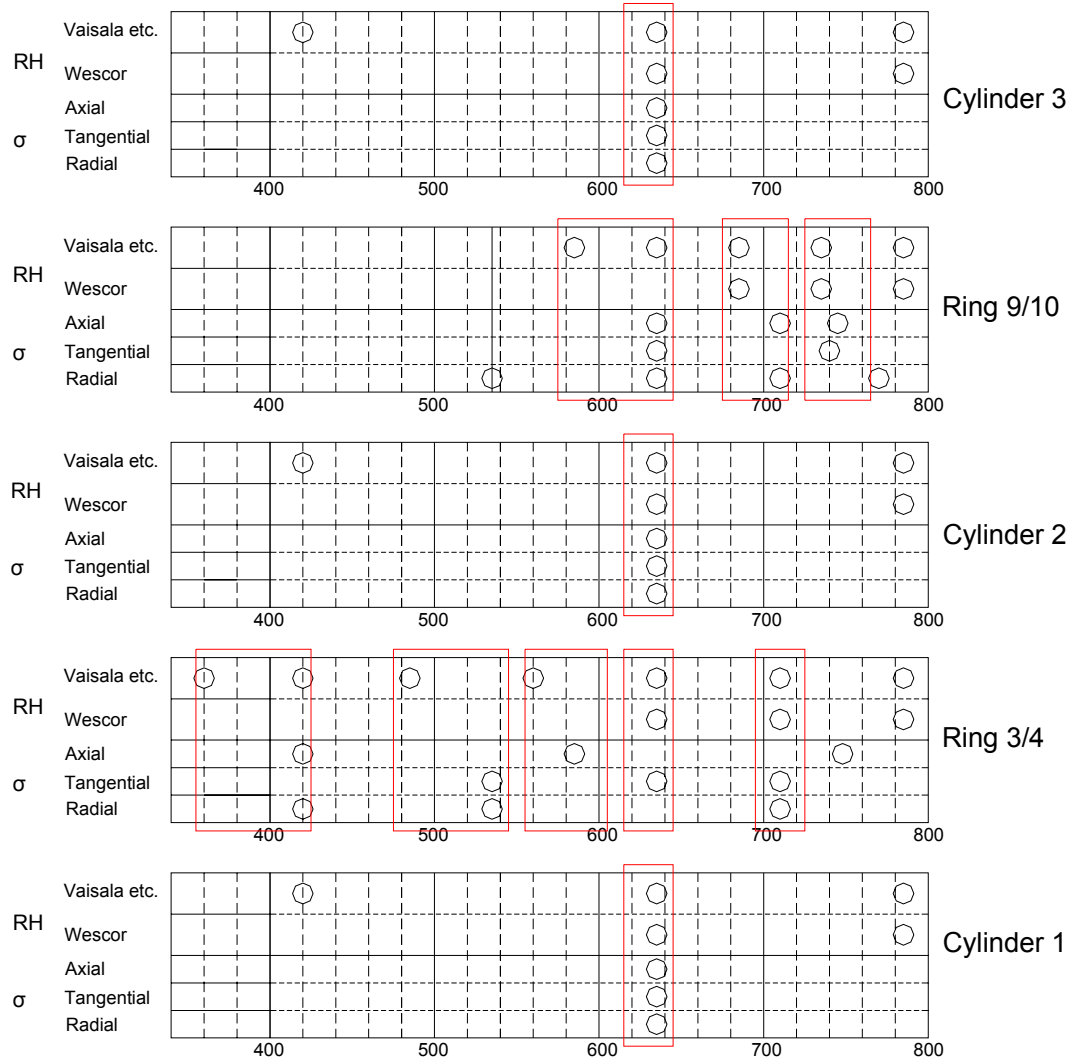


Figure 5-9. Schematic locations of sensors for total pressure and relative humidity. Horizontal position corresponds to radius (mm). Evaluated groups of sensors are marked in red.

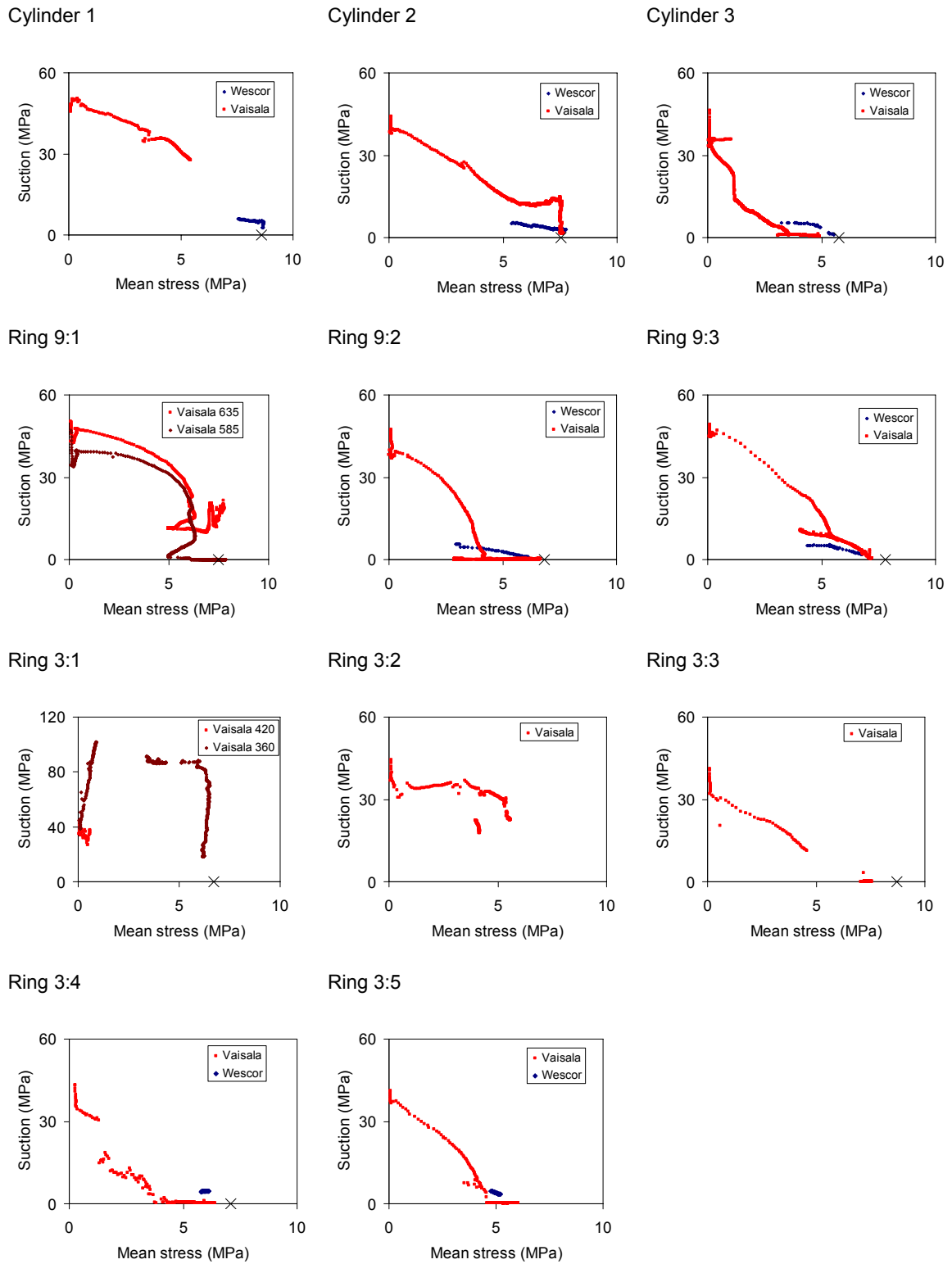


Figure 5-10. Stress-paths (mean stress vs. suction) for the hydro-mechanical evolution as displayed by the defined groups of sensors. Capacitive RH sensors (Vaisala) marked red and dark red. Psychrometers (Wescor) marked blue. Current (2007-01-01) stress levels marked \times .

6 References

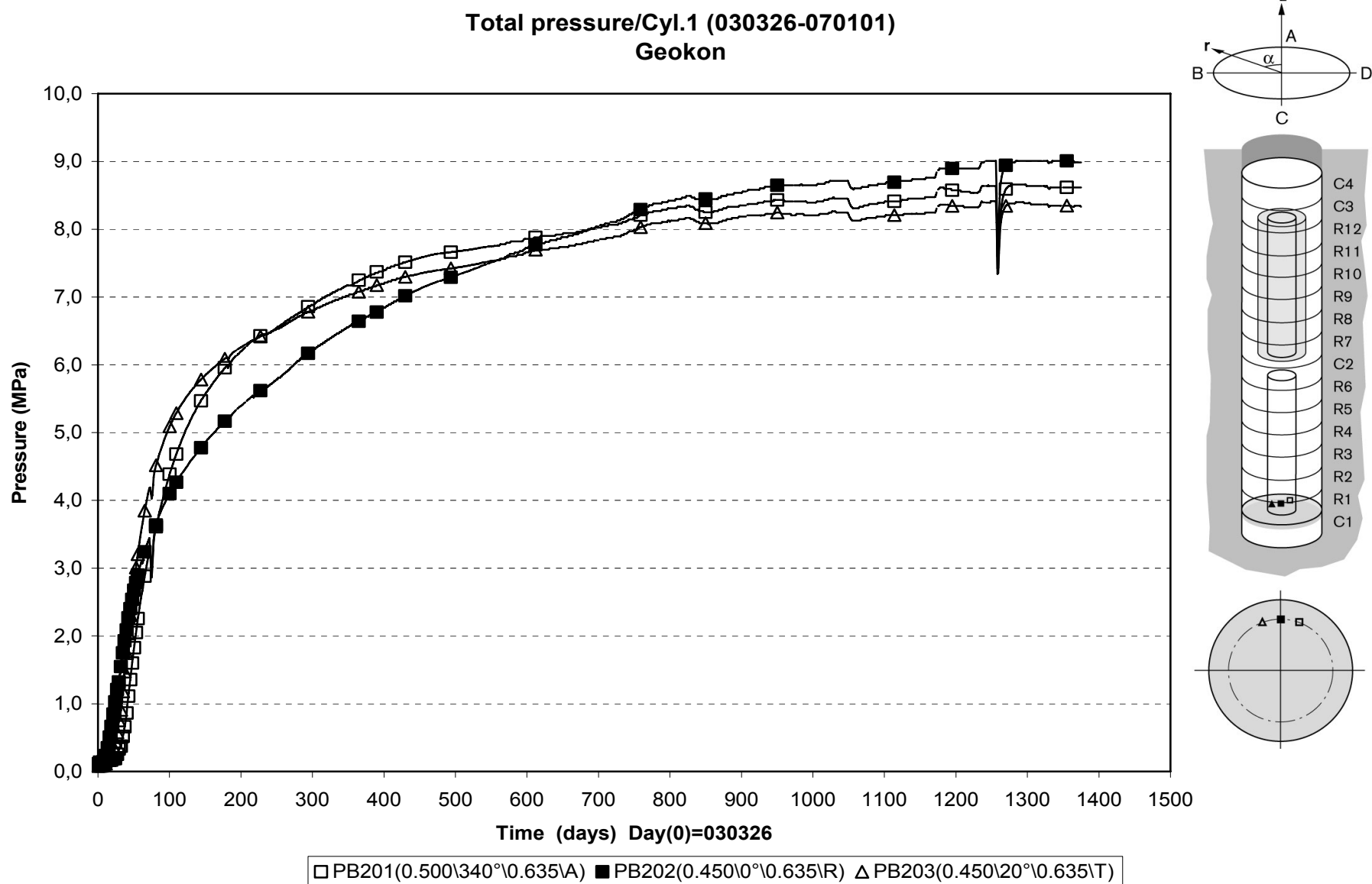
/4-1/ Sandén T and Börgesson L. Report on instruments and their positions for THM measurements in buffer and rock and preparation of bentonite blocks for instruments and cables. Temperature Buffer Test, Report R5 , 2002. SKB ITD-02-05

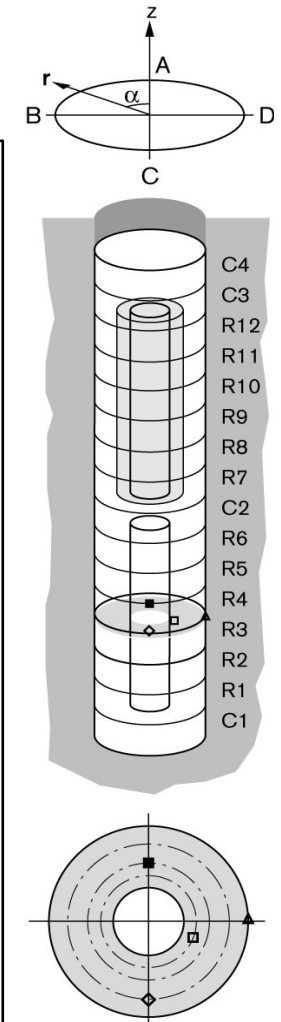
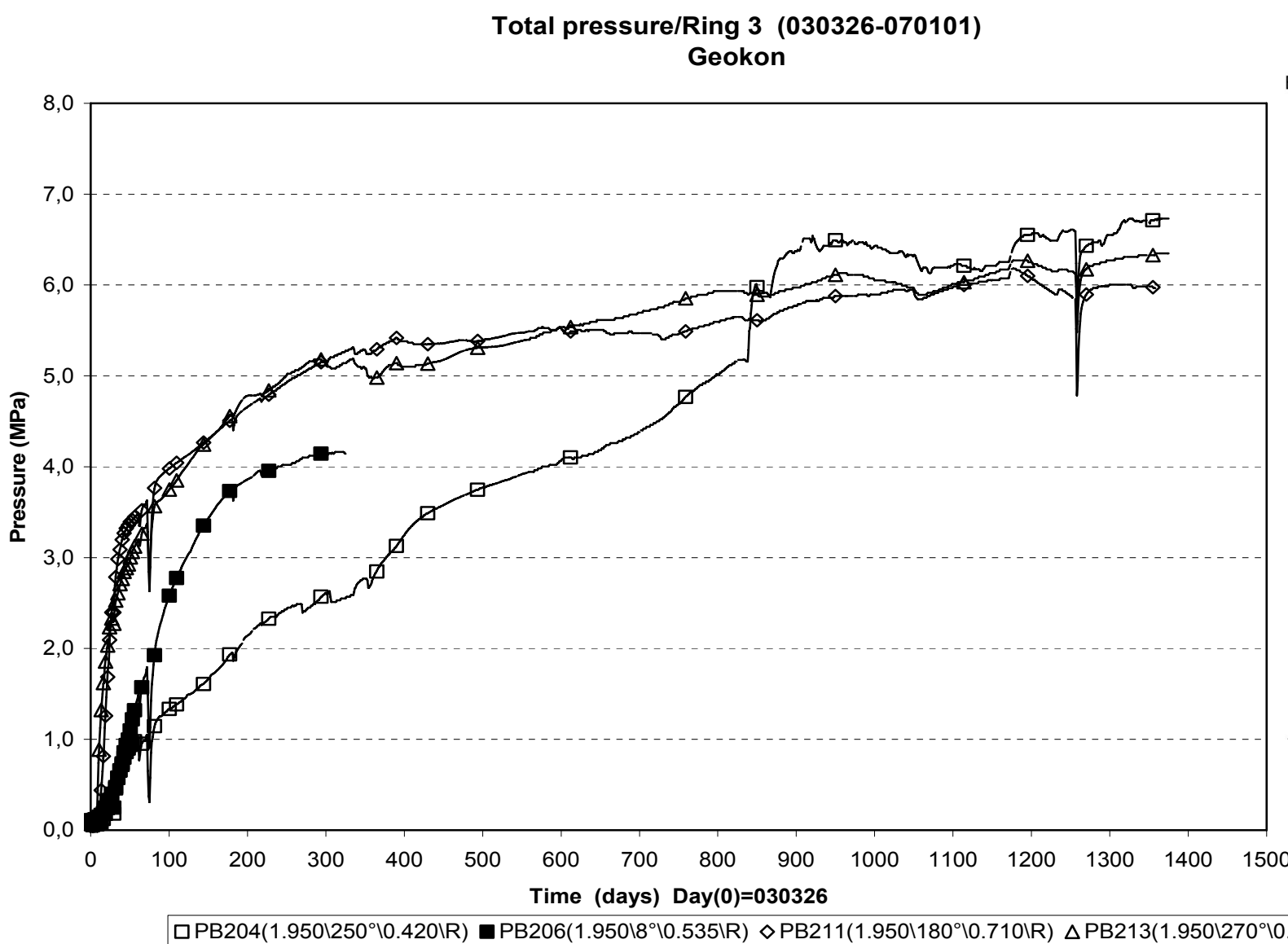
/4-2/ Garcia-Sineriz, J.L and Fuentes- Cantillana. Feasibility study for the heating system at the TBT test carried out at the Äspö HRL in Sweden. Temperature Buffer Test , October 2002. SKB IPR-03-18

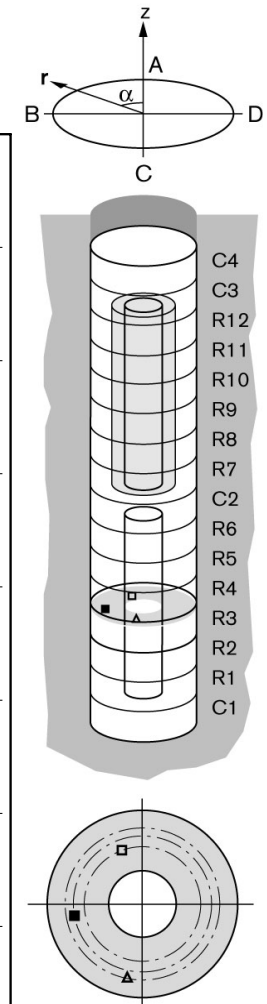
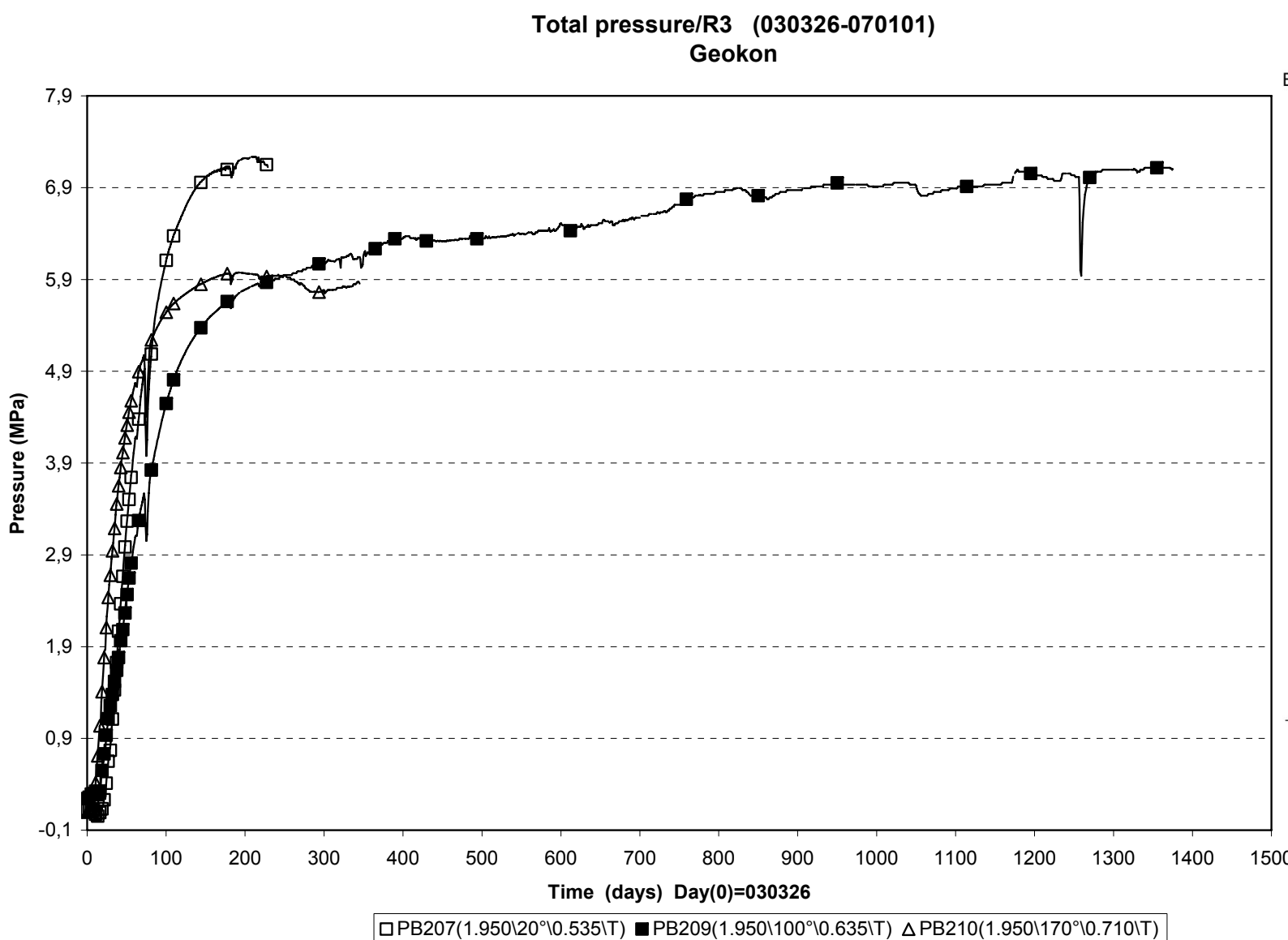
/5-1/ Goudarzi R., Åkesson M., Hökmark H. Äspö Hard Rock Laboratory. Temperature Buffer Test. Sensors data report (period 030326-060701) Report No:8, 2006, SKB IPR-06-27.

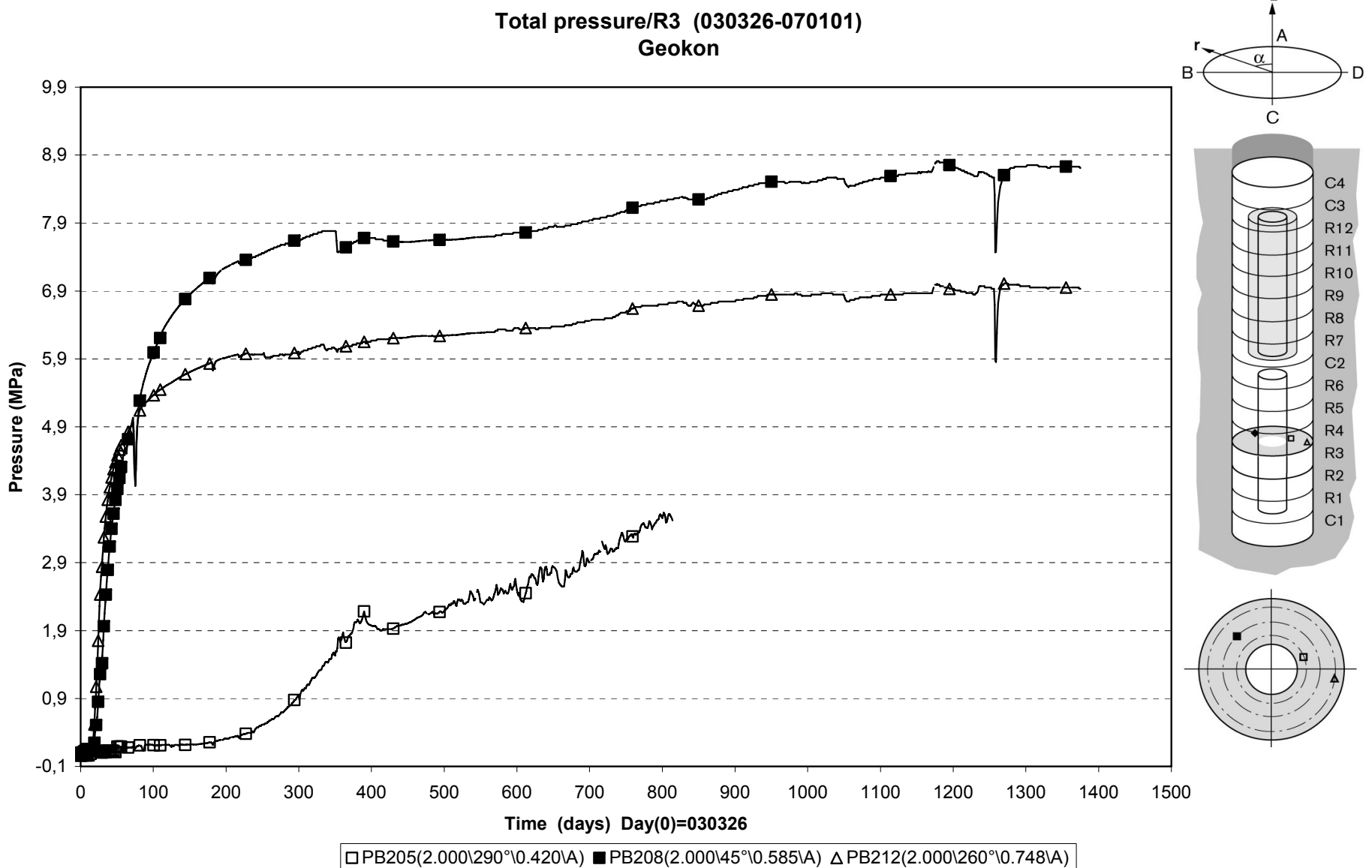
Appendix A

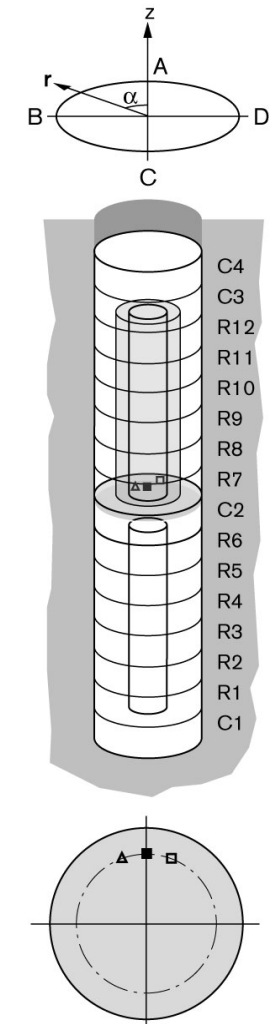
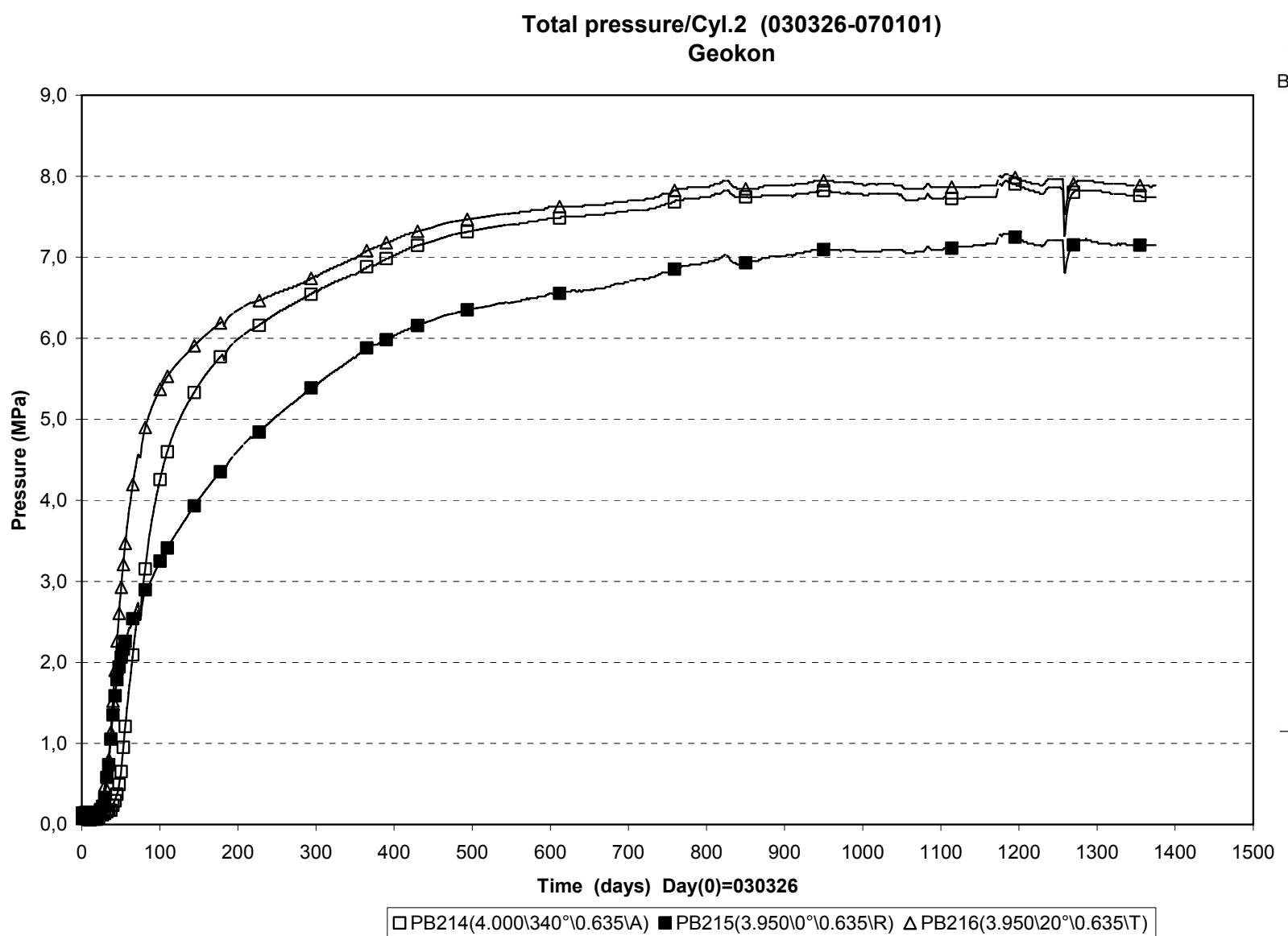
Measured data

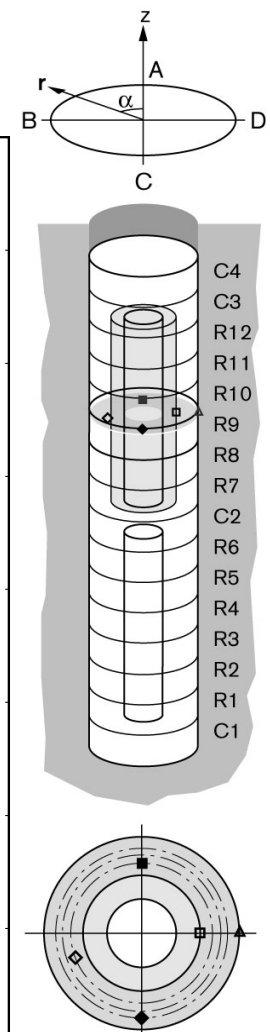
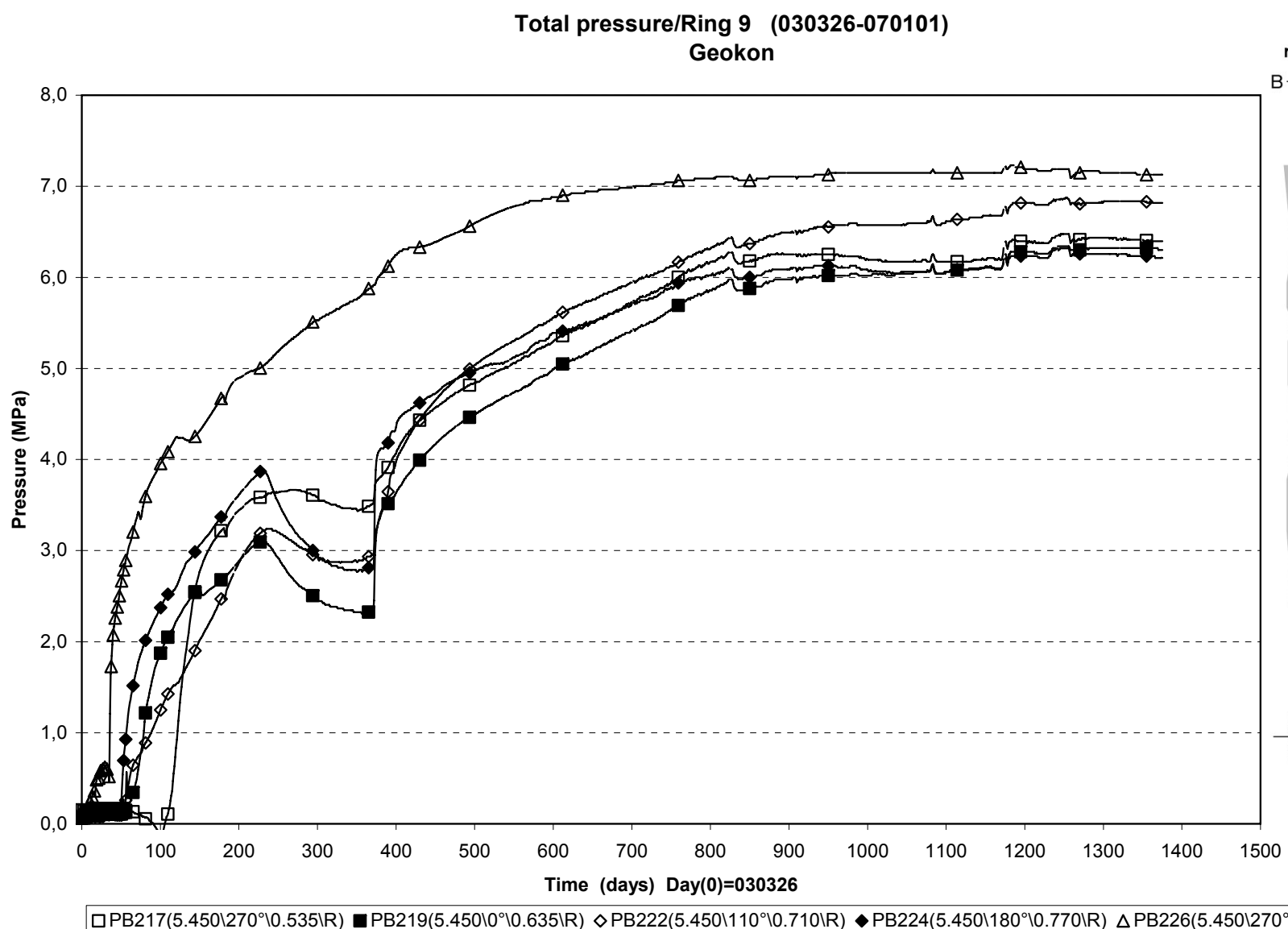


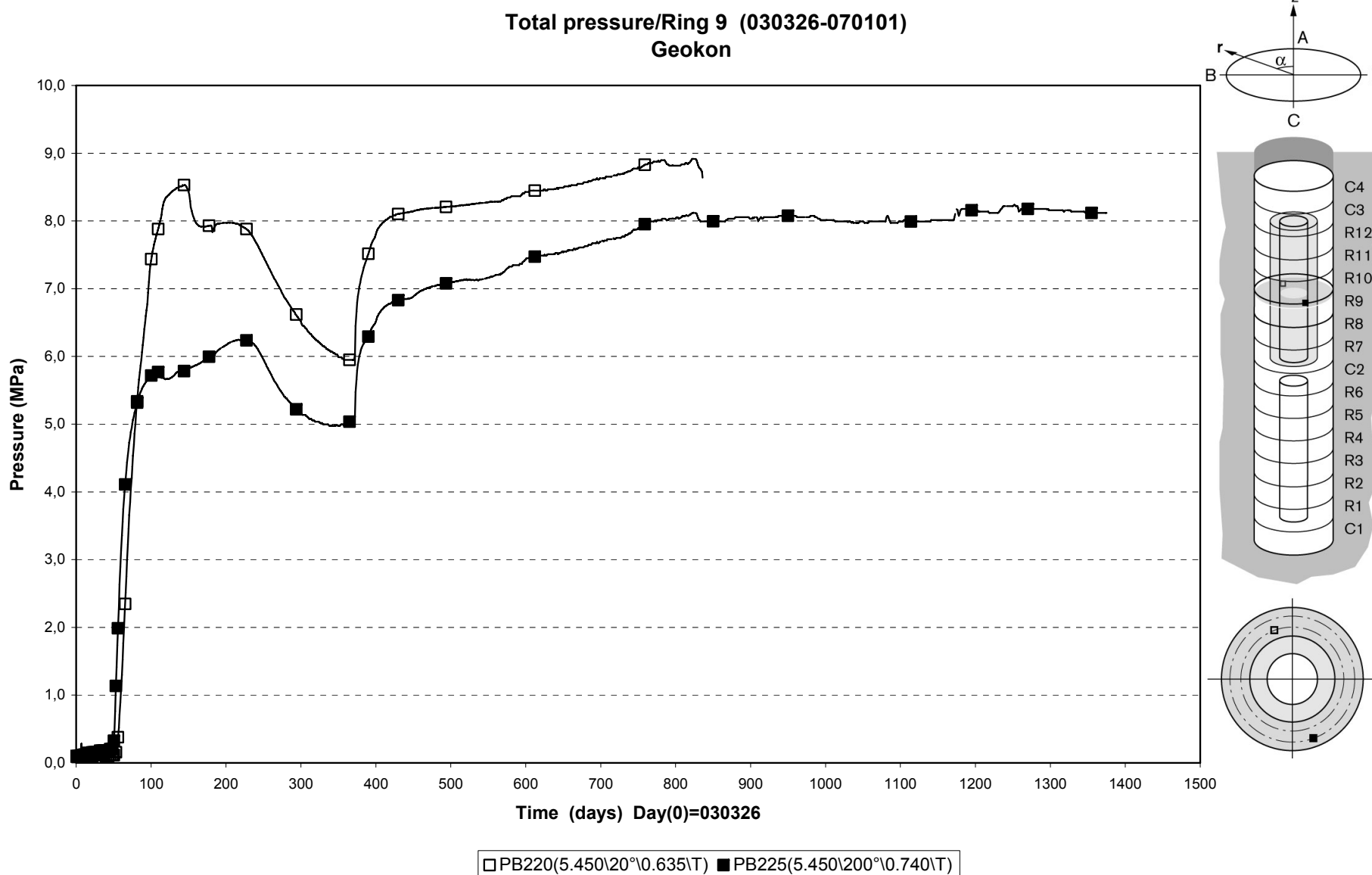


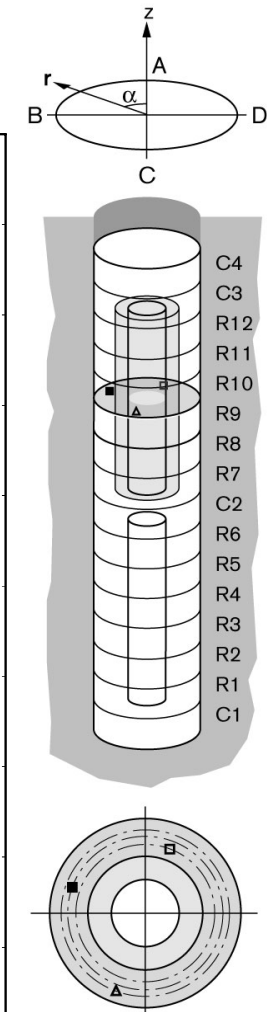
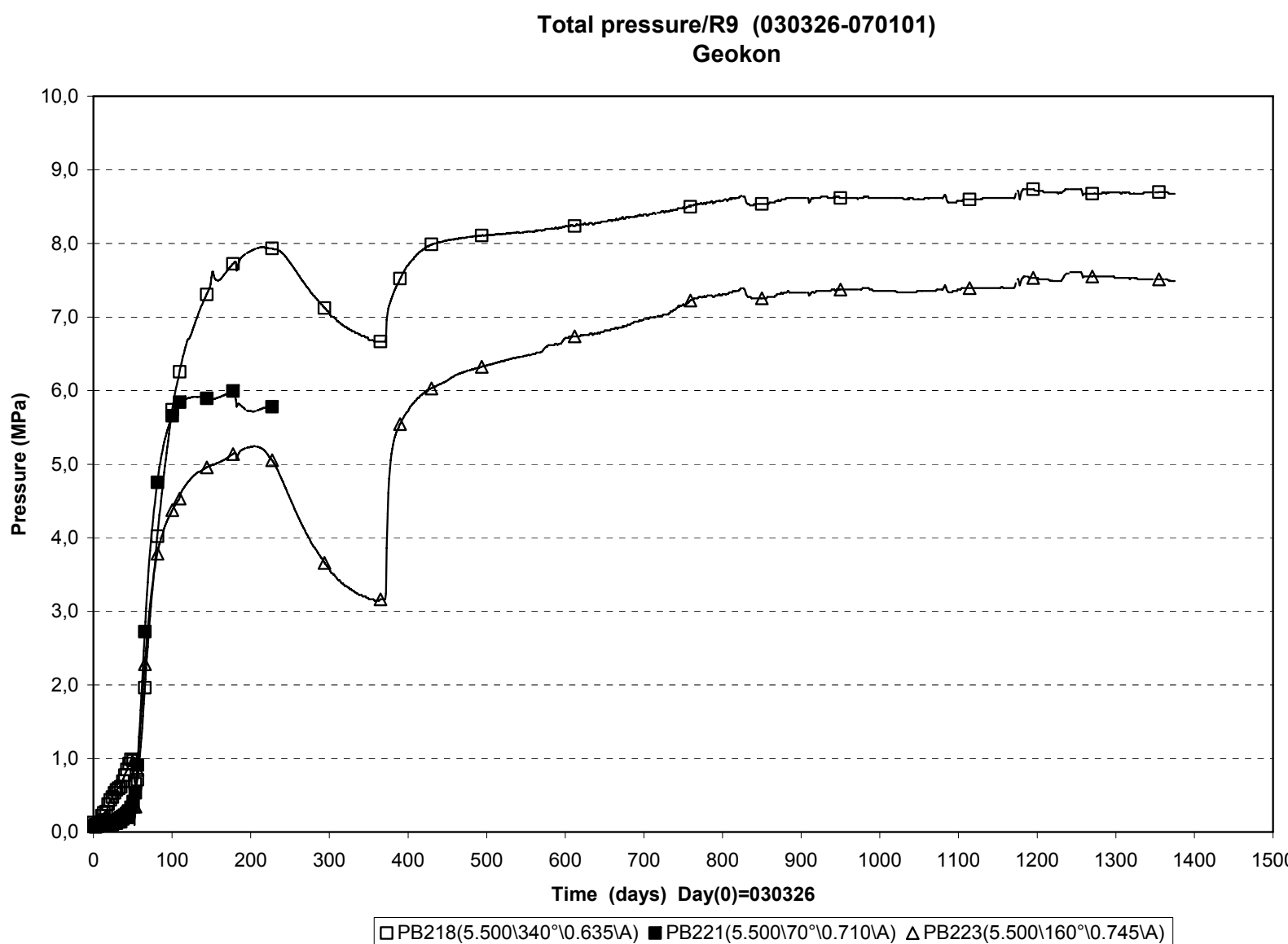


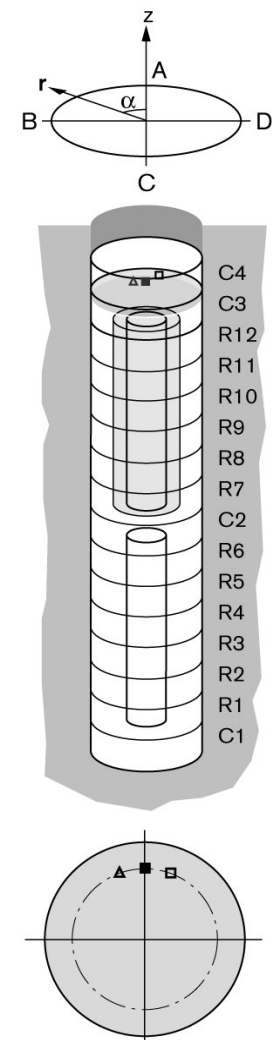
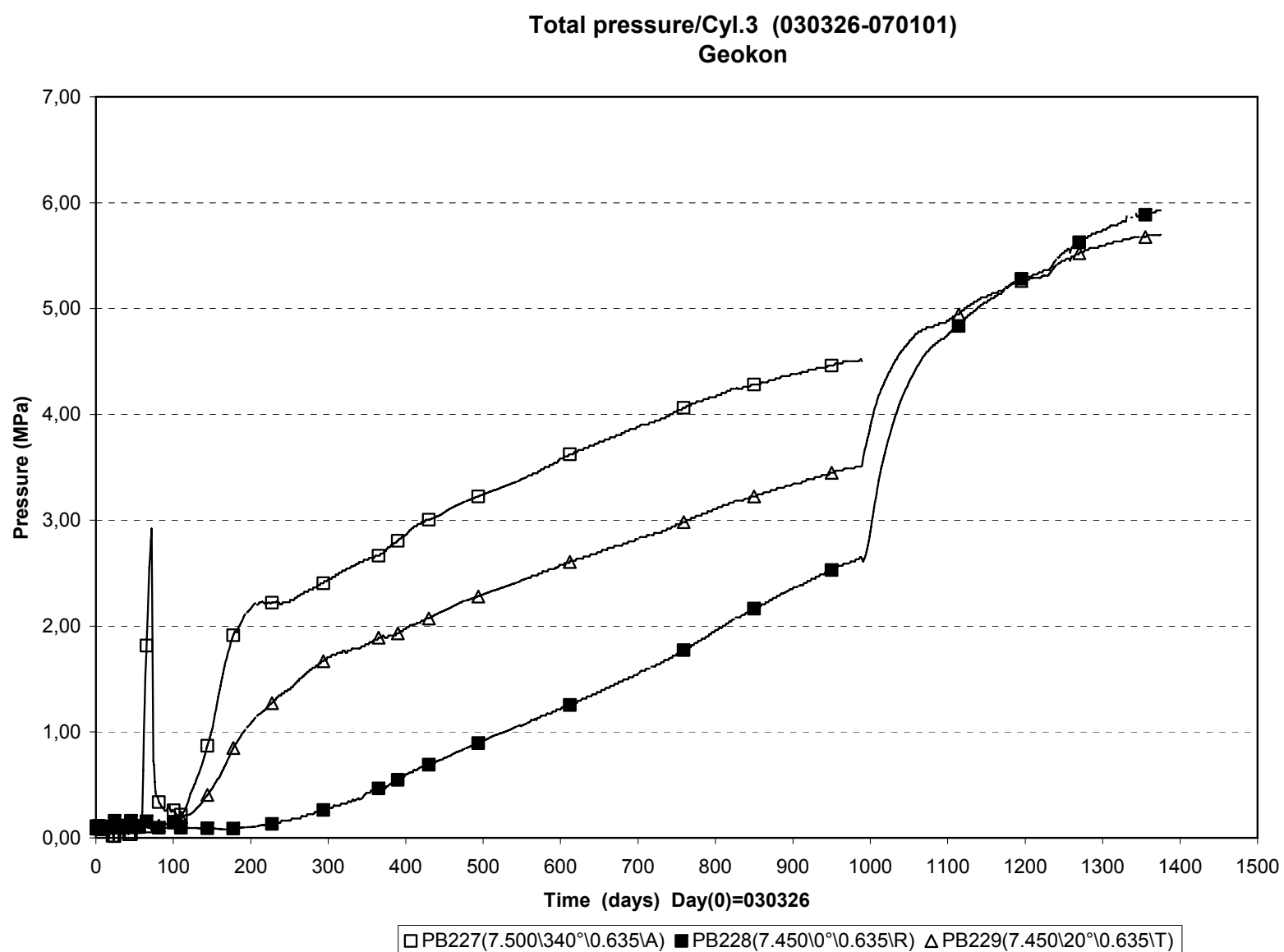


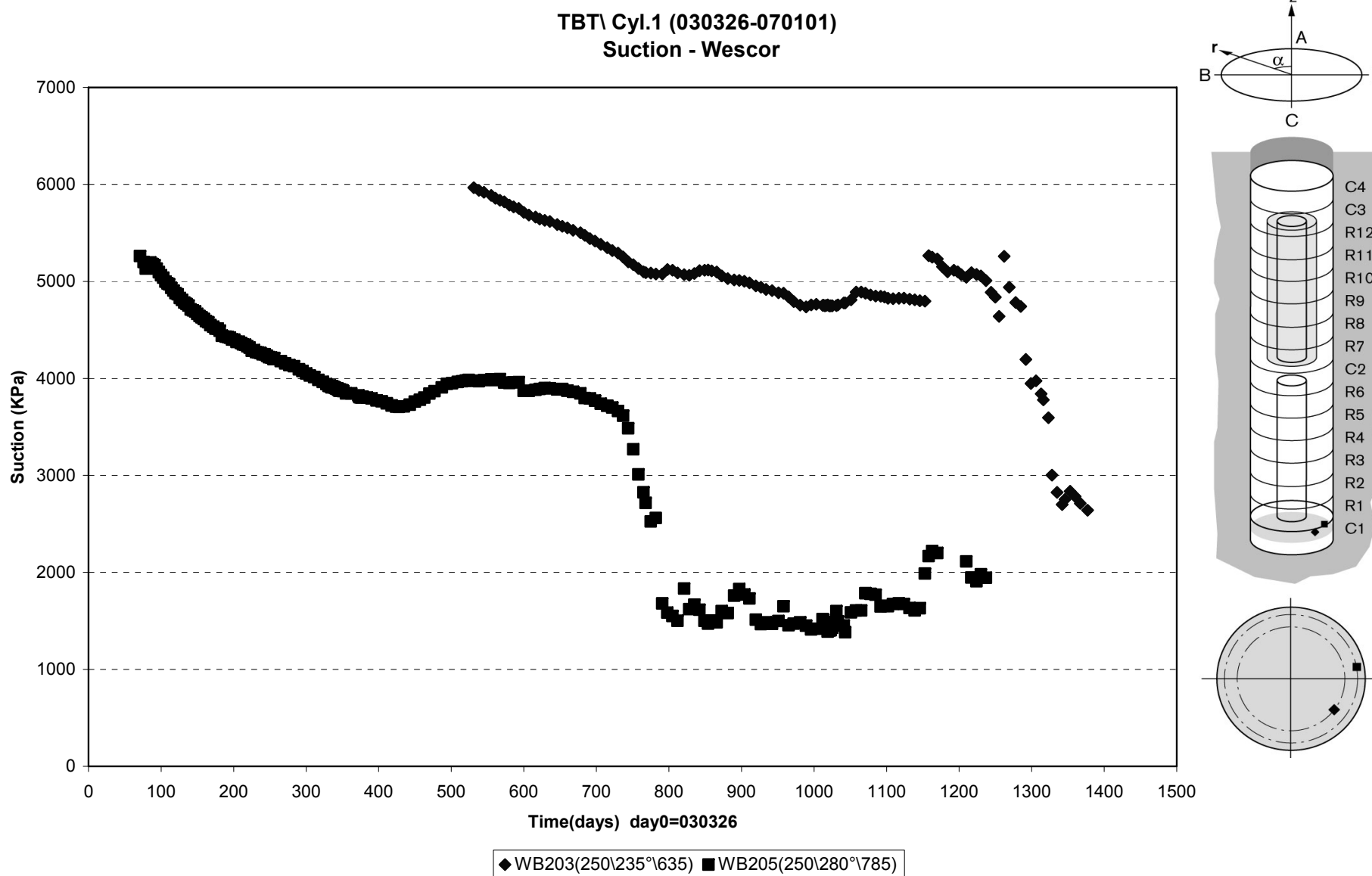


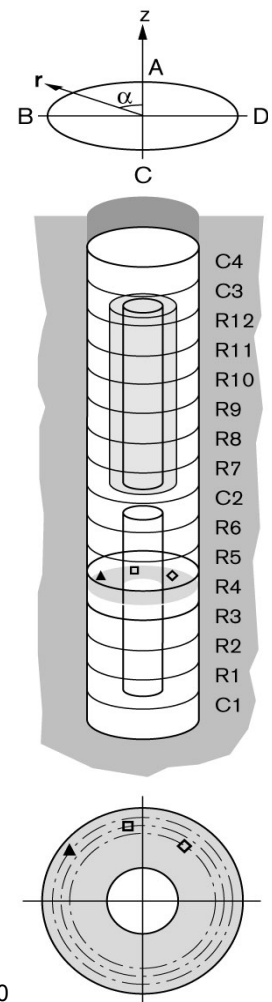
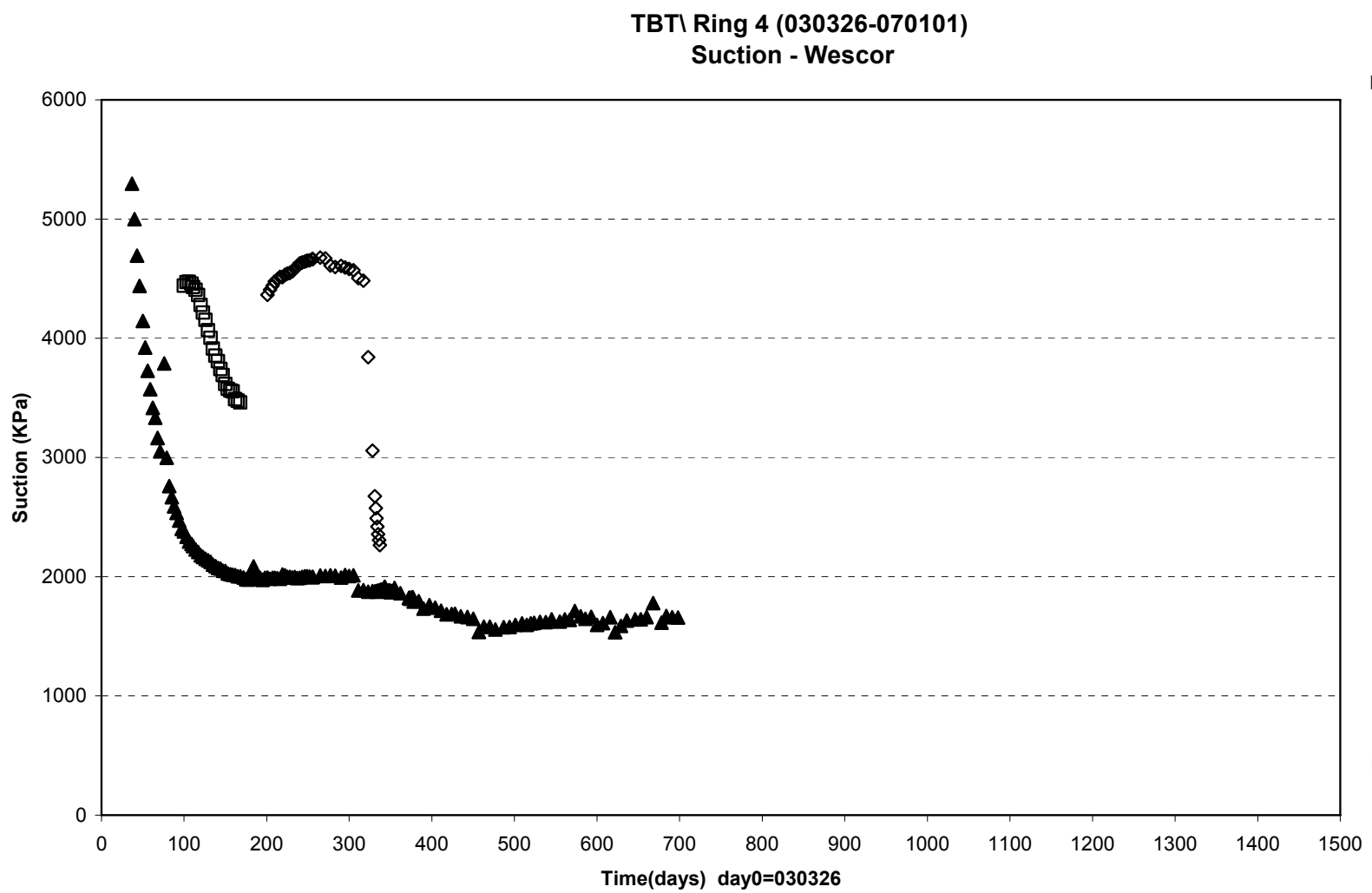




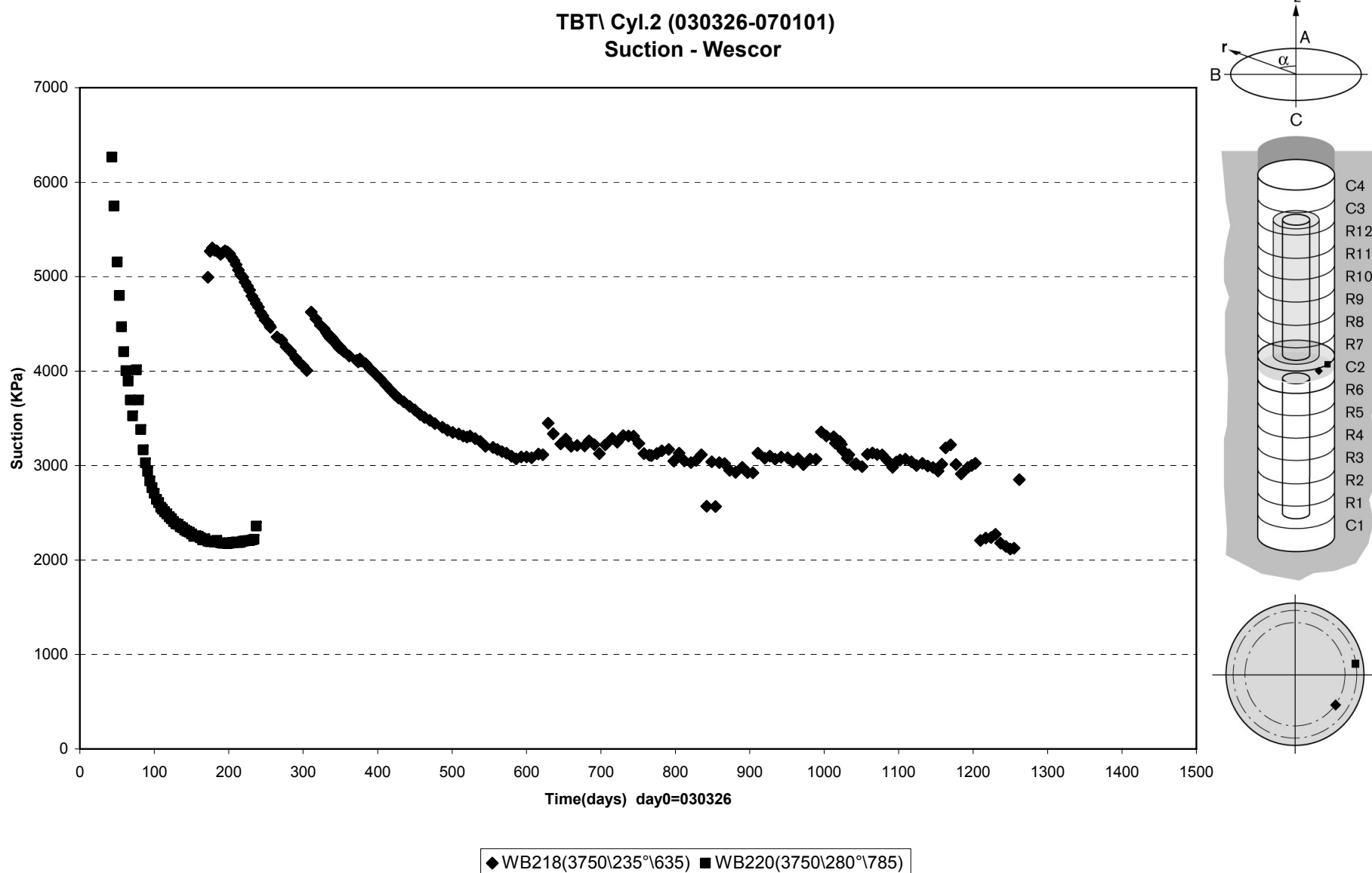


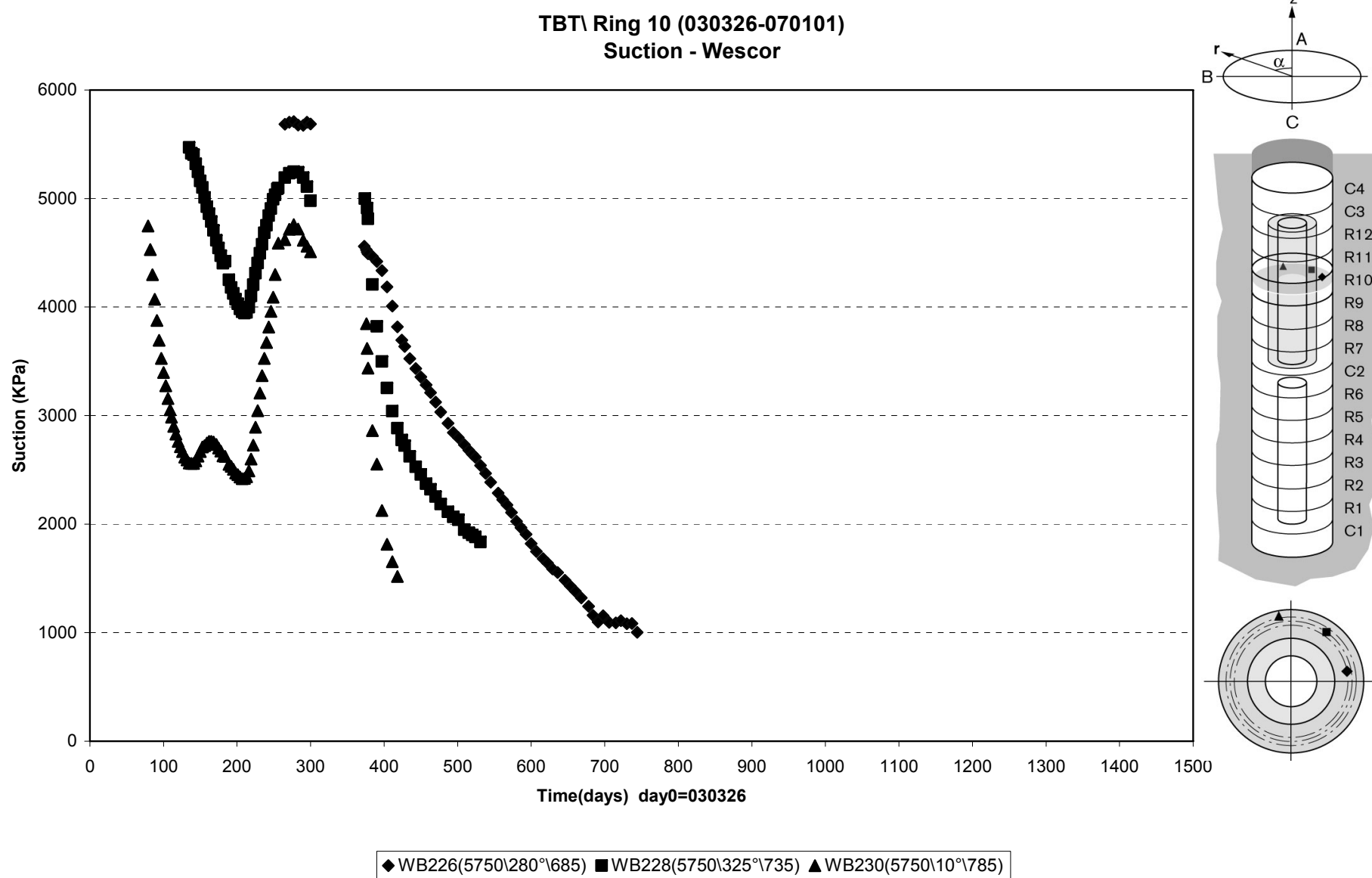


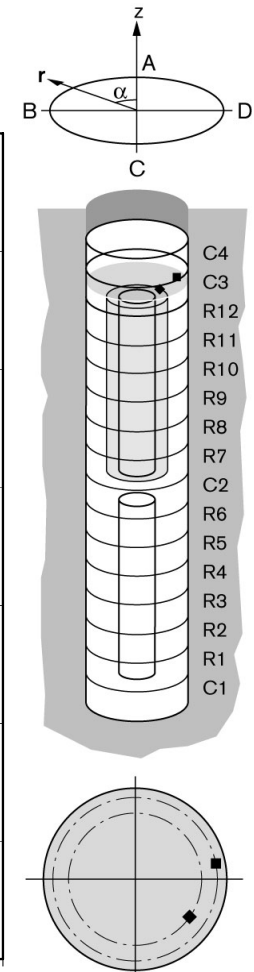
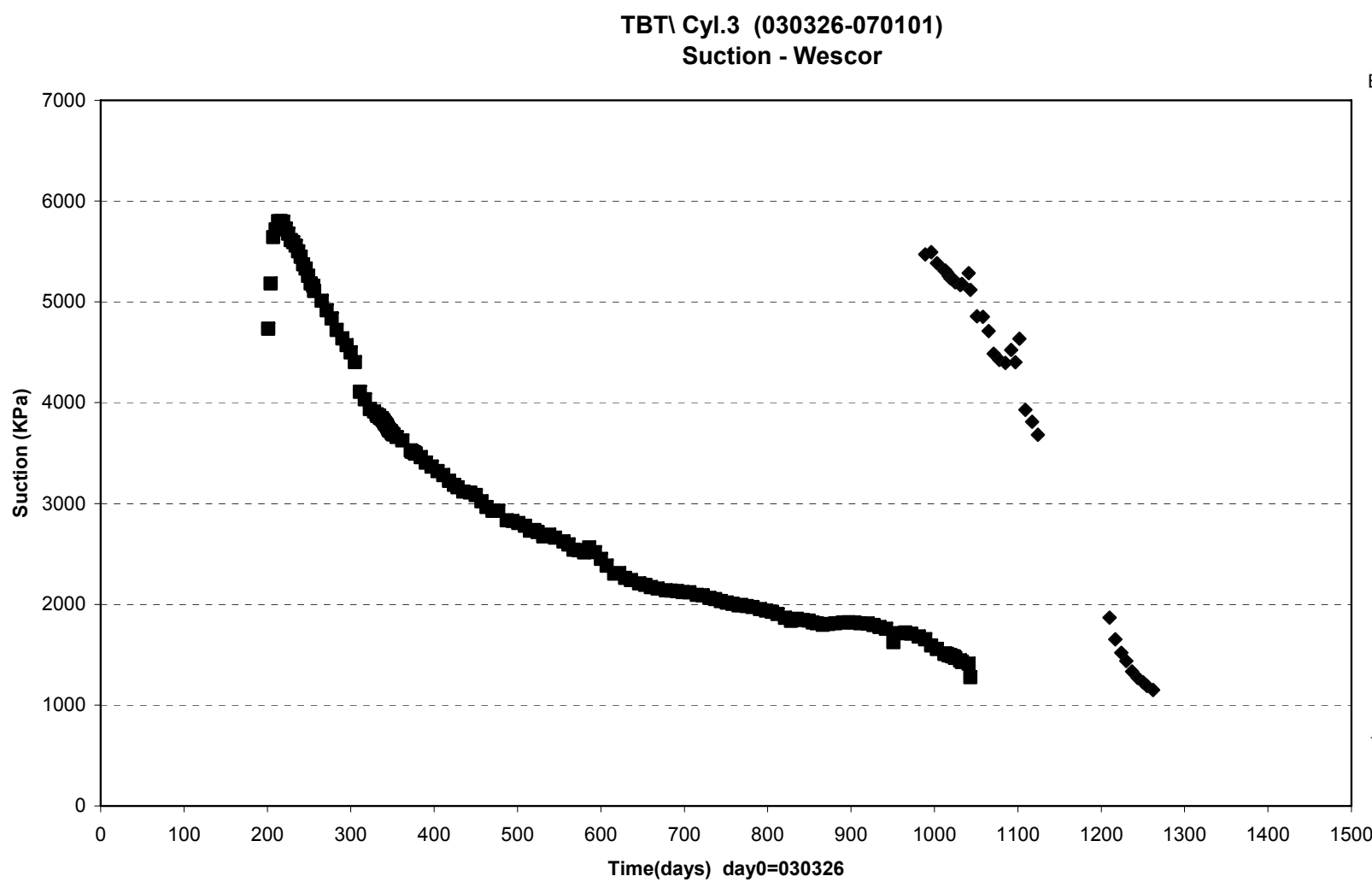


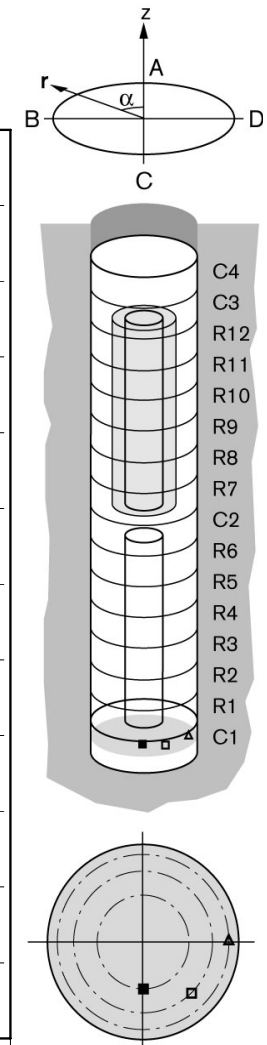
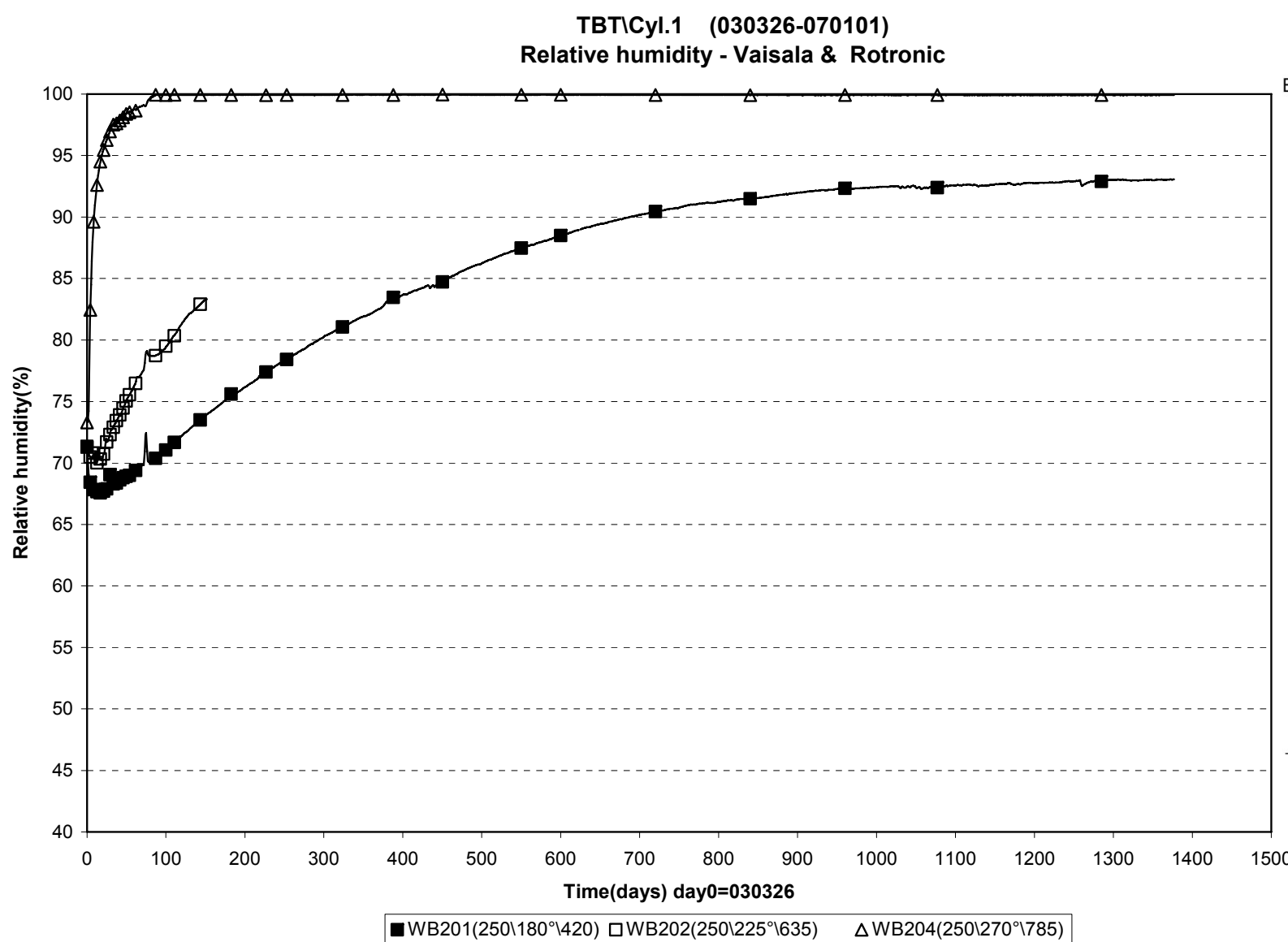


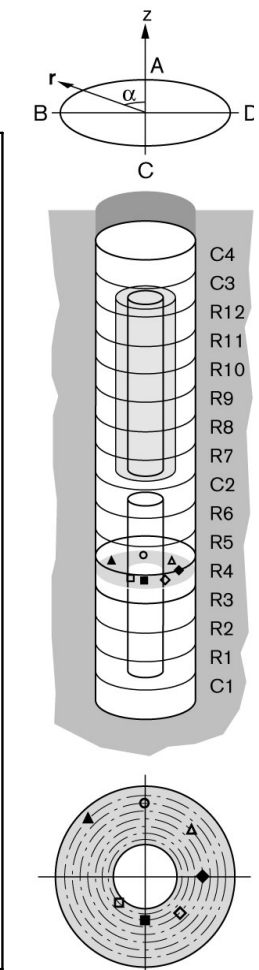
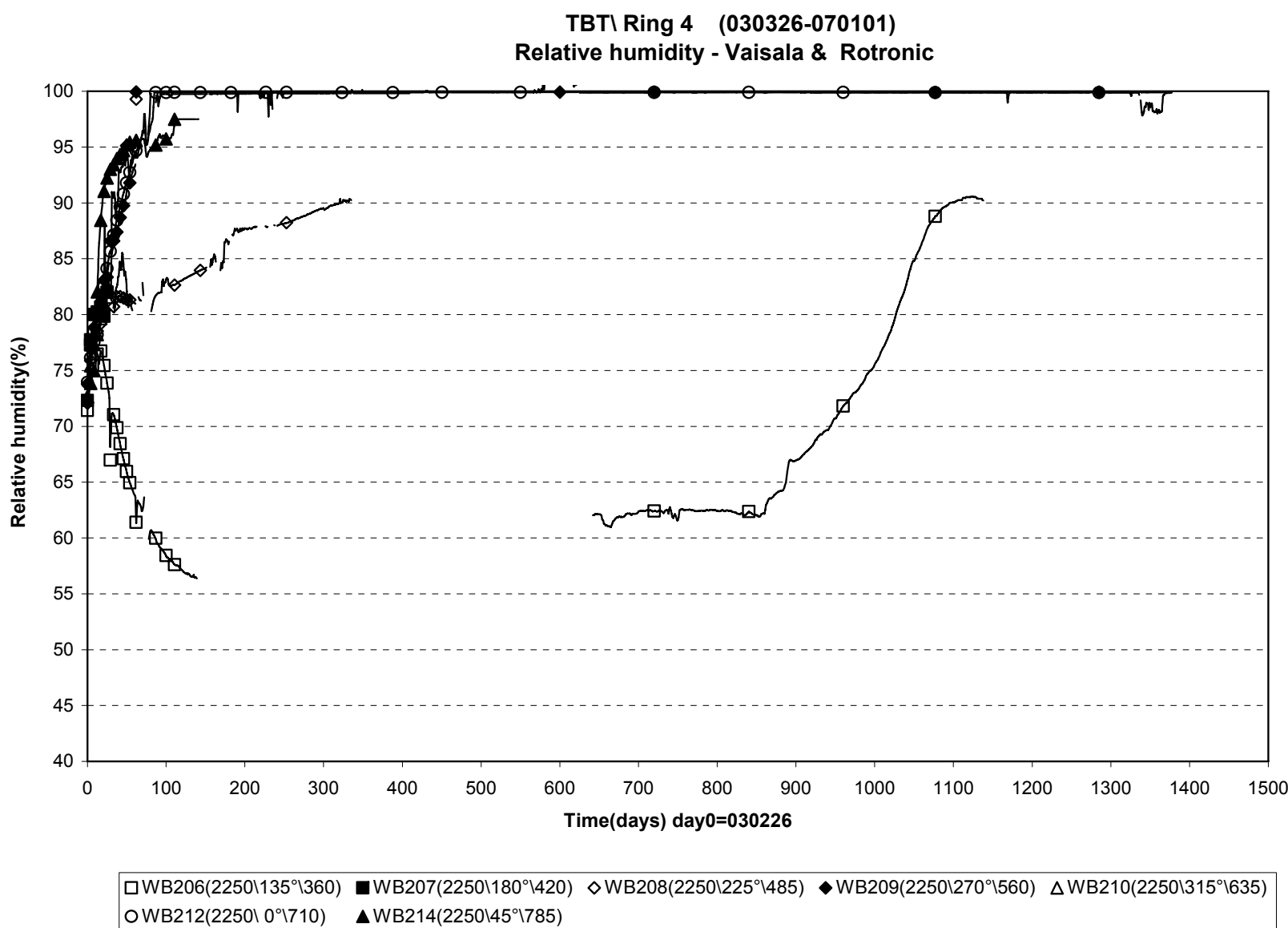
◇ WB211(2250\325°\635) □ WB213(2250\10°\710) ▲ WB215(2250\55°\785)

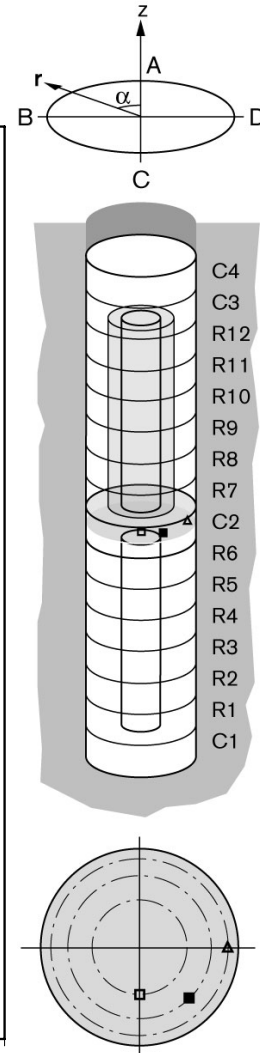
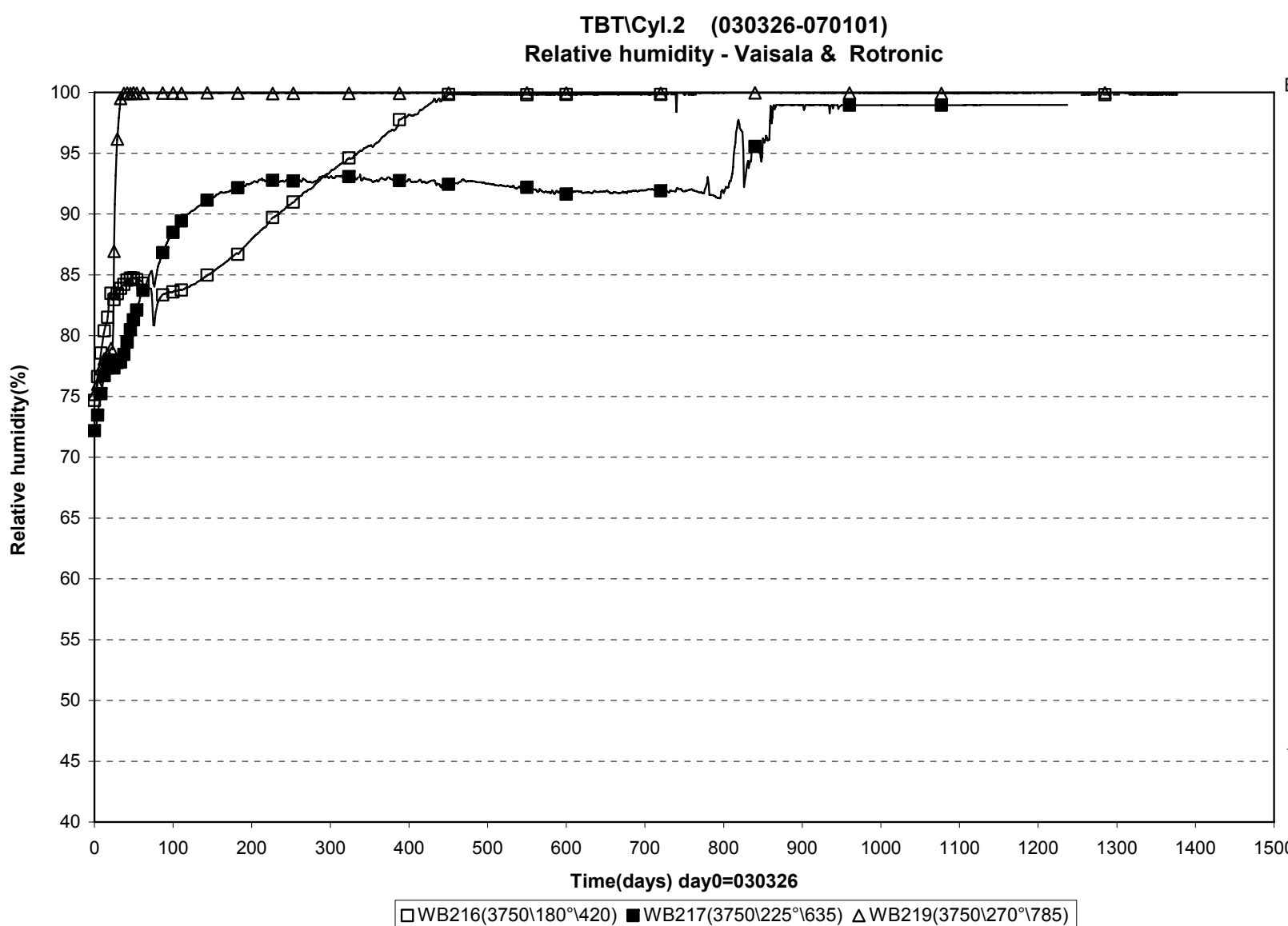


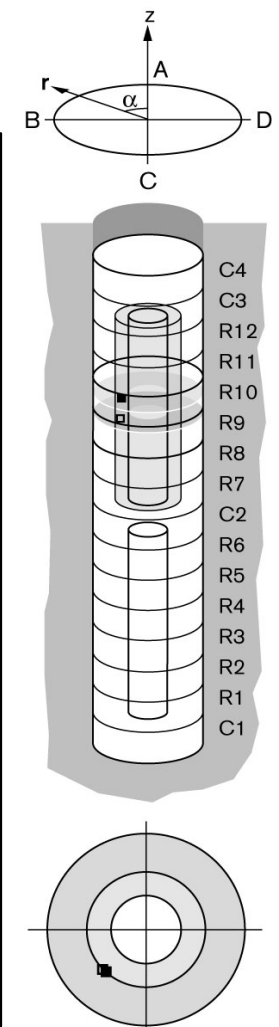
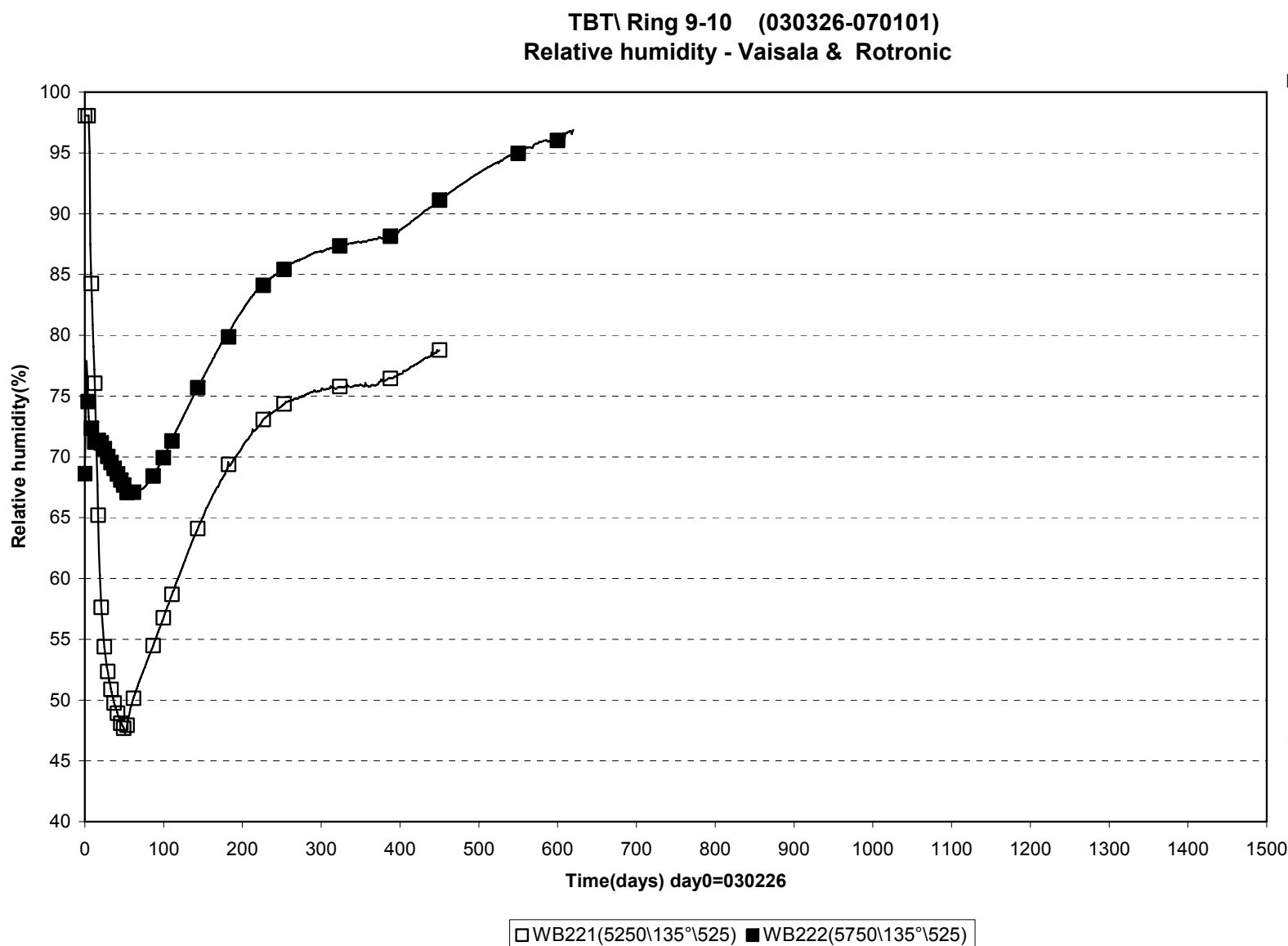


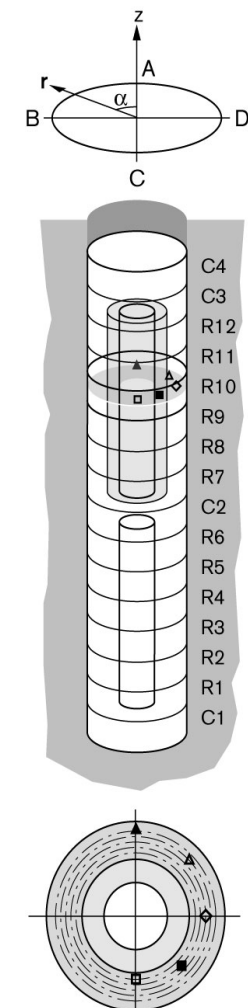
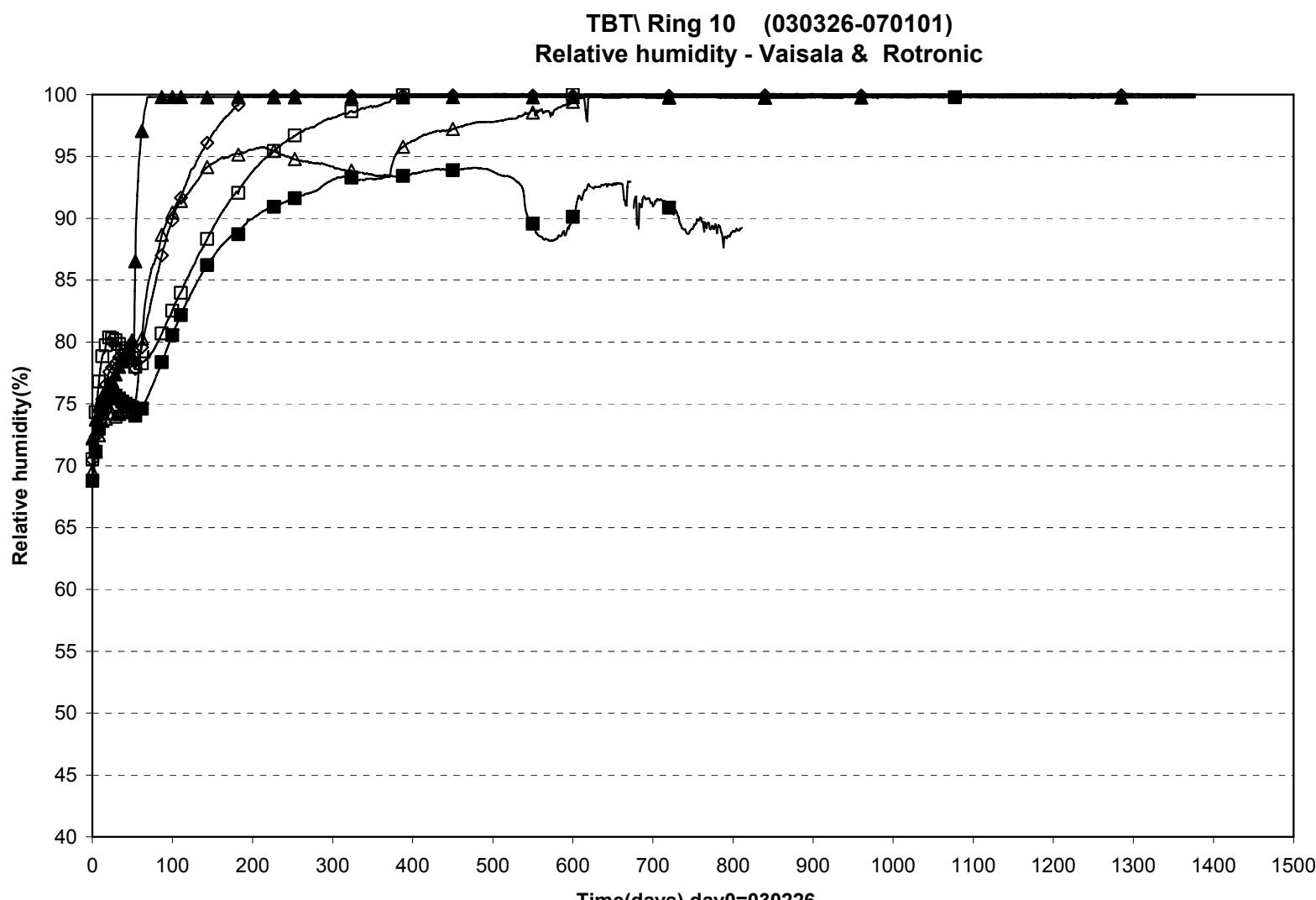


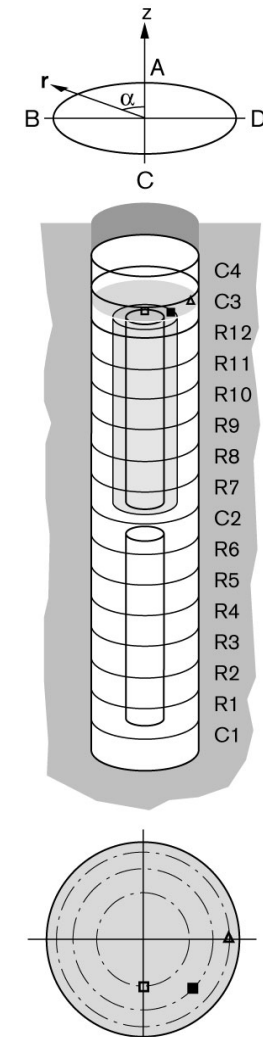
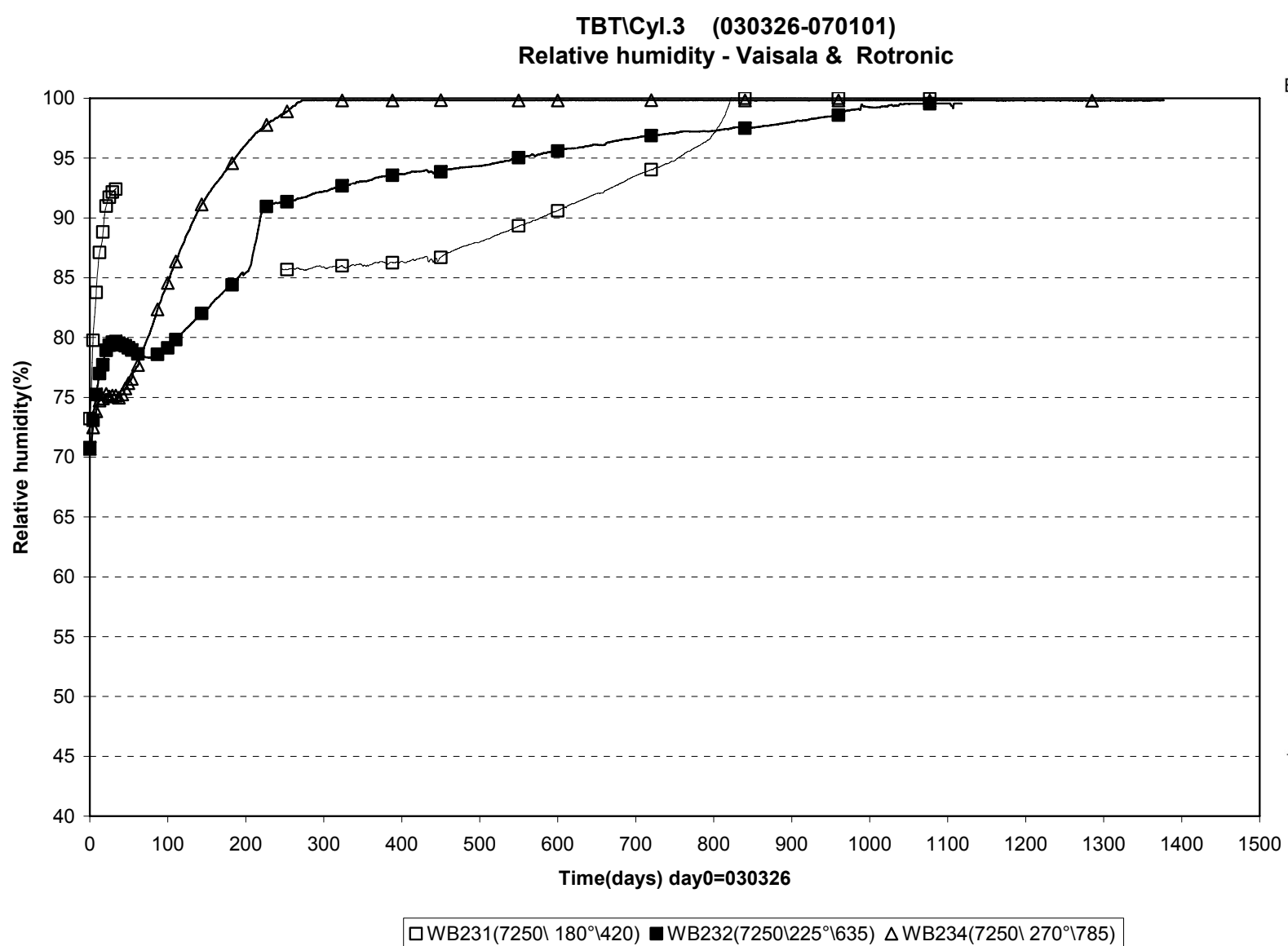


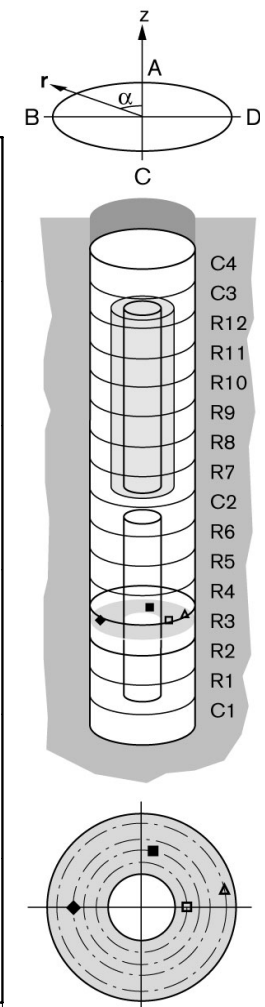
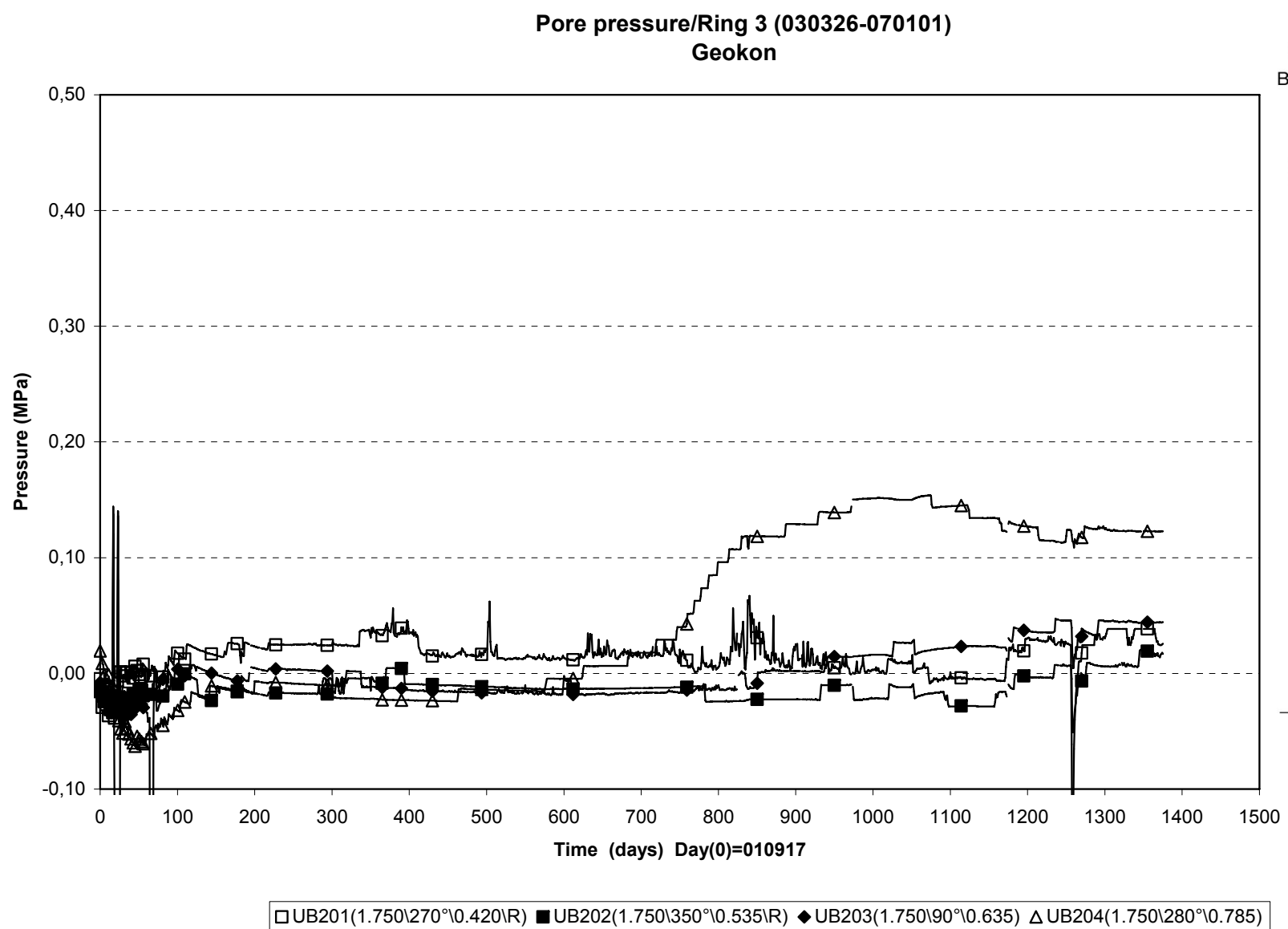


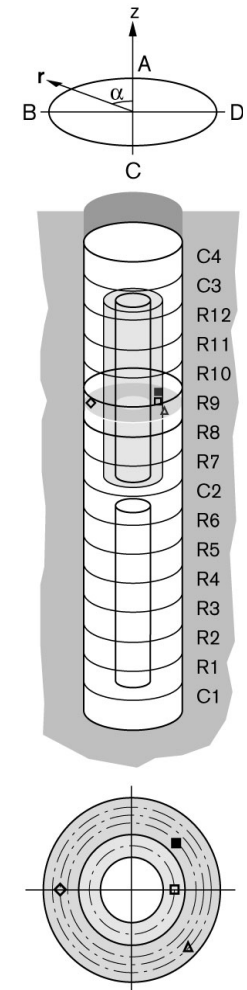
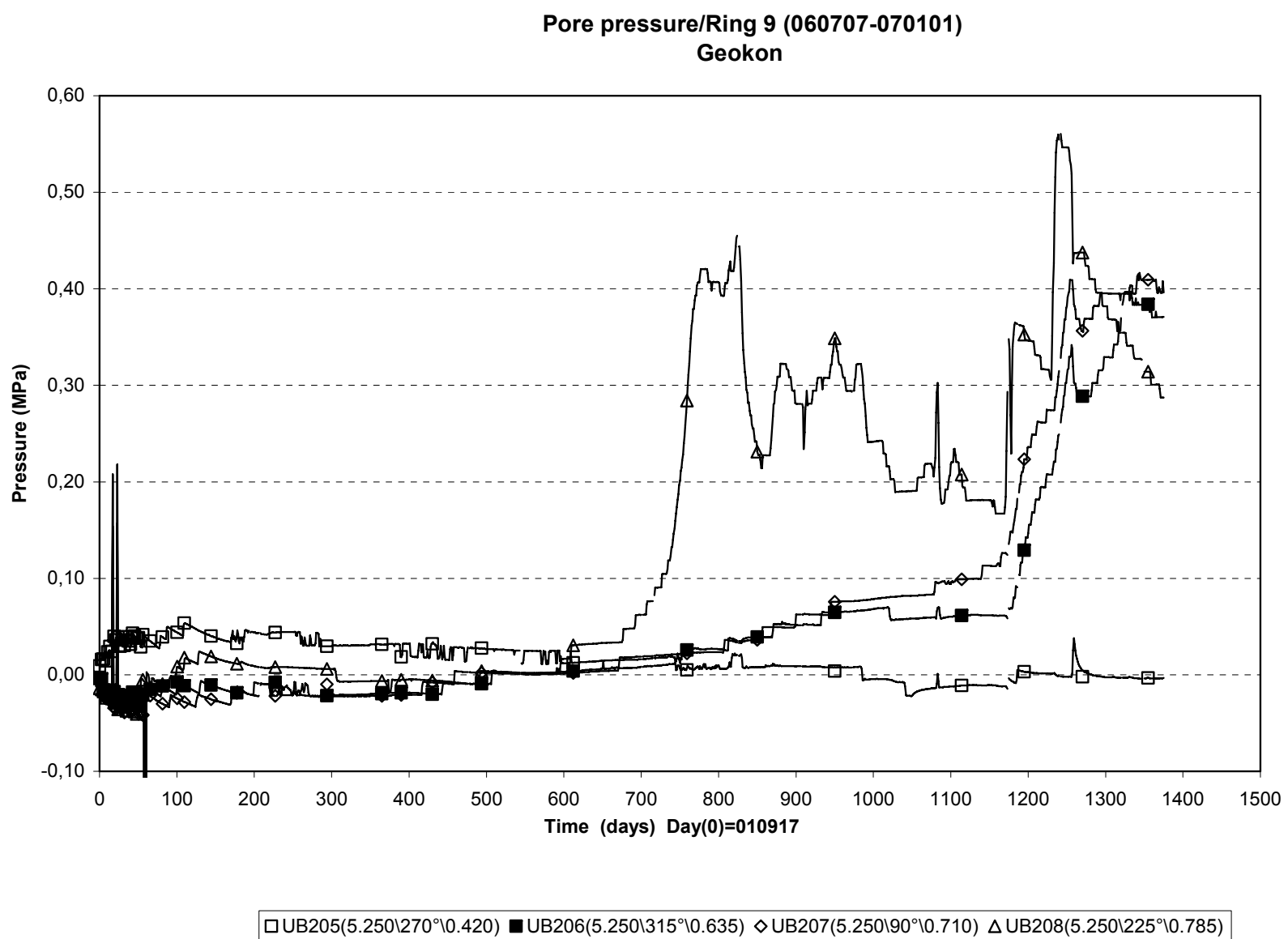




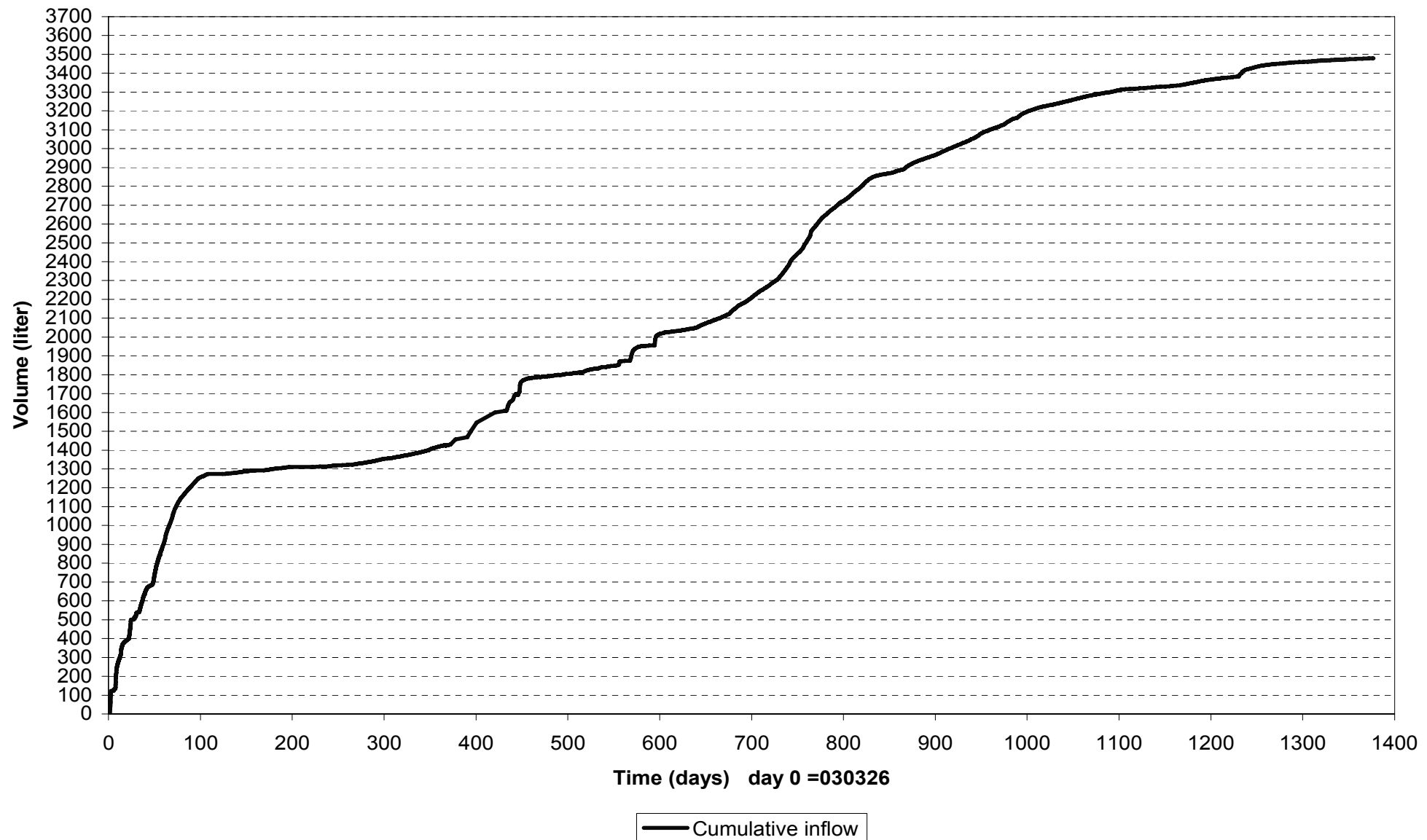




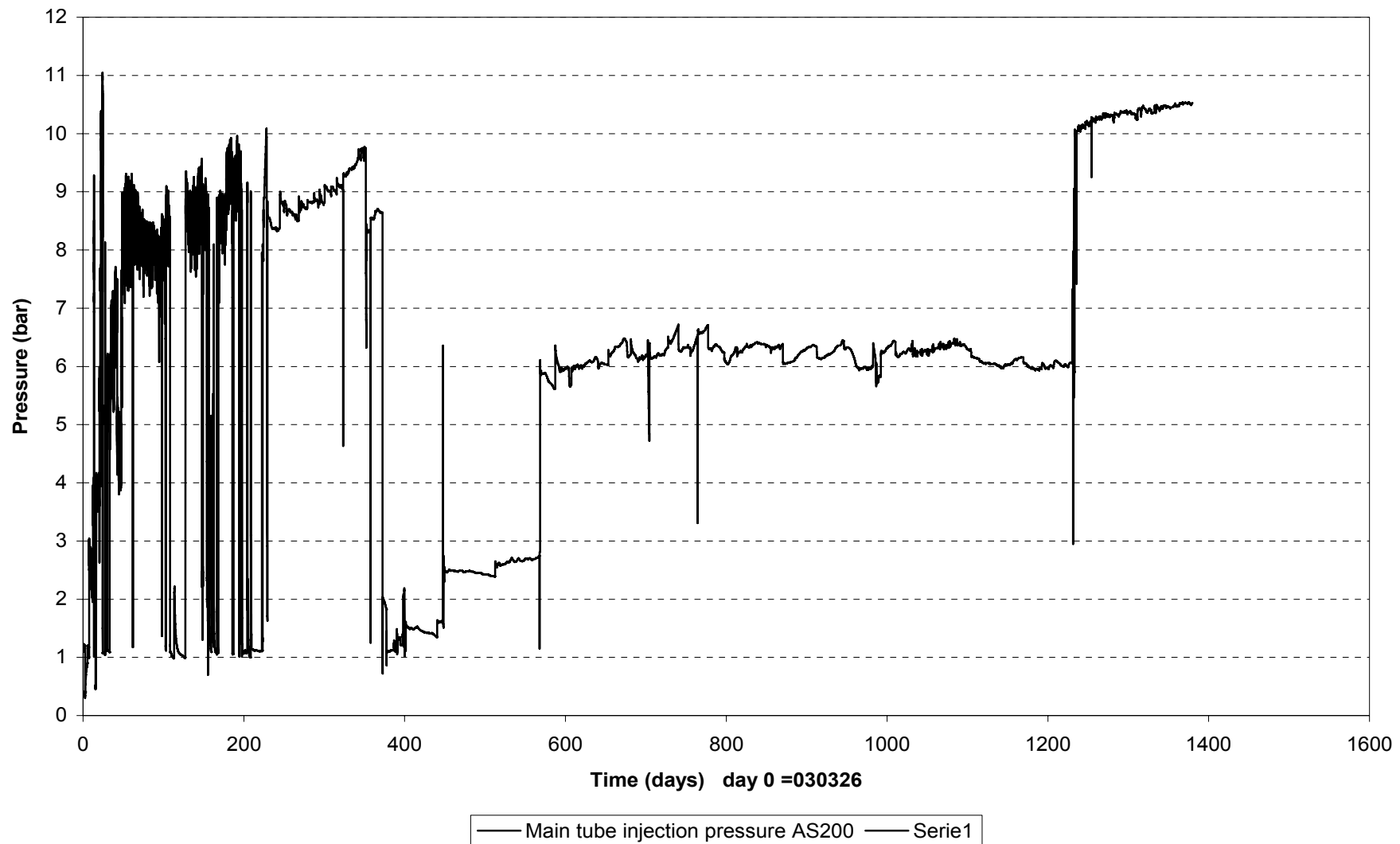




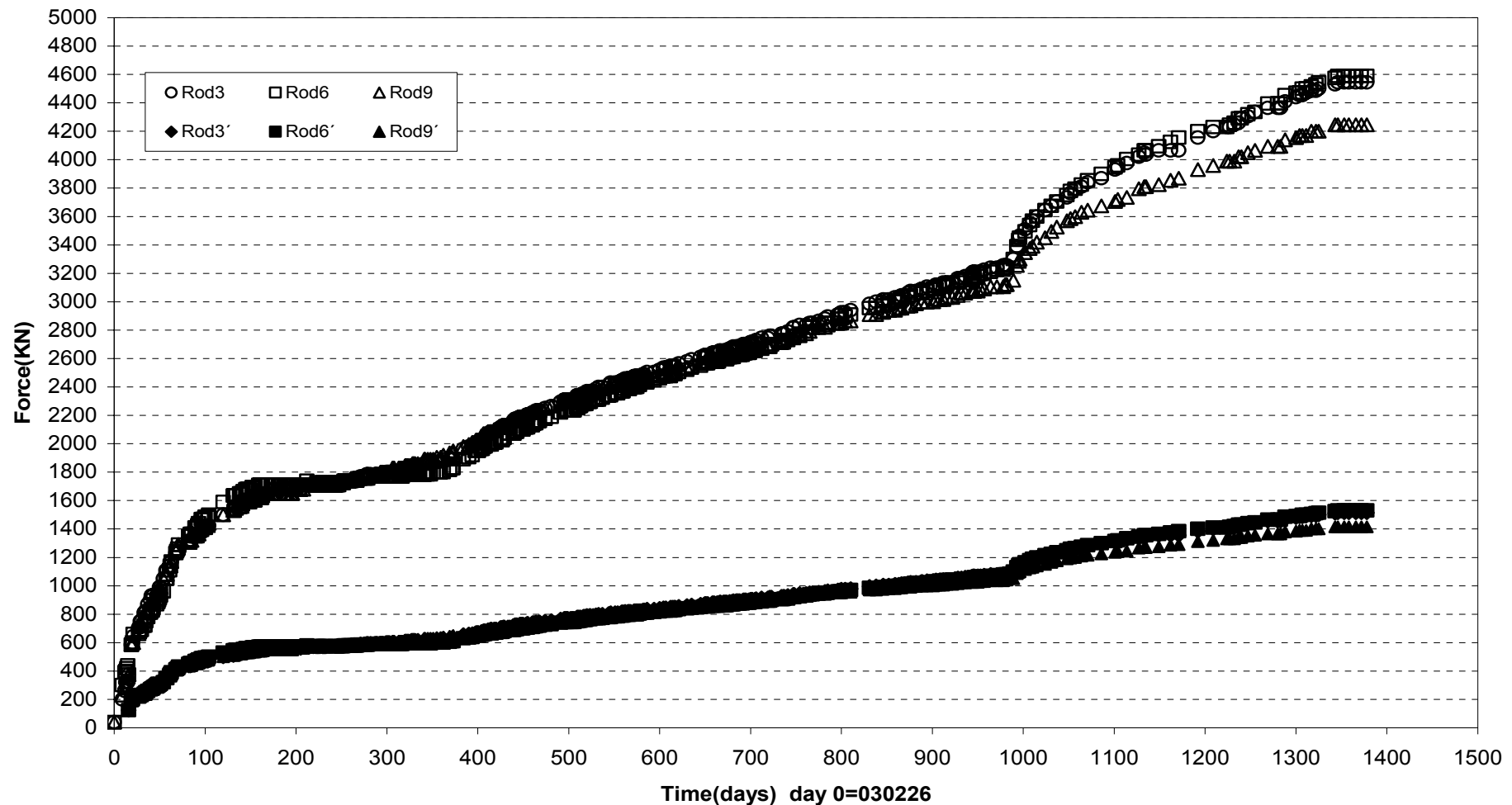
Inflow of water (030326-070101)



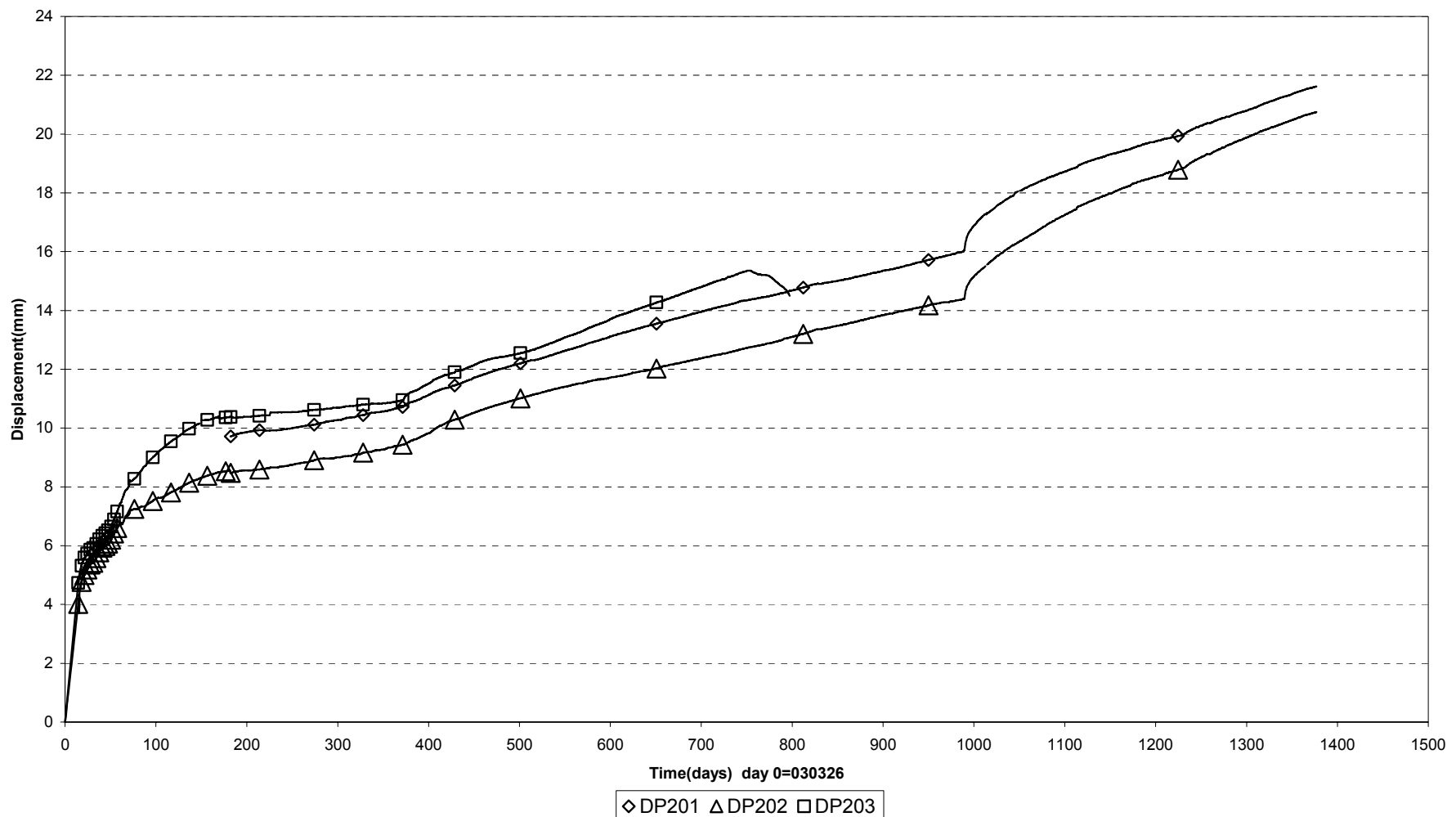
Injection pressure upstream the filter tips (030326-070101)



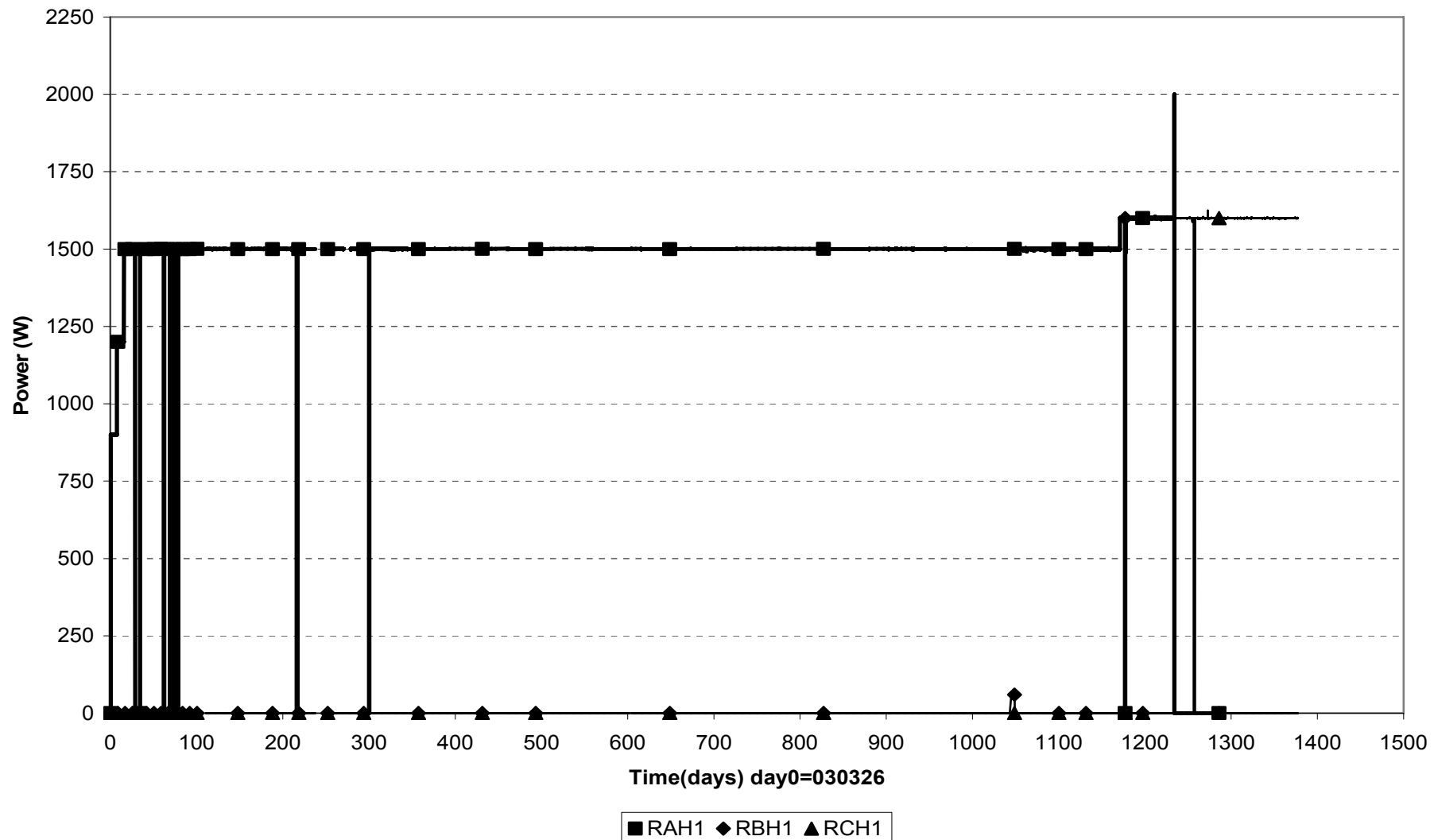
Forces on plug (030326-070101)



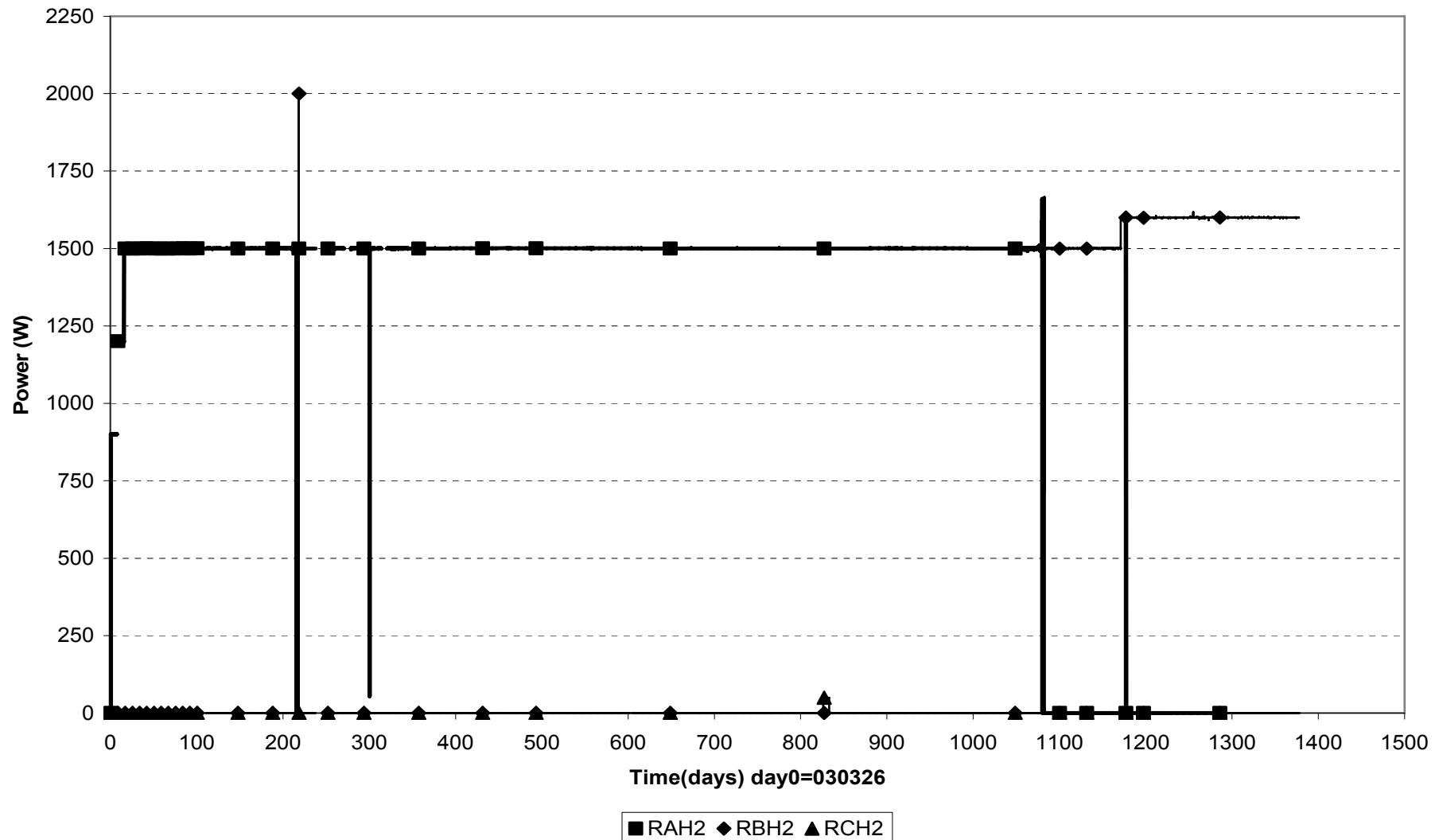
Displacement of plug (030326-070101)

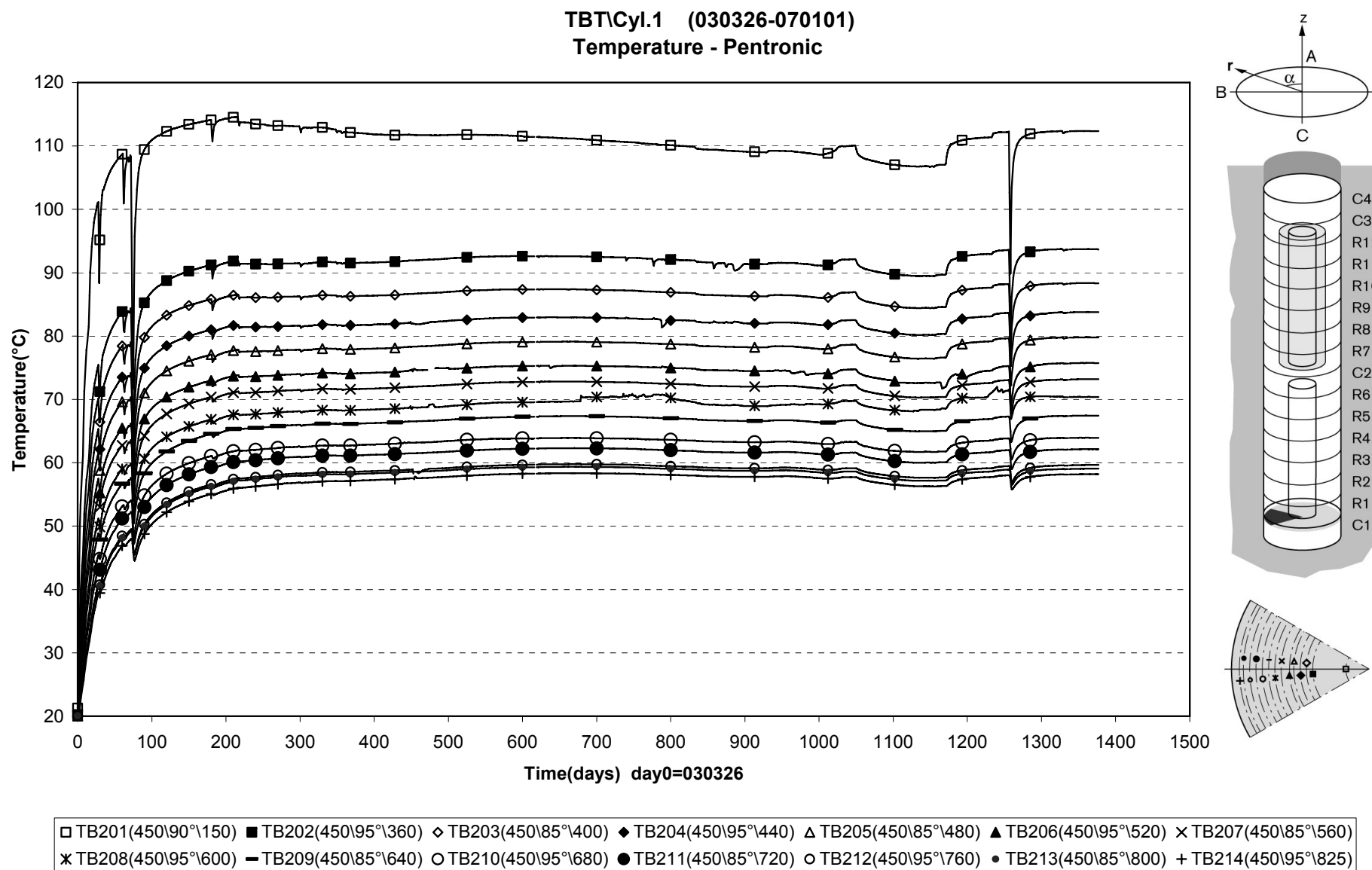


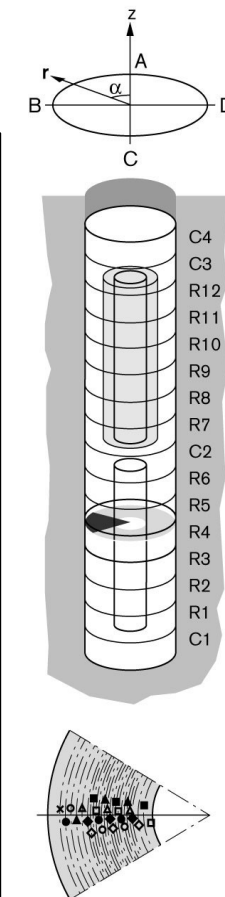
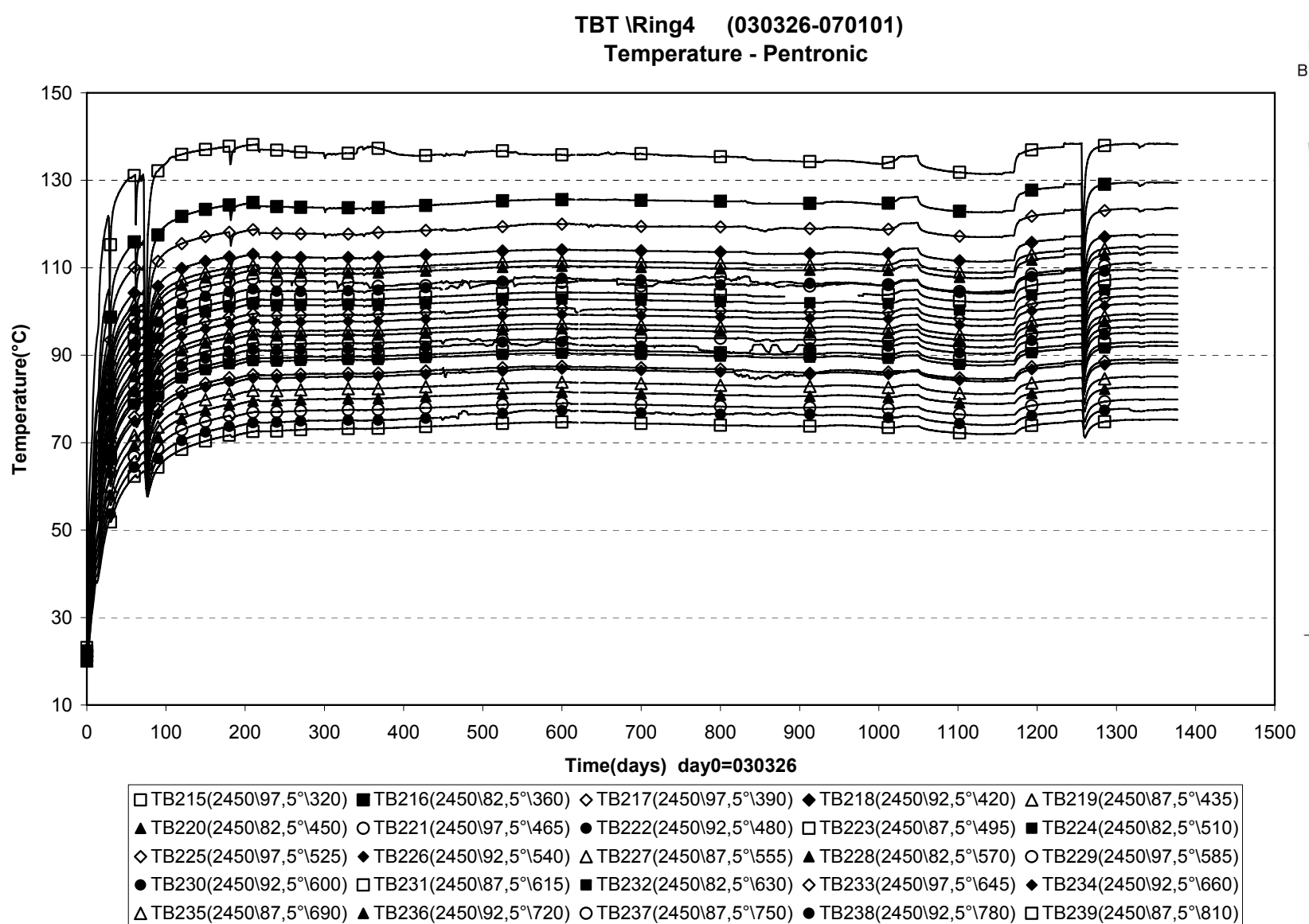
Power Heater 1 (030326-070101)

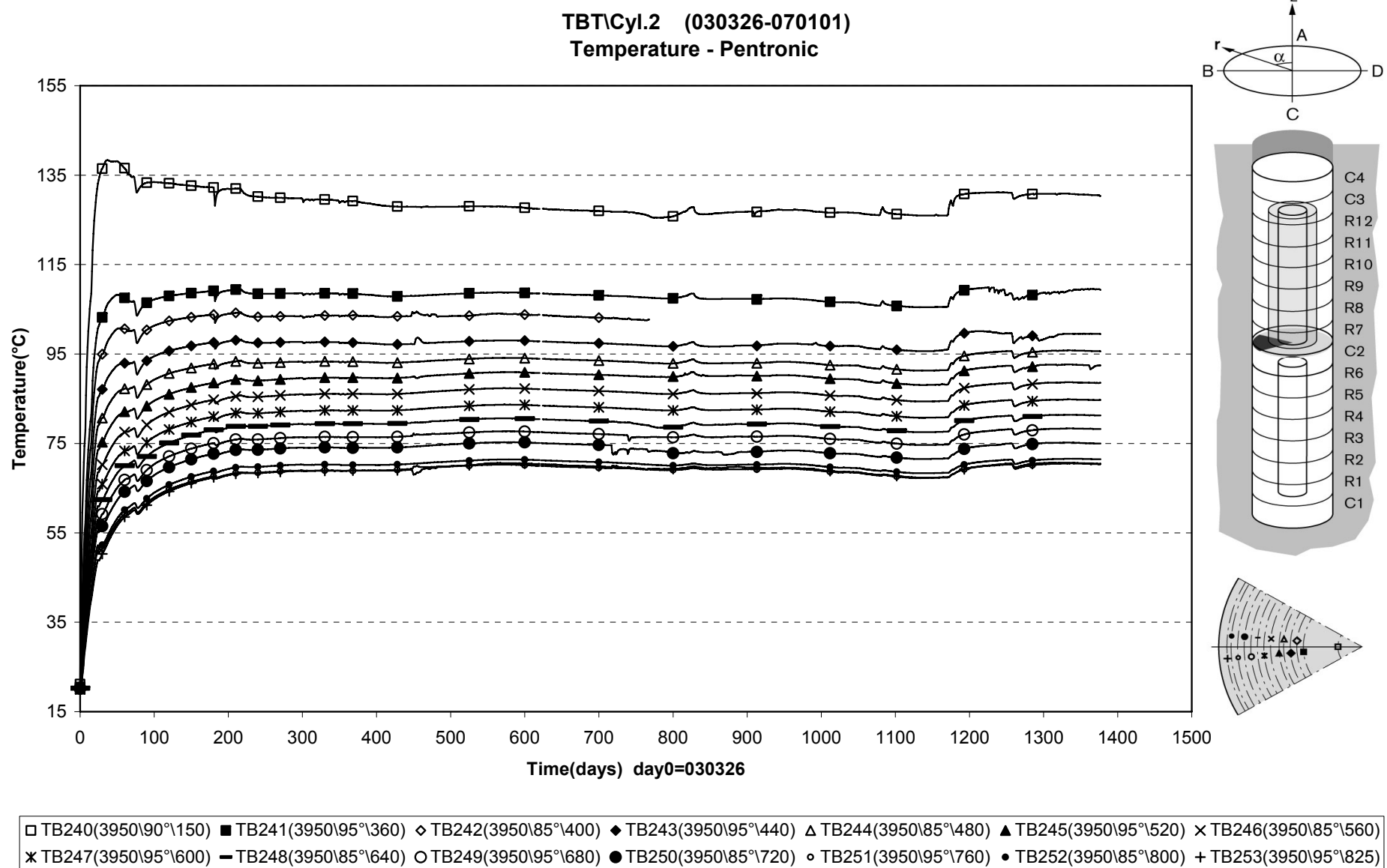


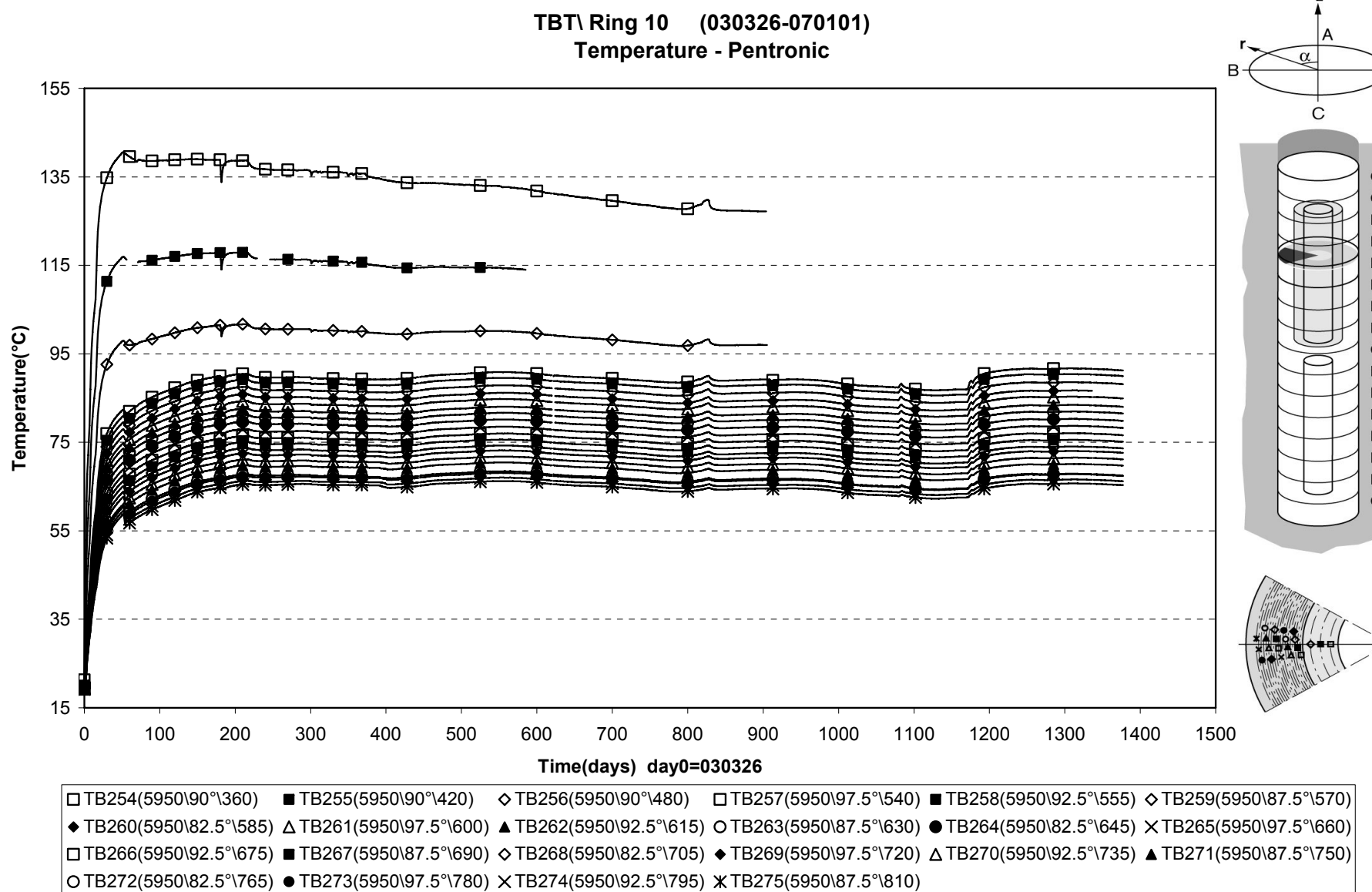
Power Heater 2 (030326-070101)

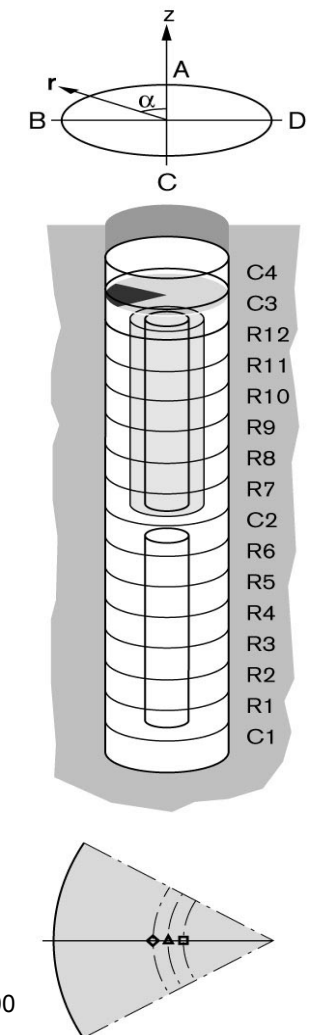
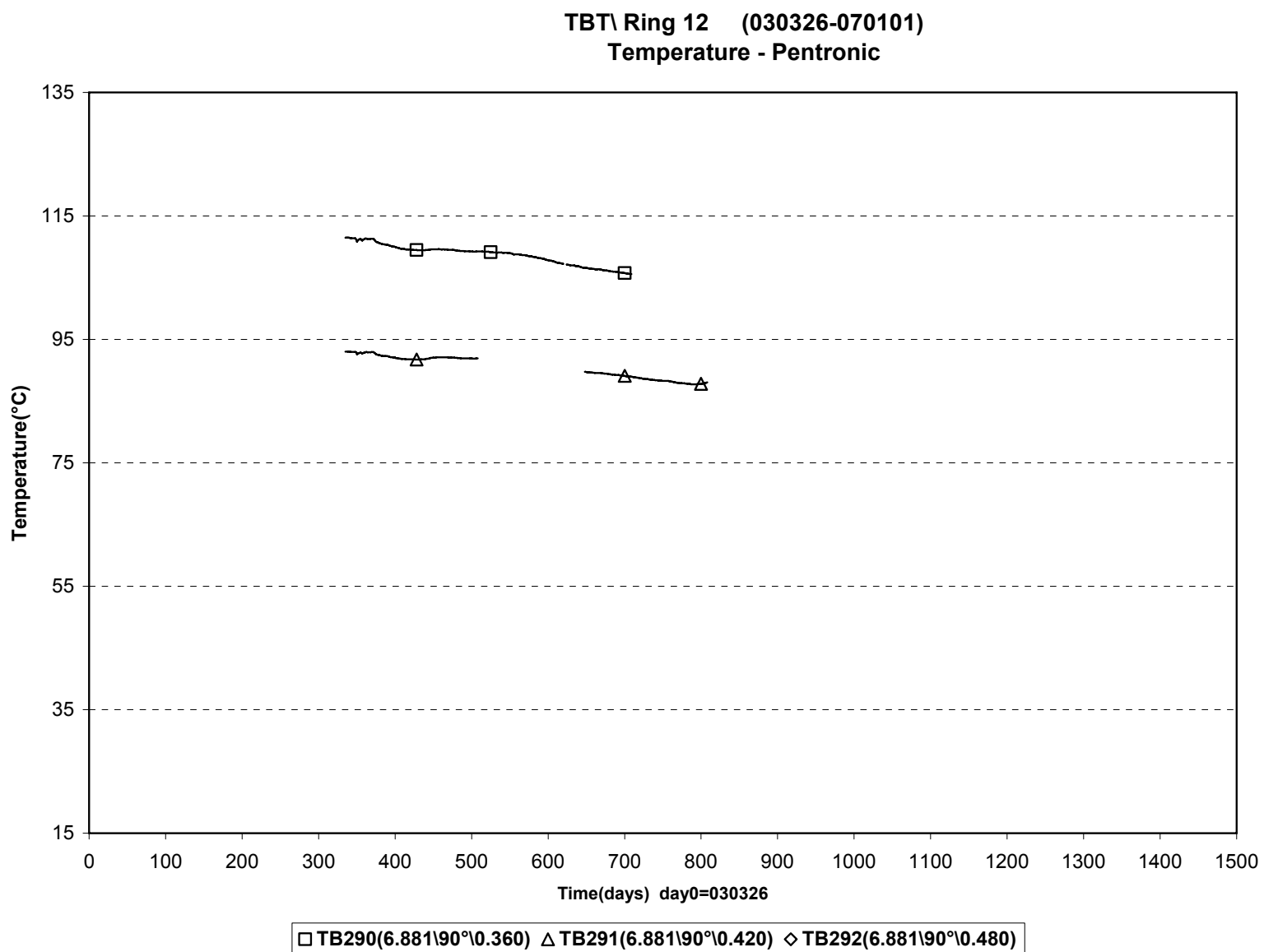




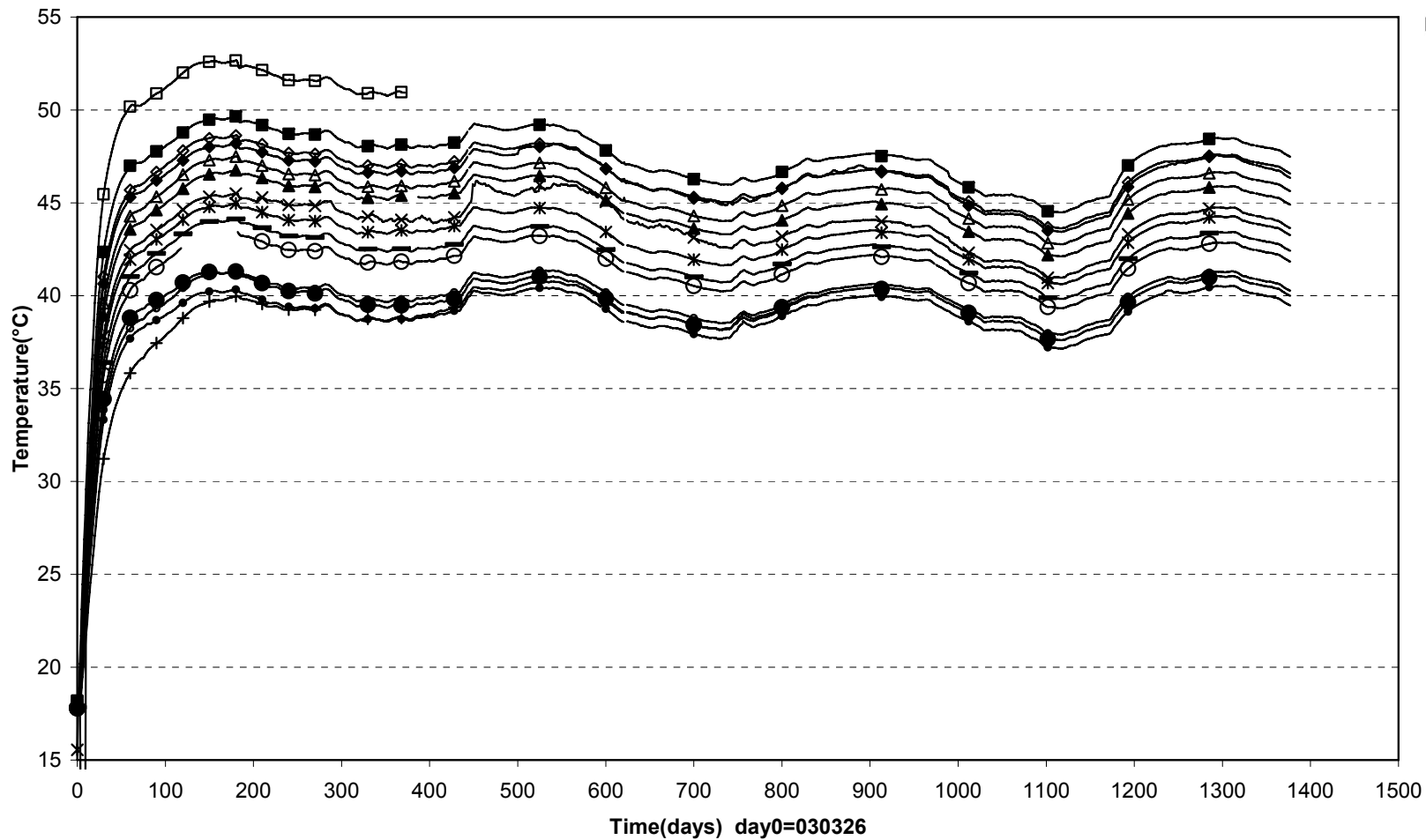




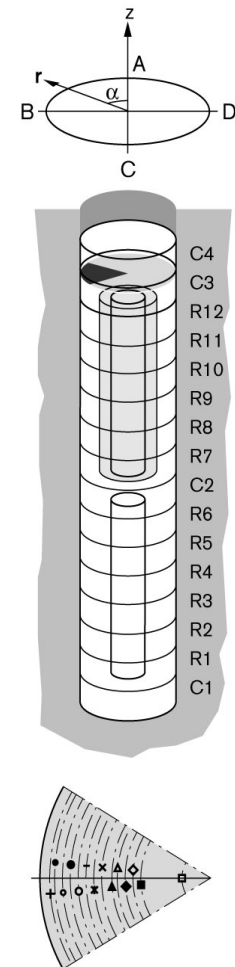




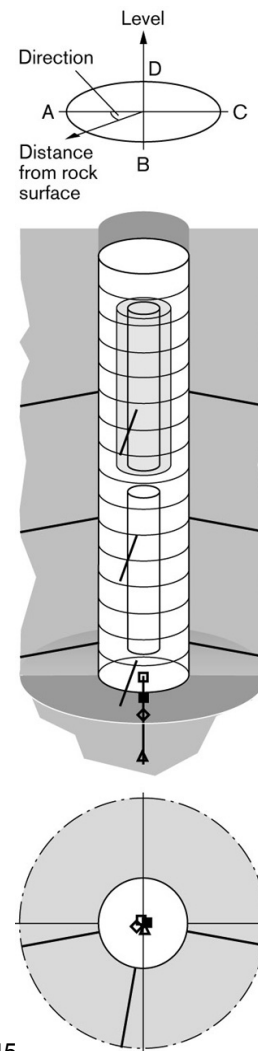
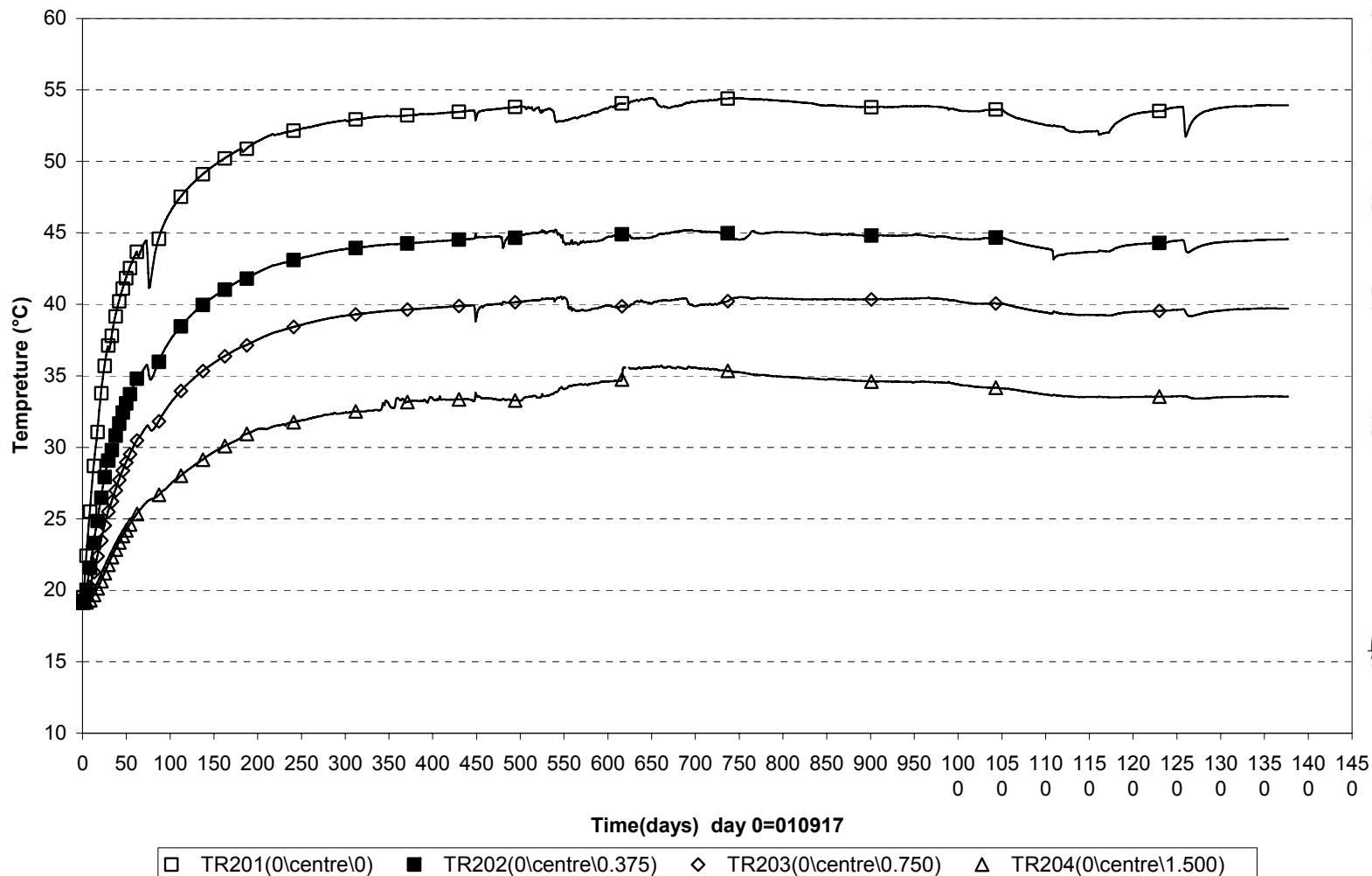
TBT\Cyl.3 (030326-070101)
Temperature - Pentronic



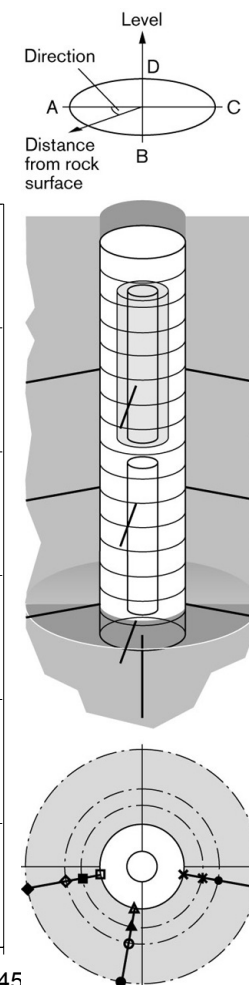
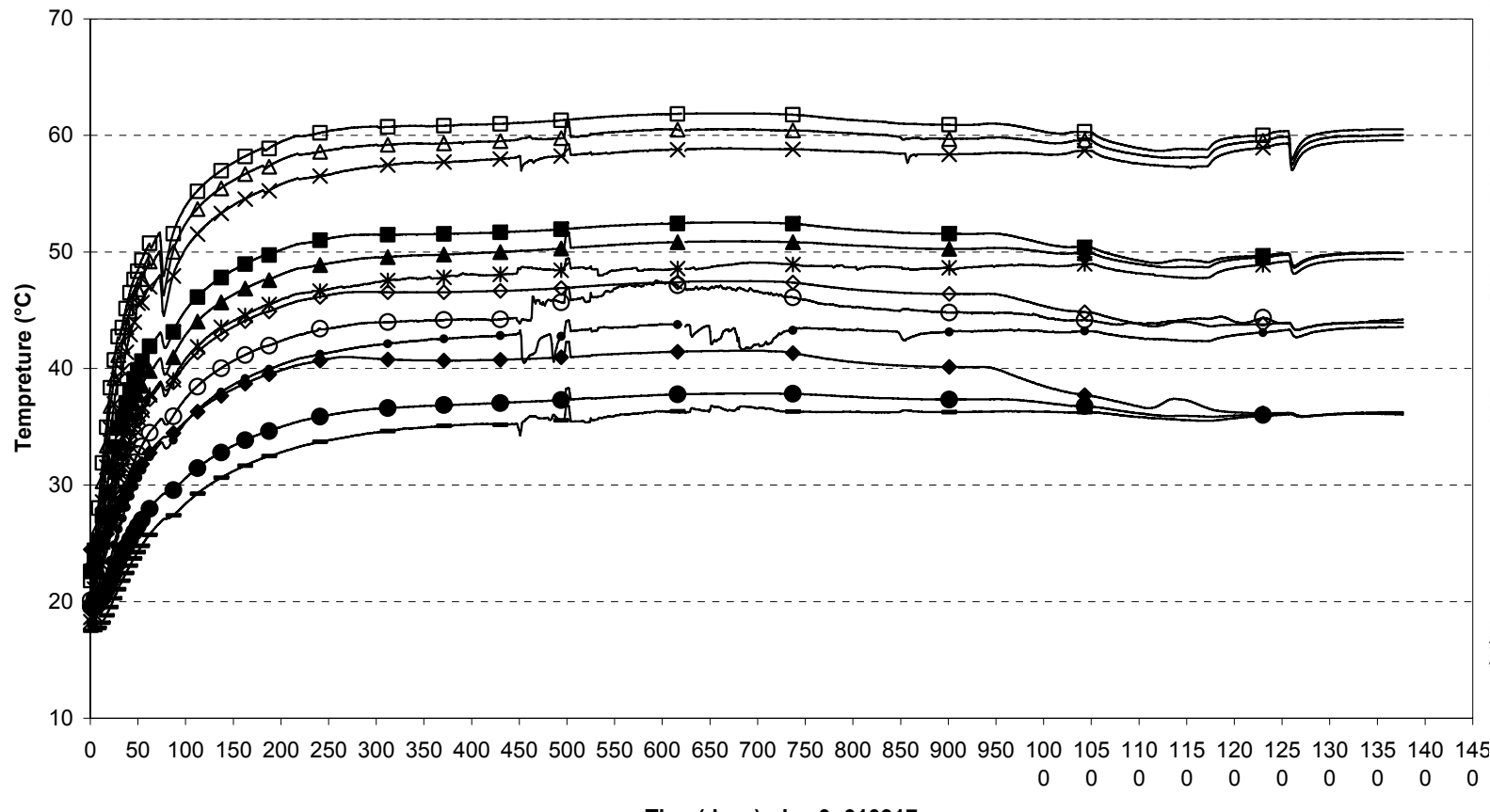
- | | | | | | | |
|-----------------------|-----------------------|-----------------------|-----------------------|-----------------------|-----------------------|-----------------------|
| □ TB276(7450\90°\150) | ■ TB277(7450\95°\360) | ◇ TB278(7450\85°\400) | ◆ TB279(7450\95°\440) | △ TB280(7450\85°\480) | ▲ TB281(7450\95°\520) | × TB282(7450\85°\560) |
| * TB283(7450\95°\600) | - TB284(7450\85°\640) | ○ TB285(7450\95°\680) | ● TB286(7450\85°\720) | ◦ TB287(7450\95°\760) | • TB288(7450\85°\800) | + TB289(7450\95°\825) |



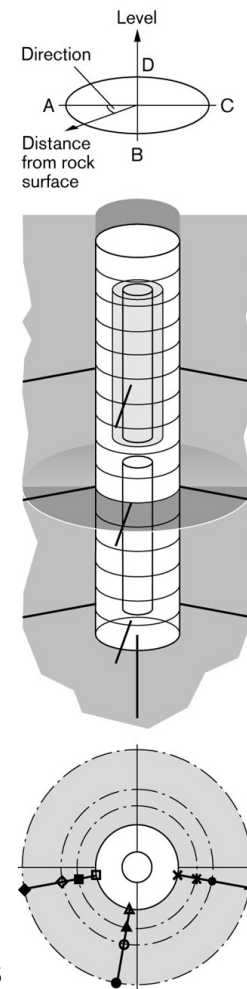
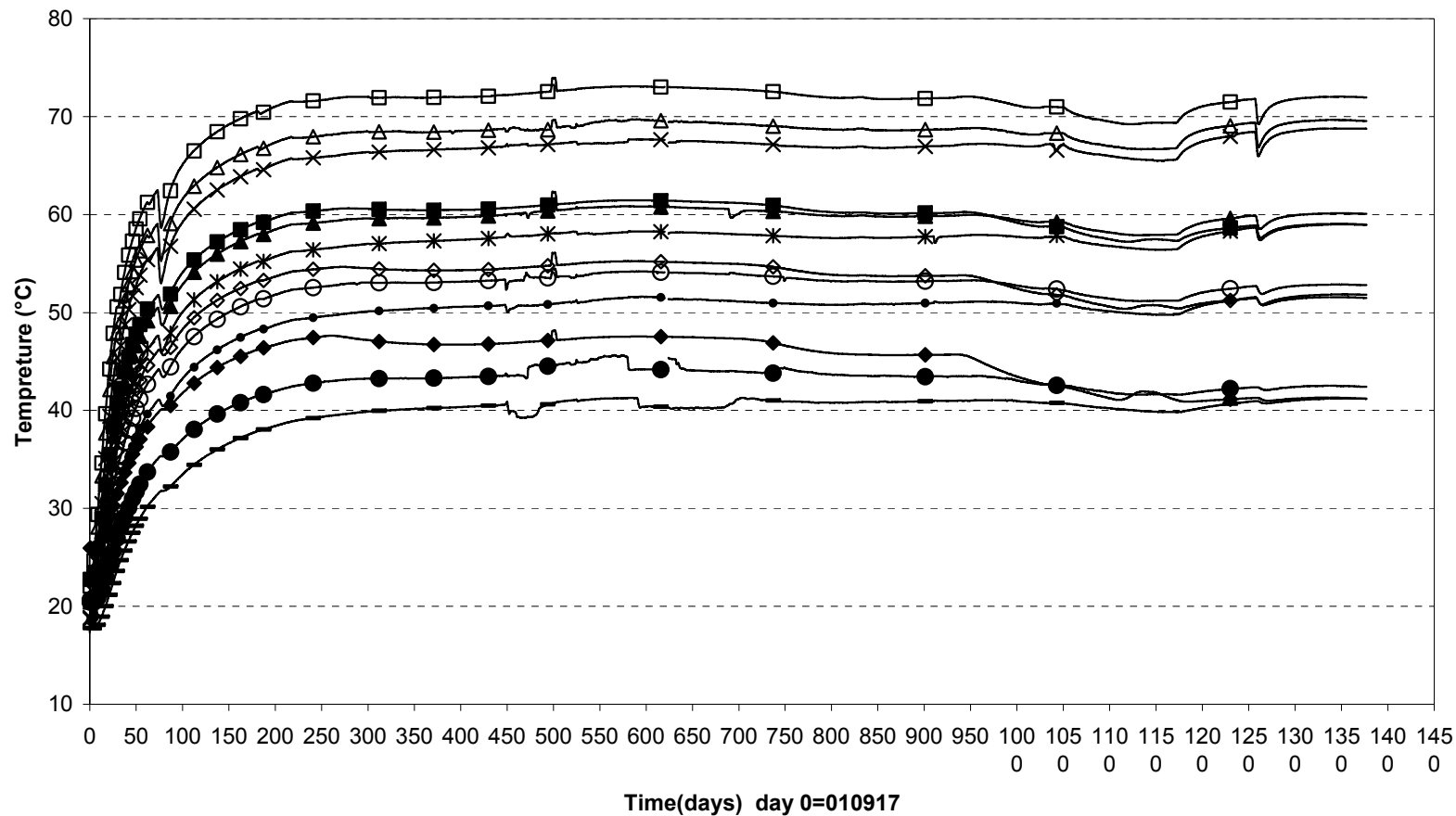
TBT\ Temperature in the rock-below the dep.hole (030326-070101)
Temperature - Pentronic



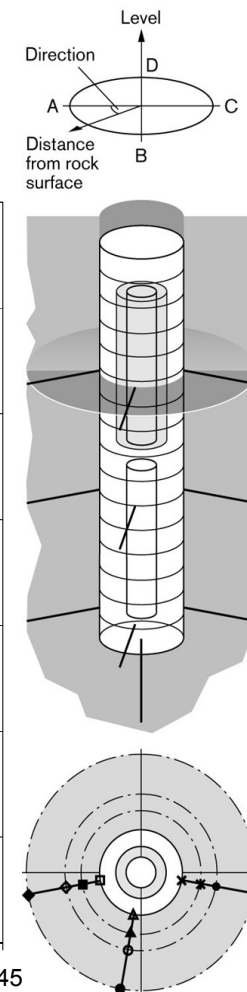
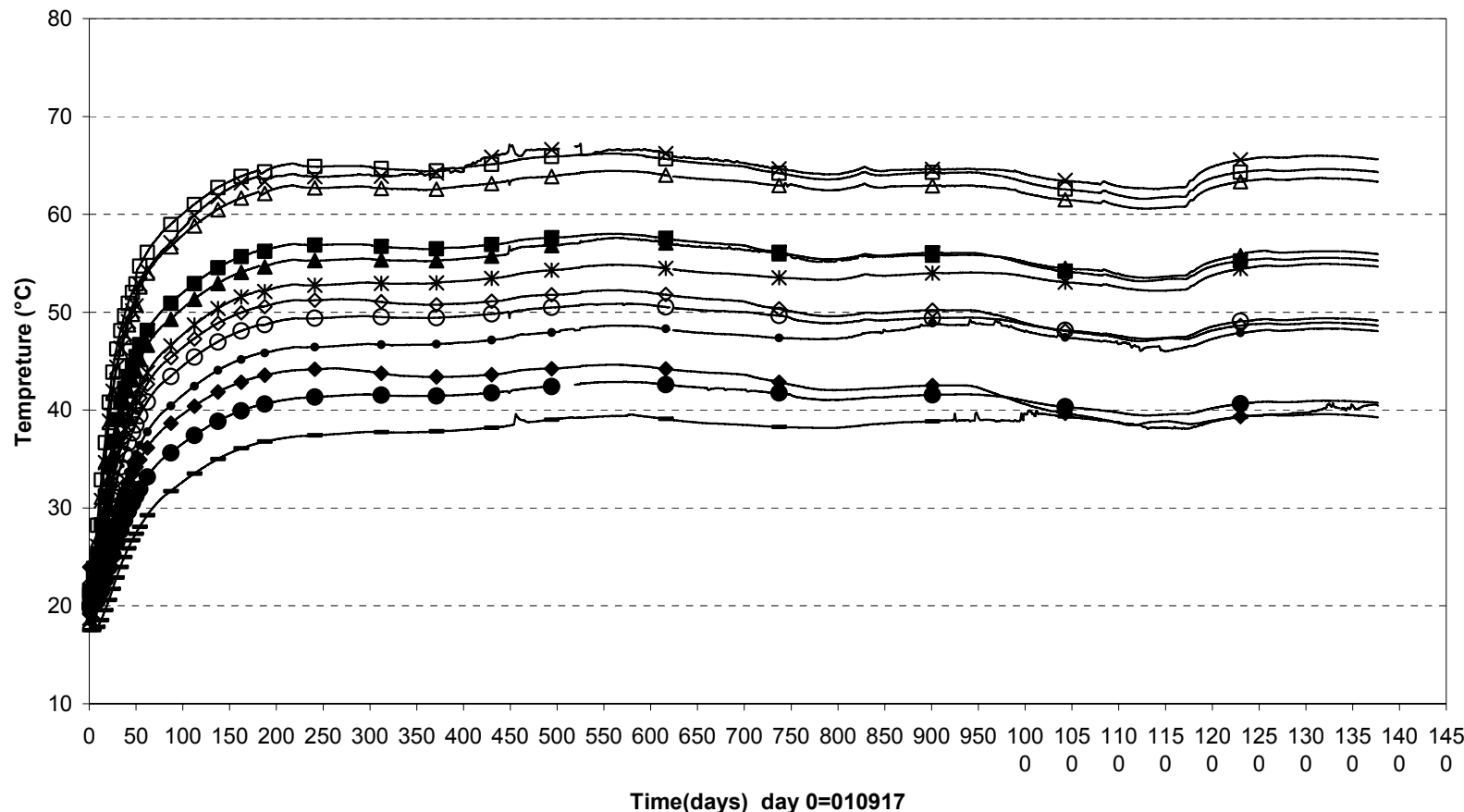
TBT\ Temperature in the rock-level 0,61 m (030326-070101)
 Temperature - Pentronic



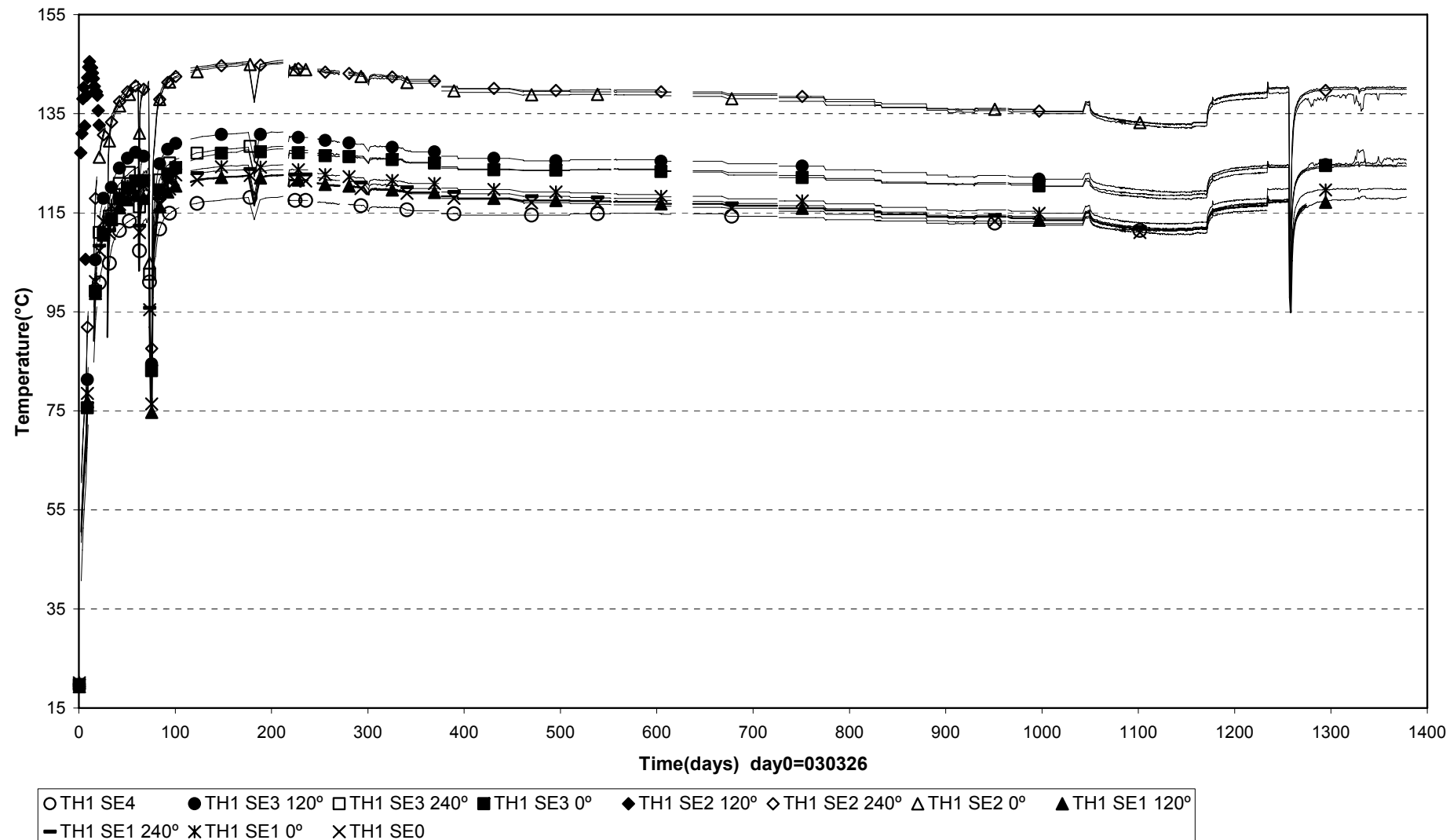
TBT\ Temperature in the rock-level 3,01 m (030326-070101)
 Temperature - Pentronic



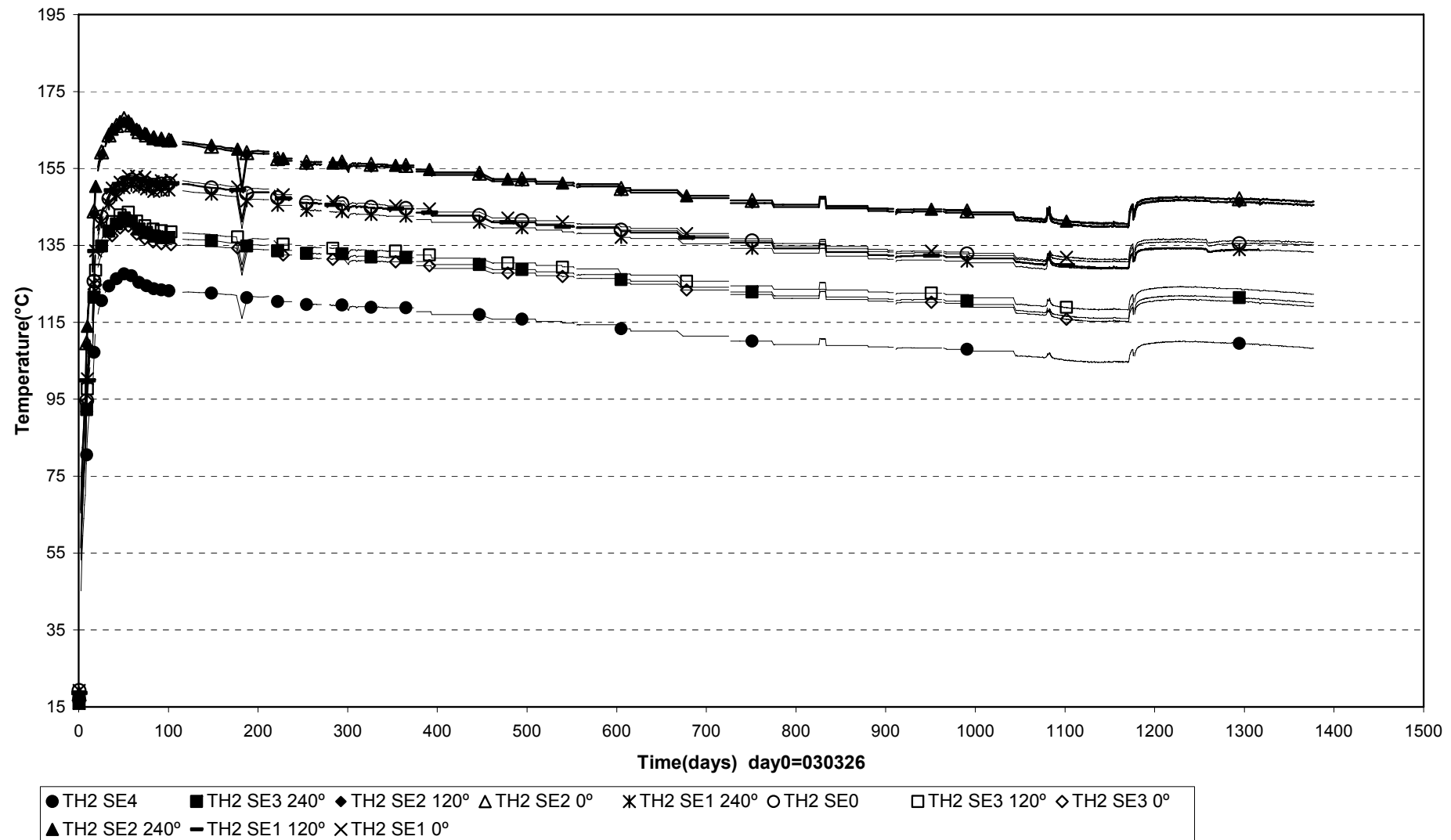
TBT\ Temperature in the rock-level 5,41 m (030326-070101)
 Temperature - Pentronic



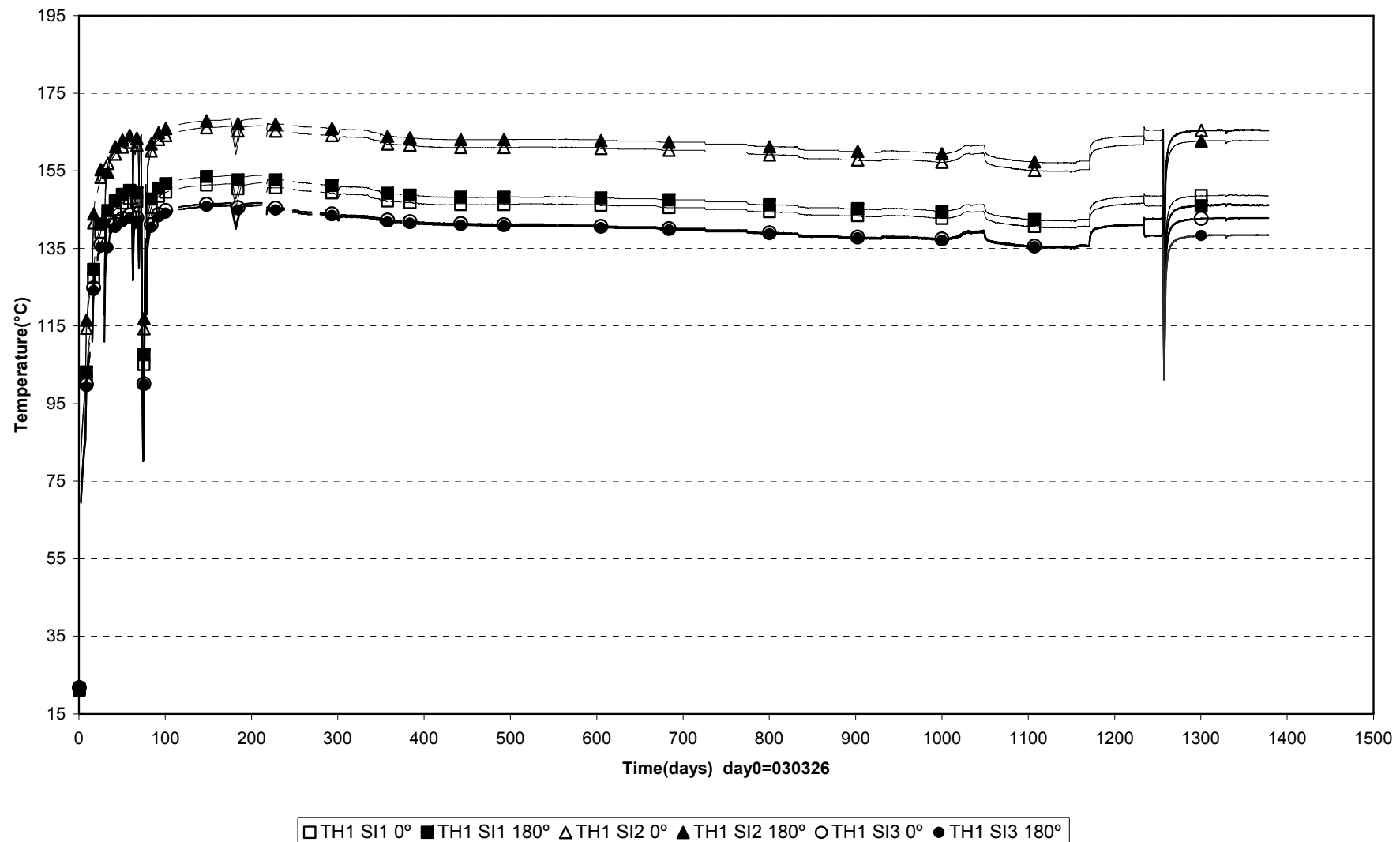
External temperatures Heater 1 (030326-070101)



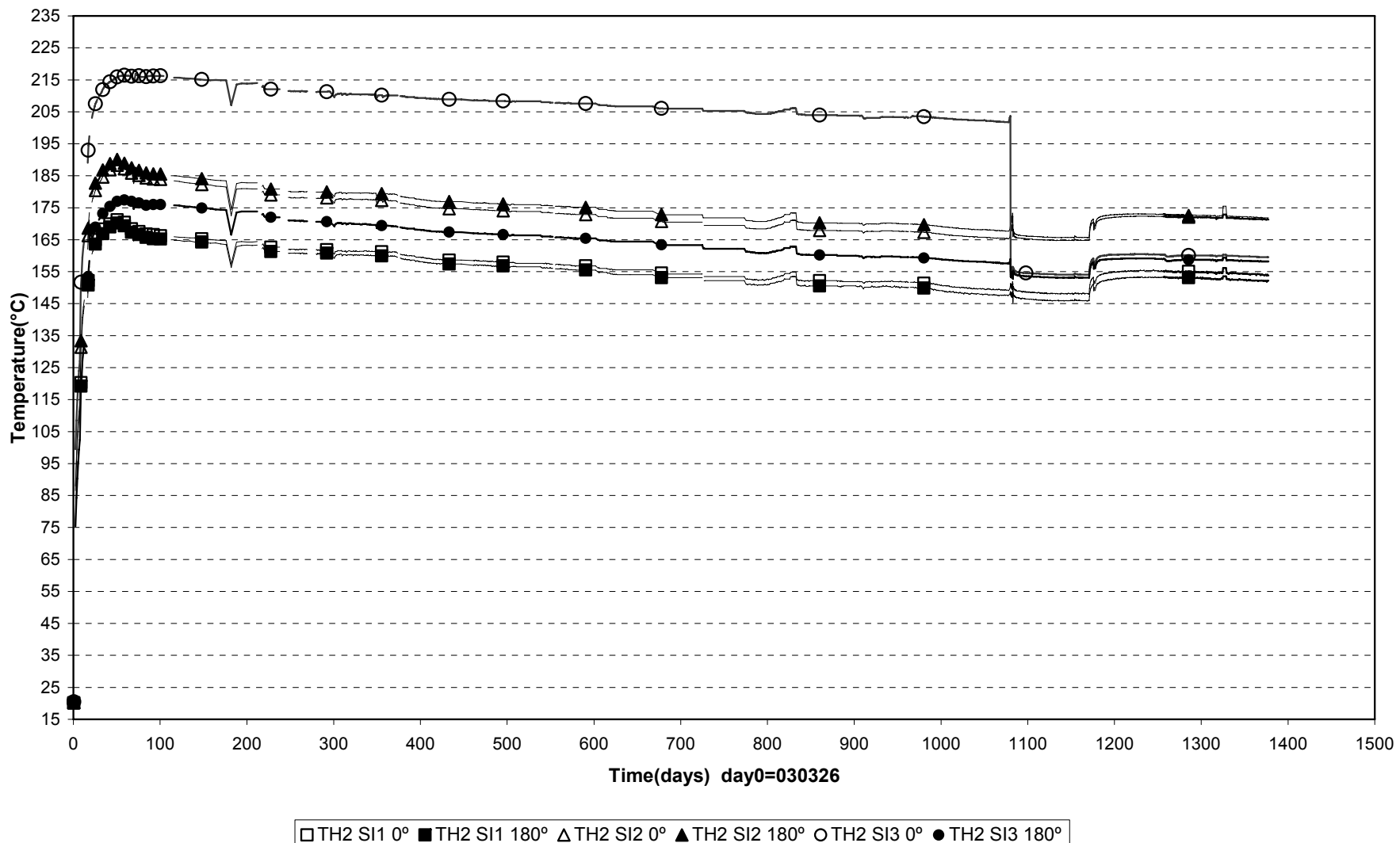
External temperatures Heater 2 (030326-070101)



Internal temperatures Heater 1 (030326-070101)



Internal temperatures Heater 2 (030326-070101)



Appendix B

Measurement from optiska sensors

DBE Technology

Fiber Optic sensors in TBT

The high temperatures and the corrosive environment yield extreme requirements on the sensor material. Never before fiber optic sensors from DBE have been implemented under these conditions and thus a few optical pressure and temperature sensors have been installed for evaluation purposes.

Two pressure sensors and two pore water pressure sensors have been installed each including a low resolution temperature grating for compensation purposes. Figure 1 and 2 show the location of each sensor in addition to all the other sensors.

Data from PB231 has presented in this report .The other three sensors are out of order.

Table 1. Numbering and position of the instruments referred to in this report

| Instrument number | Measuring section | Block | α [deg] | r [mm] | z [mm] | Remark |
|-------------------|-------------------|---------------|-------------------|------------|-------------|--|
| PB204 | 2 | Ring3 | 250 | 420 | 1950 | Total pressure radial |
| PB205 | 2 | Ring 3 | 290 | 420 | 2000 | Total pressure axial |
| PB206 | 2 | Ring 3 | 0 | 535 | 1950 | Total pressure radial |
| PB207 | 2 | Ring 3 | 20 | 535 | 1950 | Total pressure tangential |
| PB208 | 2 | Ring 3 | 45 | 585 | 2000 | Total pressure axial |
| PB209 | 2 | Ring 3 | 100 | 635 | 1950 | Total pressure tangential |
| PB210 | 2 | Ring 3 | 170 | 710 | 1950 | Total pressure tangential |
| PB211 | 2 | Ring3 | 180 | 710 | 1950 | Total pressure radial |
| PB212 | 2 | Ring 3 | 260 | 770 | 2000 | Total pressure axial |
| PB213 | 2 | Ring 3 | 270 | 875 | 1950 | Total pressure radial on the rock |
| PB230a | 2 | Ring 3 | 180 | 376 | 1950 | Fiber Optic total pressure radial |
| PB230b | 2 | Ring 3 | 180 | 428 | 950 | Fiber Optic temperature |
| | | | | | | |
| PB217 | 5 | Ring 9 | 270 | 535 | 5450 | Total pressure radial against sand |
| PB218 | 5 | Ring 9 | 340 | 635 | 5500 | Total pressure axial |
| PB219 | 5 | Ring 9 | 0 | 635 | 5450 | Total pressure radial |
| PB220 | 5 | Ring 9 | 20 | 635 | 5450 | Total pressure tangential |
| PB221 | 5 | Ring 9 | 70 | 710 | 5500 | Total pressure axial |
| PB222 | 5 | Ring 9 | 110 | 710 | 5450 | Total pressure radial |
| PB223 | 5 | Ring 9 | 160 | 770 | 5500 | Total pressure axial |
| PB224 | 5 | Ring 9 | 180 | 770 | 5450 | Total pressure radial |
| PB225 | 5 | Ring 9 | 200 | 770 | 5450 | Total pressure tangential |
| PB226 | 5 | Ring 9 | 270 | 875 | 5450 | Total pressure radial on the rock |
| PB231a | 5 | Ring 9 | 180 | 573 | 5450 | Fiber Optic total pressure radial |
| PB231b | 5 | Ring 9 | 180 | 608 | 5450 | Fiber Optic temperature |

| | | | | | | |
|---------------|----------|---------------|------------|------------|-------------|--|
| UB201 | 2 | Ring 3 | 270 | 420 | 1750 | Pore pressure |
| UB202 | 2 | Ring 3 | 350 | 535 | 1750 | Pore pressure |
| UB203 | 2 | Ring 3 | 90 | 635 | 1750 | Pore pressure |
| UB204 | 2 | Ring 3 | 280 | 785 | 1750 | Pore pressure |
| UB209a | 2 | Ring 3 | 190 | 495 | 1750 | Fiber Optic pore pressure |
| UB209b | 2 | Ring 3 | 190 | 555 | 1750 | Fiber Optic temperature |
| UB205 | 5 | Ring 9 | 270 | 420 | 5250 | Pore pressure |
| UB206 | 5 | Ring 9 | 315 | 635 | 5250 | Pore pressure |
| UB207 | 5 | Ring 9 | 90 | 710 | 5250 | Pore pressure |
| UB208 | 5 | Ring 9 | 225 | 785 | 5250 | Pore pressure |
| UB210 | 5 | Ring 9 | 160 | 420 | 5250 | Fiber Optic pore pressure and temp. |
| TB215 | 3 | Ring 4 | 97.5 | 320 | 2450 | Pentronic thermocouple thermometer |
| TB216 | 3 | Ring 4 | 82.5 | 360 | 2450 | Pentronic thermocouple thermometer |
| TB217 | 3 | Ring 4 | 97.5 | 390 | 2450 | Pentronic thermocouple thermometer |
| TB218 | 3 | Ring 4 | 92.5 | 420 | 2450 | Pentronic thermocouple thermometer |
| TB222 | 3 | Ring 4 | 92.5 | 480 | 2450 | Pentronic thermocouple thermometer |
| TB229 | 3 | Ring 4 | 97.5 | 585 | 2450 | Pentronic thermocouple thermometer |
| TB235 | 3 | Ring 4 | 87.5 | 690 | 2450 | Pentronic thermocouple thermometer |
| TB239 | 3 | Ring 4 | 87.5 | 810 | 2450 | Pentronic thermocouple thermometer |
| TB254 | 6 | Ring 10 | 90 | 360 | 5950 | Pentronic thermocouple thermometer |
| TB255 | 6 | Ring 10 | 90 | 420 | 5950 | Pentronic thermocouple thermometer |
| TB256 | 6 | Ring 10 | 90 | 480 | 5950 | Pentronic thermocouple thermometer |
| TB260 | 6 | Ring 10 | 82.5 | 585 | 5950 | Pentronic thermocouple thermometer |
| TB267 | 6 | Ring 10 | 87.5 | 690 | 5950 | Pentronic thermocouple thermometer |
| TB275 | 6 | Ring 10 | 87.5 | 810 | 5950 | Pentronic thermocouple thermometer |

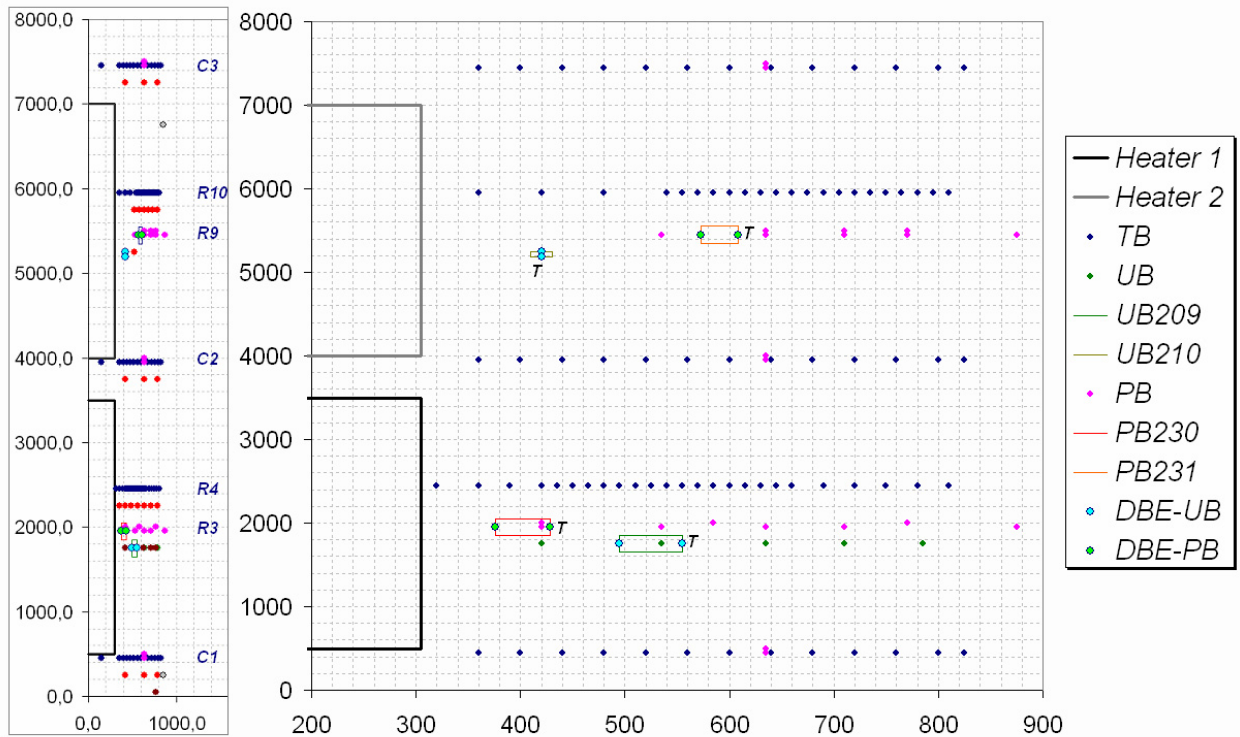


Fig. 1. Vertical location and radial distance of each sensor in mm

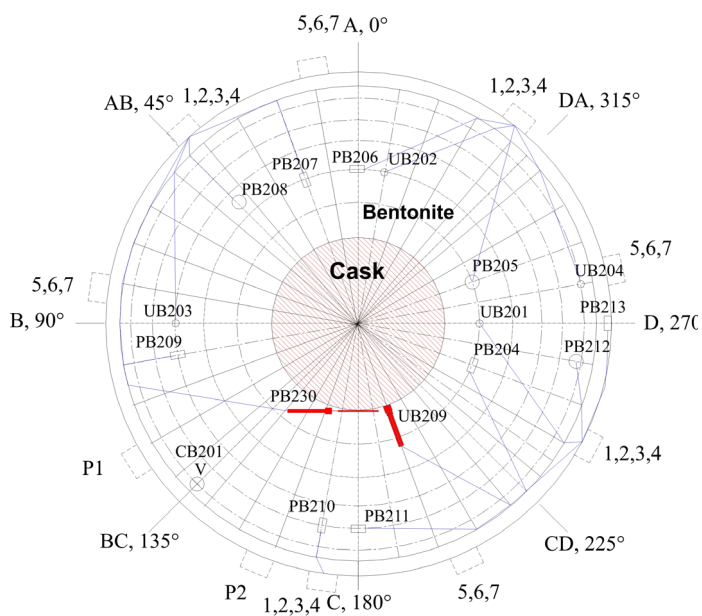


Fig. 2a. Radial location of sensors in Ring 3 horizontal cross-sections of the lower canister

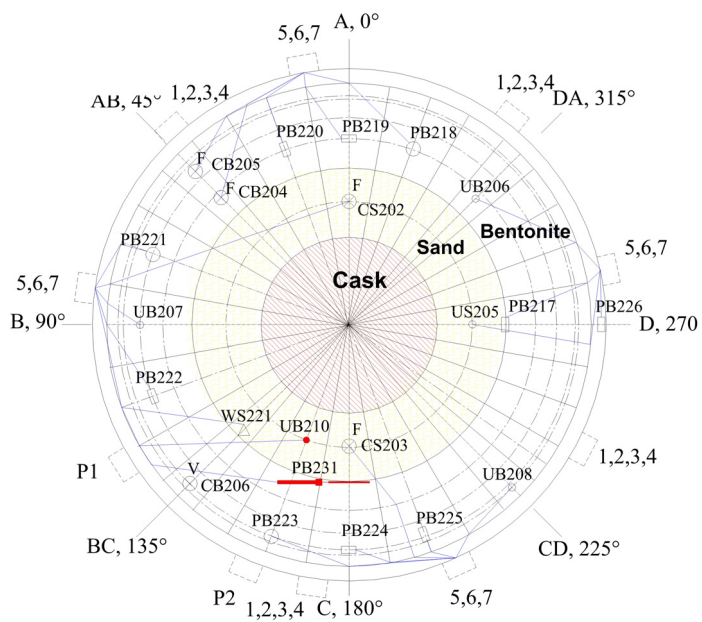
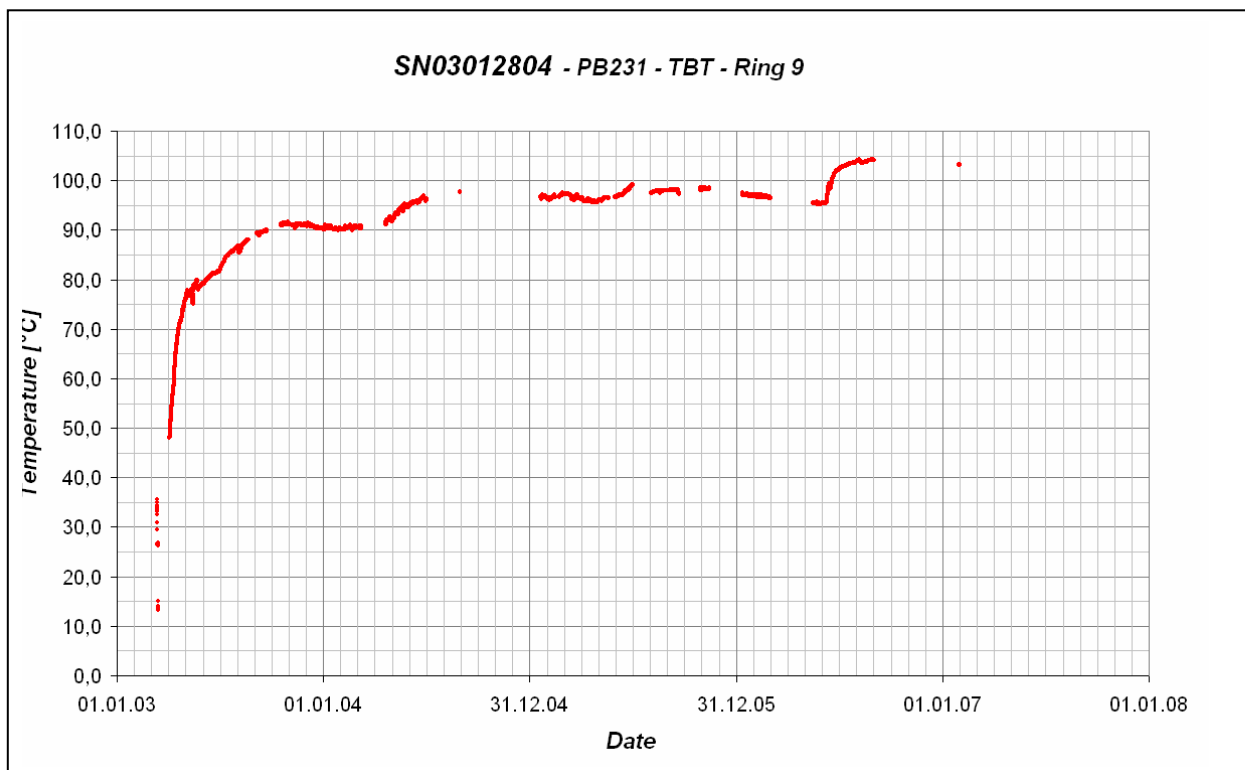


Fig. 2b. Radial location of sensors in Ring 9 horizontal cross-sections of the upper canister

Data update of FO-sensor PB231 (the other three sensors failed)



SN03012804 - PB231 - TBT - Ring 9

